THE UNIVERSITY *of* EDINBURGH

THE ELECTRICAL AND OPTICAL PROPERTIES OF VANADIUM TELLURITE GLASSES

BY

BRIAN W FLYNN

Thesis presented for the degree of
Doctor of Philosophy of the
University of Edinburgh

March 1977

ABSTRACT

Glasses in the system V_2O_5-TeO_2 were prepared at intervals throughout the glass-forming composition range. The vanadium valence state was varied for each composition by the addition of elemental tellurium to reduce the melt. A chemical analysis method was devised to determine the V^{4+}:V_{total} ratio.

Conductivity and thermopower measurements were made as functions of composition, valence ratio and temperature. The conductivity was found to increase as the total vanadium content increased and to be $2\frac{1}{2}$ to 3 orders of magnitude greater than that of a V_2O_5-P_2O_5 glass of similar V_2O_5 content. A maximum in conductivity was observed as the vanadium valence ratio was varied. This maximum was shifted to values around V^{4+}:V_{total} = 0.2 from the theoretically predicted value of 0.5. At temperatures above 250 K the conductivity varied exponentially with temperature with activation energies in the range 0.25 to 0.40 eV. Below this temperature there was a continuous decrease in slope of the conductivity down to the lowest temperature at which measurements were made.

Thermopower was found to be negative and temperature independent above 250 K, while below this temperature it decreased in an activated manner with an activation energy of 0.02 eV. As a function of valence ratio the thermopower followed the behaviour predicted by Heikes and Ure, with the exception that the change of sign occurred at V^{4+}:V_{tot} ratios of around 0.2, instead of the theoretically predicted value of 0.5.

Measurements were made of the optical absorption coefficient as functions of photon energy, composition, valence ratio and temperature. Temperature and composition did not affect the absorption spectrum significantly except that an absorption band appeared below the fundamental absorption edge as the glasses were reduced.

The high electric field and a.c. properties of the glasses were also measured. These are consistent with hopping conduction of carriers between V^{4+} and V^{5+} sites. This data gives indirect indications of an inhomogeneous glass structure.

ACKNOWLEDGEMENTS

I would like to express my thanks and appreciation for the help and guidance received from my supervisors, Dr A E Owen and Dr J M Robertson.

The assistance of the academic and technical staff of the Department of Electrical Engineering is gratefully acknowledged, in particular, the help from Mr D J Reynolds with the chemical analysis work.

I wish to thank my colleagues in the Department during the period of this work for helping to make it stimulating and enjoyable.

I am grateful to the Science Research Council for a studentship.

Finally, I would like to thank Mrs Diane Bilton for her excellent typing of the text.

TABLE OF CONTENTS

TABLE OF CONTENTS (continued) *page no*

TABLE OF CONTENTS (continued) *page no*

TABLE OF CONTENTS (continued) *page no*

TABLE OF CONTENTS (continued) *page no*

TABLE OF CONTENTS (continued) *page no*

CHAPTER 1 : INTRODUCTION

1.1 ELECTRONIC TRANSPORT IN CRYSTALLINE SOLIDS

In metals and crystalline semiconductors such as silicon, germanium, III-V and II-IV compounds, electronic charge transport can be described by the 'free-electron' approach within the limits of the effective mass approximation. Carriers have wide bands of allowed energy and the mobility is high (usually in the range 10^{-2} to 1 $m^2\ V^{-1}\ s^{-1}$) implying a large mean free path. In this situation charge transport is limited by scattering of the carriers.

There is also a large class of crystalline materials for which these concepts are invalid because they have narrow bands of allowed energy. This implies that the curvature of the E,K diagram is small and the effective mass (m*), determined by the relation, $m^* = h^2\left(\frac{d^2E}{dK^2}\right)^{-1}$ is large. As a consequence, carriers have low mobilities and short mean-free-paths resulting effectively in their localisation. Conduction takes place by hopping between localised states when conditions of temperature and pressure allow. Examples of materials which show this behaviour are certain transition-metal oxides and some organic compounds such as anthracene. The essential feature is a small degree of overlap of the wave functions forming the 'conduction' and 'valence bands' as in a molecular crystal.

The subject of this thesis is electronic transport in transition-metal oxide *glasses*, ie, narrow-band materials with the additional feature of a disordered structure.

1.2 AMORPHOUS SOLIDS AND GLASSES

Crystalline solids are ordered structures in which the atoms or molecules are positioned in a regular periodic lattice with long-range order making it possible to predict the position of an atom, within the limit of vibrational motion, at many site spacings from an arbitrarily chosen reference site. Glasses, on the other hand do not have long-range order and are often described as having a "frozen-in liquid-like structure", i.e. they are mechanically rigid networks which retain the structural features of the liquid state. Figure 1.1 (a)[1] is a schematic representation of a glassy network of atoms in two dimensions. The position of the nearest neighbours to a given atom can be determined by X-ray diffraction but at distances of several site spacings the periodicity of the structure diminishes rapidly. Figure 1.1(b) is a radial distribution function for a typical glass in which the positions of the first, second and third nearest neighbours can be distinguished but subsequent peaks merge with the parabola predicted by a model consisting of a series of randomly positioned point atoms. Glasses yield an X-ray diffraction pattern similar to that of a micro-crystalline powder, i.e. broad rings vanishing rapidly with increasing diffraction angle, confirming the lack of long-range order.

1.3 PREPARATION OF GLASSES AND AMORPHOUS SOLIDS

Amorphous solids are prepared by methods which prevent crystallisation. This can be done in a number of ways, e.g. thermal evaporation, R.F. sputtering, vapour phase reaction, glow discharge decomposition and by rapid quenching of the liquid. In all of these

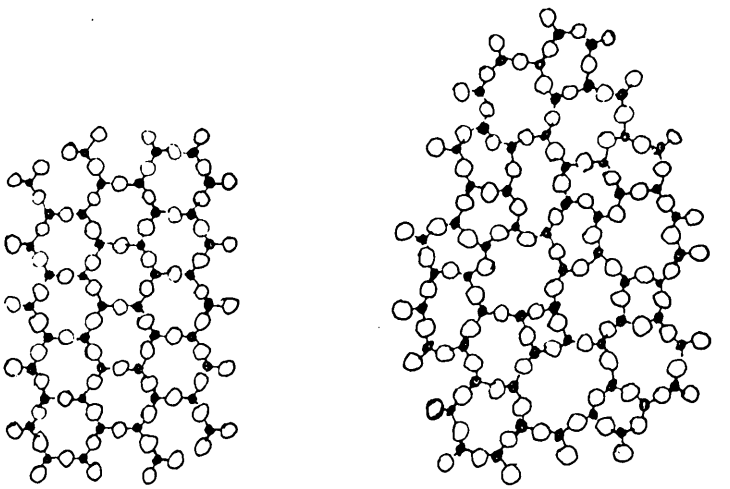

Fig. 1.1 (a) Two dimensional representation of crystalline network of atoms along with a glassy network (after Zachiarasen, Ref. 1).

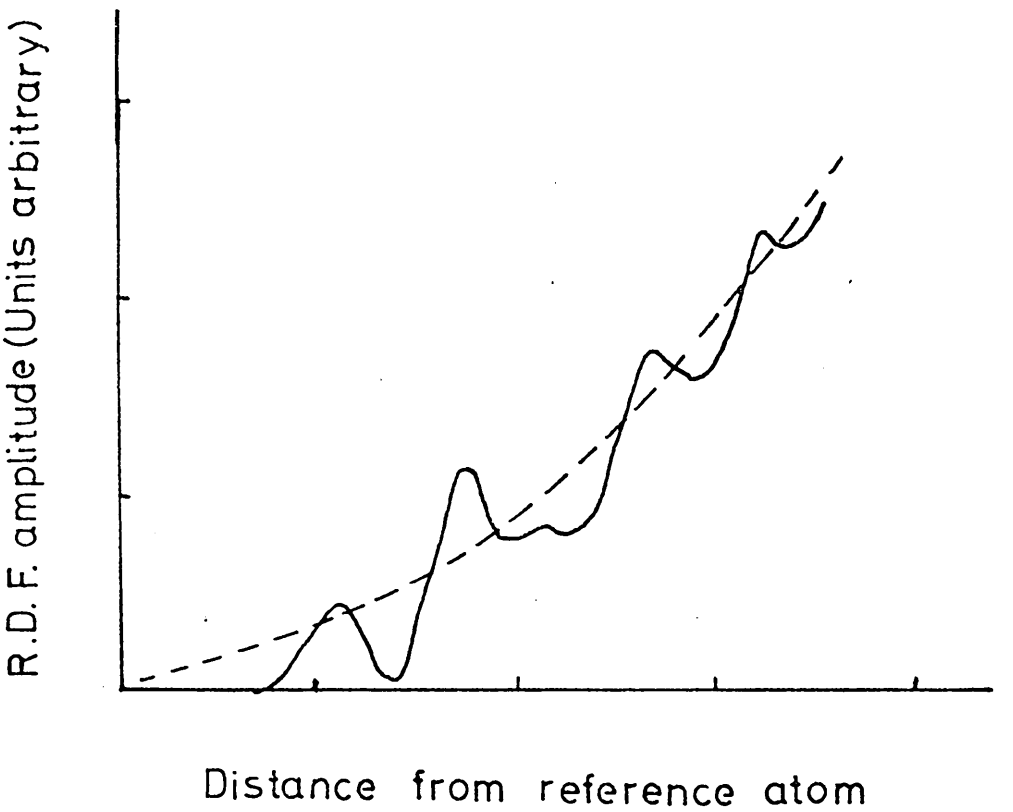

Fig. 1.1 (b) Radial distribution function of a typical glass.

methods, except the last, the solid is deposited from the vapour or some other highly energetic form, such as a plasma in the case of R.F. sputtering.

Techniques such as neutron bombardment, ion bombardment and shock-wave transformation can be used to produce non-crystalline solids by disordering the crystalline material. In the case of quartz, shock-wave transformation is found to give a material with identical properties to those of ordinary fused silica (i.e. density and refractive index are almost the same). This is thought[2] to be the result of melting and subsequent quenching at the shock front as it progresses through the crystal.

This thesis is entirely concerned with glasses, or vitreous solids quenched from the melt by ordinary cooling techniques , i.e. melts of several grams or more cooled naturally by pouring onto a metal block at room temperature (estimated cooling rate 10 - 10^2 degrees/sec.).

1.4 GLASS-FORMATION

Figure 2(a) shows a typical volume-temperature curve for a material in its liquid, glassy and crystalline forms. As the temperature of the liquid is reduced through its freezing point, T_f, it may either freeze into a crystalline solid, with a discontinuous change in volume, or if cooling is rapid enough to prevent nucleation it may continue as a super-cooled liquid below T_f until a temperature T_g, at which there is a change in slope to that of the crystalline form. This temperature (T_g), known as the glass transformation temperature, defines the transition between the super-cooled liquid state and the solid glassy state. It should be noted that T_g is

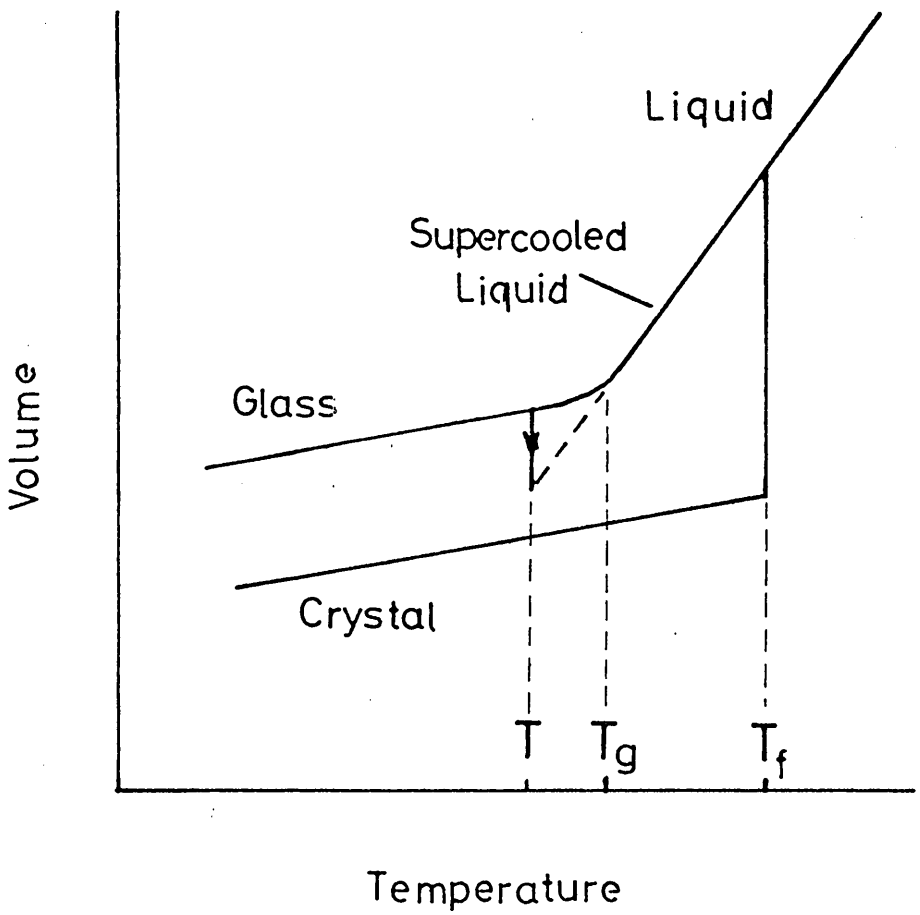

Fig. 1.2 (a) Relation between the glassy, liquid and solid states.

dependent upon the cooling rate during glass-formation. It rises with increasing cooling rate, so it is not a uniquely defined temperature for a given composition (unlike the melting and boiling points). The glassy state is unstable and the ease with which it reverts to the crystalline form is dependent upon the composition, temperature and thermal history of the glass.

The first order thermodynamic properties of glass such as volume, heat content and entropy (See Figure 1.2(a)) are continuous functions of temperature through T_g but second order properties such as thermal expansivity (See Figure 1.2(b)) and specific heat capacity are discontinuous. The properties of a glass depend upon the rate of cooling during manufacture e.g. a rapidly cooled glass has a greater tendency to contract as it ages than one which has been slowly cooled.

The physical properties in different regions of a glass ingot tend to vary. This is a result of difficulty in ensuring an even cooling rate throughout the bulk and can give rise to undesirable mechanical stresses in the glass. These effects can be virtually elimated by an annealing treatment in which the glass is heated for a long period at a temperature somewhat below the transformation temperature and then cooled slowly. This procedure relieves mechanical stresses within the glass without introducing further stresses on cooling and also ensures uniform physical properties throughout the glass.

1.5 GLASS-FORMERS AND MODIFIERS

Oxides such as SiO_2, P_2O_5 and B_2O_3 are known to be good "glass-formers". The strong co-valent bonding between oxygen and the positive

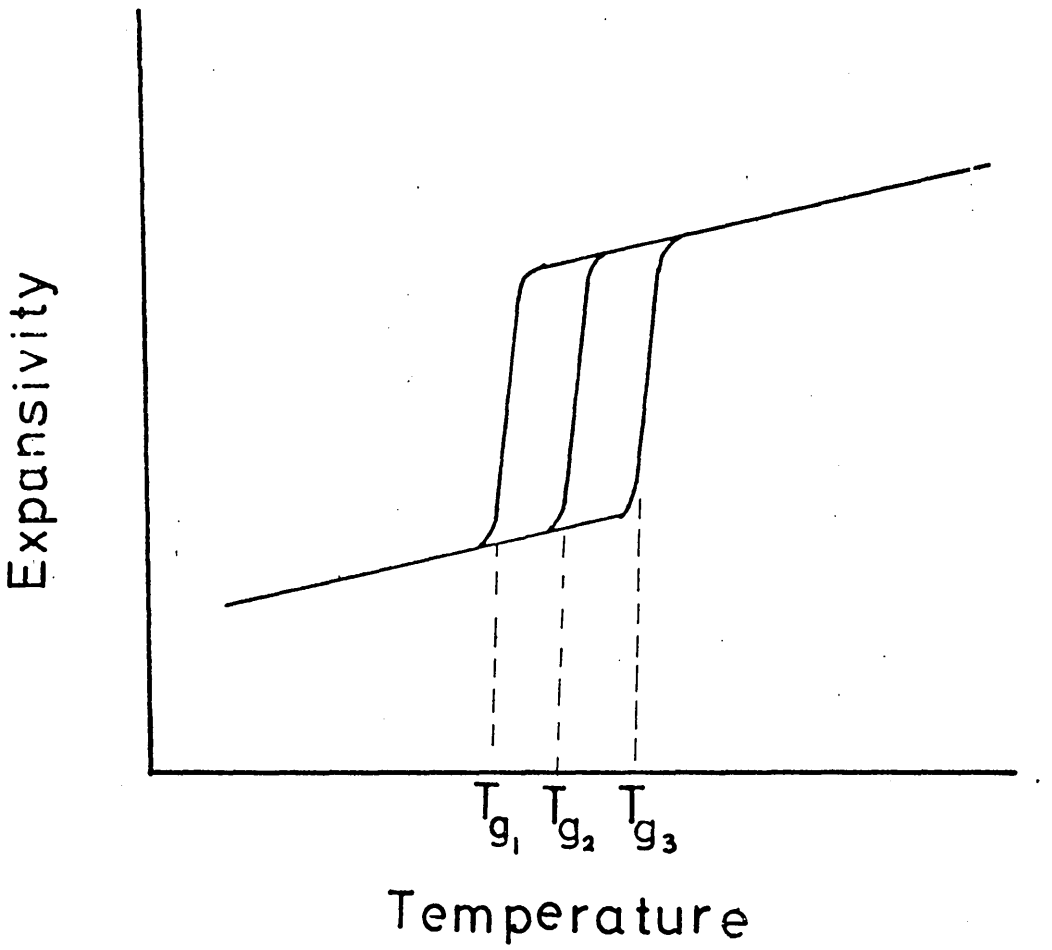

Fig. 1.2 (b) Second order thermodynamic properties (e.g. expansivity) as a function of temperature.

ions facilitates the formation of 3-dimensional networks of atoms. In SiO_2 and P_2O_5, oxygen tetrahedra are the basic structural units but boric oxide (B_2O_3) glasses are formed from essentially planar triangles of oxygen atoms around boron atoms. Silicon, phosphorous and boron are considered to be good network-formers. On the other hand elements such as sodium which normally form ionic bonds are referred to as "modifiers". In the case of sodium, for example, the introduction of sodium oxide into silica is thought to cause a breakdown of the Si-O network through the formation of non-bridging oxygen ions. This is often illustrated schematically as follows:

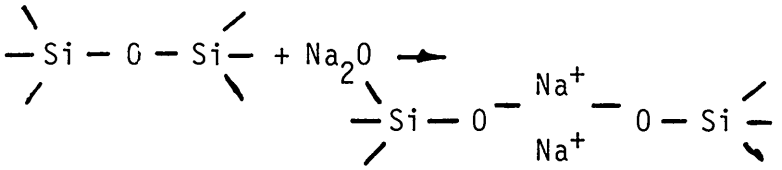

The sodium ions occupy the "holes", or interstices, between the non-bridging oxygen ions in the Si-O network. Van Wazer[3] and Stevels[4] predict that, as the proportion of modifier is gradually increased, the network breaks down, first to cross-linked and branched chains and finally to unbranched chains.

The oxides of metals such as aluminium, magnesium and lead are known as "intermediate oxides", as they do not form glasses on their own but can be incorporated in large amounts into the networks of glasses.

1.6 MACROSTRUCTURE IN GLASSES

In binary and ternary glasses, i.e. glasses composed of more than one compound, the structure is often complicated by phase separation arising during the formation of the glass. Figure 1.3

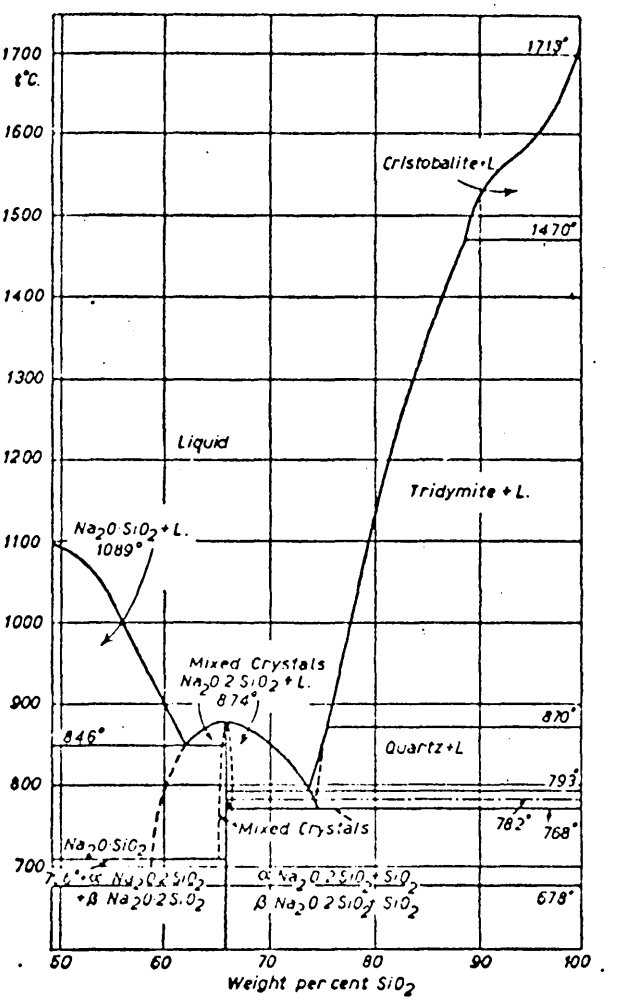

Fig. 1.3 Phase equilibrium diagram of the soda-silica system from 50 to 100 m.p.c. SiO_2 (after Jones, Ref. 2).

shows the phase equilibrium diagram of the soda-silica[2] system from 50 to 100 molar per cent (m.p.c.) SiO_2. At temperatures above 1713°C pure SiO_2 is a liquid but if 25 m.p.c. Na_2O is added to the melt the liquidus temperature is lowered to 793°C. In the intervening region below the liquidus temperature, crystals of tridymite form with the remainder of the material staying in the liquid phase. At no point in this diagram is the co-existance of two liquid phases observed, but in some compositions, e.g. the CaO - SiO_2 system; there is an extensive region at the silica-rich side of the phase equilibrium diagram where two immiscible liquid phases co-exist. On quenching, a melt of this type would remain phase separated and the resulting glass would consist of macroscopic regions of two different compositions corresponding to the liquid phases.

1.7 ELECTRONIC PROPERTIES OF DISORDERED SOLIDS

The quantum mechanics of typical "wideband" semiconductors (e.g. Si, Ge, III - V and II - VI compounds) predict that an electron can move through the periodic potential of a perfect crystalline lattice with an energy in certain "allowed" bands which are separated by "forbidden" gaps. The bandwidth in such materials is typically 5 → 10eV. The effect of chemical impurities and imperfections in the crystal structure is to introduce energy states into the forbidden gap. The electrons in these states are localised (i.e. their wave functions are not continuous throughout the lattice) and cannot move through the lattice unless:

(i) sufficient energy is supplied to excite them into the conduction band

or (ii) there are a sufficient number of localised states in the

forbidden gap for their wave functions to overlap and form an impurity band within the forbidden gap

or (iii) the carriers jump or "hop" instantaneously from one localised state to another with the absorption or emmission of a phonon.

In a non-crystalline semiconductor the effect of disorder is to introduce a high density of localised states (typically 10^{25} m^{-3}) into the forbidden gap. There are several different models which describe the electronic structure of a non-crystalline semiconductor, but a common feature is that they postulate tails of states extending into the gap from the valence and conduction bands.

Mott and Twose[5] have applied Anderson's[6] results to the localisation of electrons in non-crystalline materials and they show that below a certain critical density of states, all states are effectively localised. Since the density of states varies with energy a transition occurs from localised to extended stares (i.e. the wave functions become continuous throughout the solid) at an energy Ec. This is known as Anderson localisation and Ec is called the mobility edge because the mobility of electrons in extended states is orders of magnitude greater than in those which are localised. Figure 1.4(a) shows the variation of mobility with energy across an energy gap.

Davis and Mott[7] suggest that the density of states function of an amorphous semiconductor is as shown in Figure 1.4(b); the conduction and valence bands have shoulders of localised states extending into mobility gap. A narrow (<0.1eV) band of localised states of sufficient density to effectively pin the Fermi energy over a wide range of

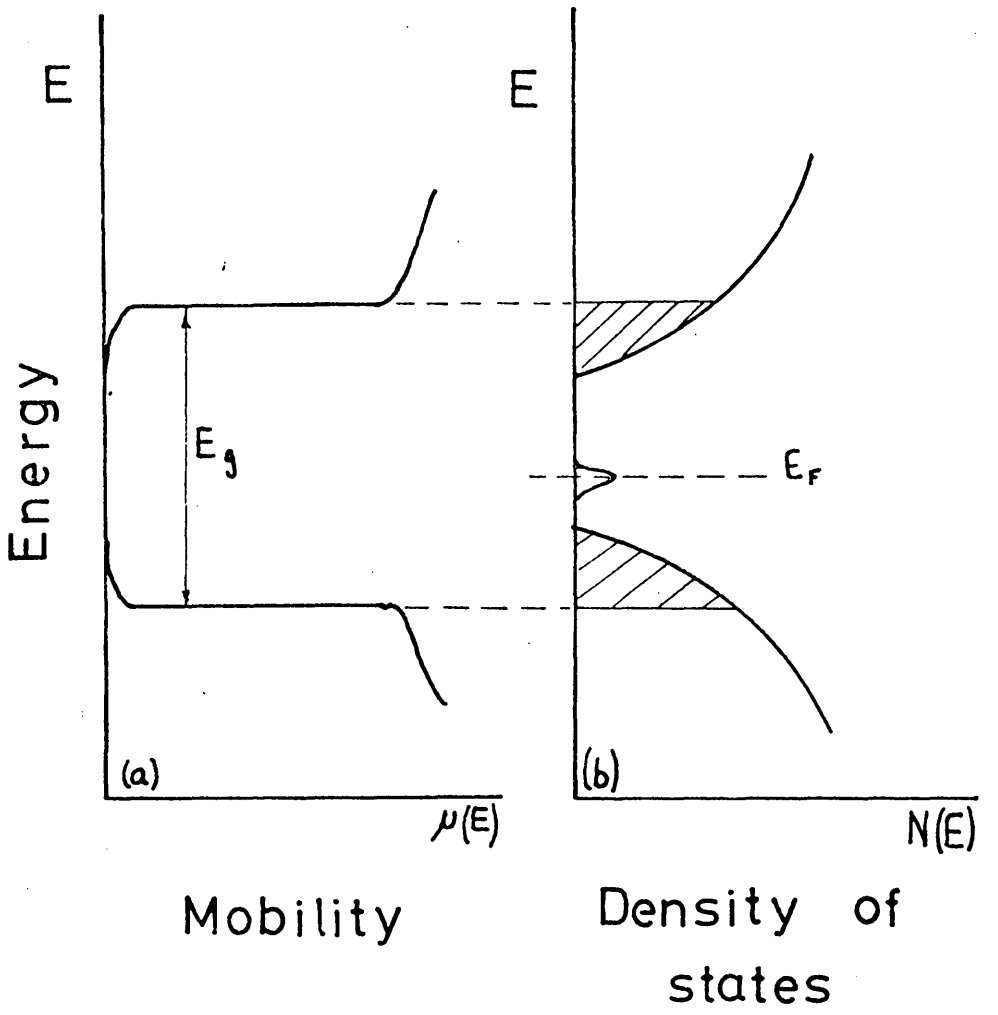

Fig. 1.4 Variation of (a) the mobility and (b) the density of states across an energy gap (after Mott and Davis, Ref. 9).

temperature is assumed to exist near the centre of the gap. From this model three mechanisms which will determine the behaviour of electronic conduction at different temperatures can be distinguished:

(i) Conduction due to the excitation of carriers into the extended states. If the main charge carriers are holes then,

$$\sigma = \sigma_o \text{ Exp } \{ \frac{-(E_F - E_V)}{kT} \}$$

(ii) Conduction by carriers excited into the localised states at the band edges, ie . at E_a and E_b. Again if the main current is carried by holes and conduction occurs by hopping then,

$$\sigma = \sigma_1 \text{ Exp } \{ \frac{-E_F - E_b + W_H)}{kT} \}$$

Where W_H is a hopping activation energy

(iii) Conduction by hopping of carriers between localised states near the Fermi level giving a conductivity temperature dependence of the form

$$\sigma = \sigma_2 \text{ Exp } (\frac{-\Delta W_D}{kT})$$

Where ΔW_D is half the width of the defect band shown in Figure (4). At very low temperatures ($kT < 2W_D$) Mott[8] argues that carriers will not necessarily hop to nearest neighbour sites, but will hop, in preference, to sites of closer energy. This "variable range hopping" mechanism gives rise to a temperature dependence of the form

$$\sigma = A \text{ Exp } (\frac{B}{T^{\frac{1}{4}}})$$

Figure 1.5[9] shows schematically the behaviour of the different conduction mechanisms, described in (i), (ii) and (iii), as functions of temperature when $\sigma_0 > \sigma_1 > \sigma_2$.

Thus, in amorphous semiconductors formed from typical wide-band materials the effect of disorder is essentially to modulate electronic transport (conductivity) by trapping and release to and from localised and extended states. Amorphous Si and Ge and the chalcognide glasses, at or near room temperature, are probably good examples of this situation. As mentioned in paragraph (1.1), however, there is also a large class of semiconductors where carriers are localised even in the absence of disorder because of the narrow width of the allowed energy bands. Examples of such materials are the transition-metal oxides, e.g. V_2O_5, Fe_2O_3, NiO etc., and certain organic compounds such as anthracene. In these materials structural disorder has a secondary effect in controlling the conduction process. This thesis is concerned with the latter situation, i.e. semiconductors in which disorder has a secondary effect on charge transport and in particular with vanadium oxide glasses in the V_2O_5 - TeO_2 system.

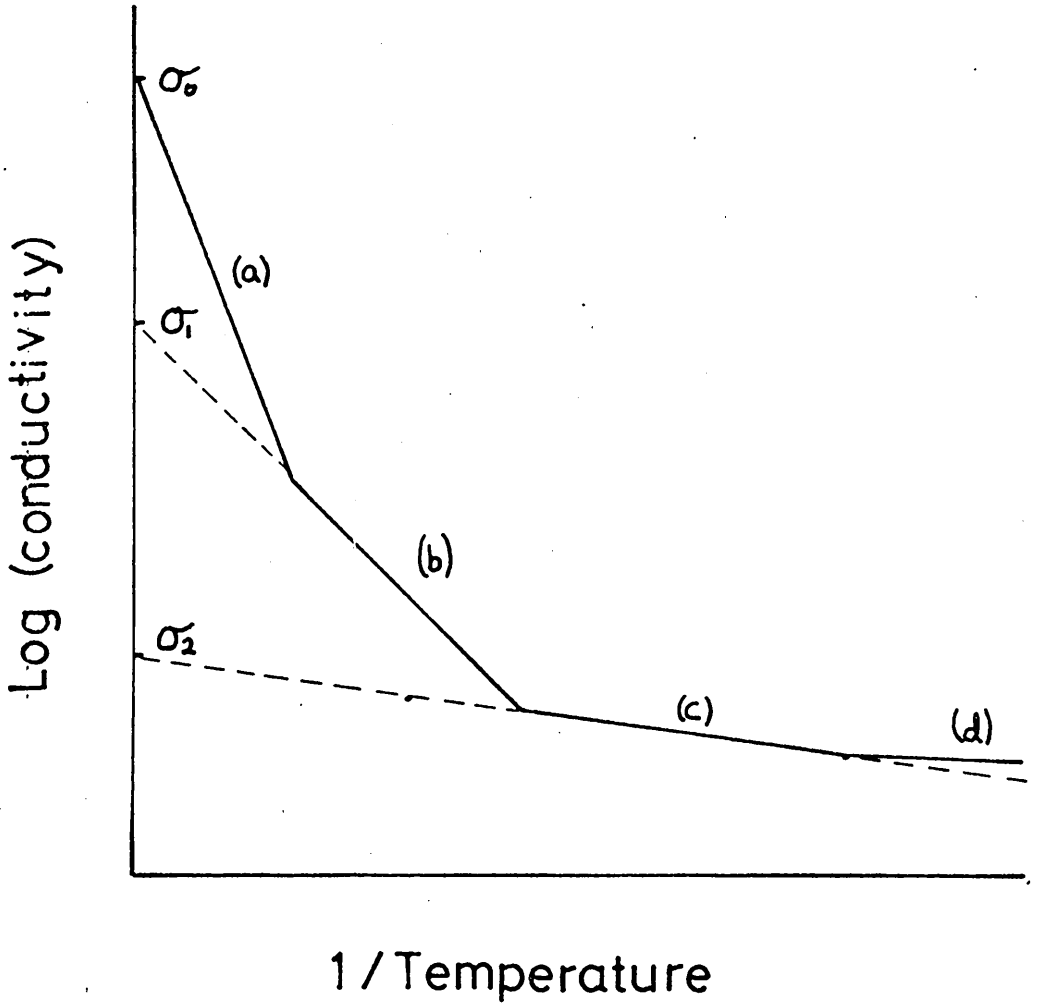

Fig. 1.5 Illustration of the temperature dependence of conductivity expected on the basis of the model in Fig. 1.4 (after Mott and Davis, Ref. 9).

CHAPTER II : CRYSTALLINE TRANSITION-METAL OXIDES

2.1 CONDUCTION IN 3d SYSTEMS

The transition metals are characterised by the progressive filling of the 3d electron shell which lies below the outermost 4S shell. On oxidation, the 4S shell loses its electrons and the 3d shell gains electrons by an amount determined by the degree of oxidation. The large number of oxides which can be formed by the transition metals is due to their ability to form stable compounds in which the outermost d-electron shell is partially filled. The stable oxides of vanadium are listed below, with, in parenthesis, the electronic configuration of their 3d shell (after Morin)[10].

$$V_2O_5(d^0) \; ; \quad V_2O_4(d^1) \; ; \quad V_2O_3(d^2) \; ; \quad VO(d^3)$$

To discuss conduction in the oxides of transition metals it is instructive to consider first the energy band situation in the metals themselves. Slater[11] has calculated the energy band structure of the 3d transition metals using the cellular and tight binding methods. It is usually found that the 4S band is at least 10 eV and overlaps the 3d band, which in nickel, for example is 2.8 eV wide. On the other hand, the 3d band can hold ten electrons per atom while the 2p band can hold two electrons for each atom. This difference in electron content increases the difference in the "per-electron" bandwidths between the two bands. In nickel the 3d-bandwidth is only 1/15th that of the 4S band. This means that electrons in the 3d band have a high effective mass and low mobility (see Section 1.1), thus electronic transport in the metals takes

place in the 4S band with the mobility being lowered by transitions into the 3d band.

In the oxides, the 3d-bandwidth is reduced by the increased separation between the metal ions, reducing the overlap of the 3d wave functions. de Boer and Verwey[12] in 1937 and Mott[13] in 1949, concluded that the 3d-bandwidth tends to zero and that the electrons will be localised. This occurs in the oxides of Cr, Mn, Fe, Co, Ni and Cu which are insulators when pure and stoichiometric, but would be expected to behave as metals on the simple energy-band theory of Wilson which does not take into account the interaction between electrons. Figure 2.1 (after Morin)[10] illustrates the decrease of 3d-bandwidth with increasing atomic weight and superimposed on this is a curve showing the increase in effective mass $(\frac{m^*}{m})$ of carriers in the 3d-band as the bandwidth reduces to zero.

2.2 MIXED VALENCE SEMICONDUCTORS

In Section 2.1 it was seen that the oxides of Cr, Mn, Fe, Co, Ni and Cu are insulators when pure and stoichiometric. For conduction to take place, according to de Boer and Verwey[12], it is necessary that there are ions of the same element but of different valency present at crystallographically equivalent lattice points. For pure, stoichiometric NiO, for example, this can be achieved thus,

$$2\ Ni^{2+} \rightleftharpoons Ni^{3+} + Ni^{+}$$

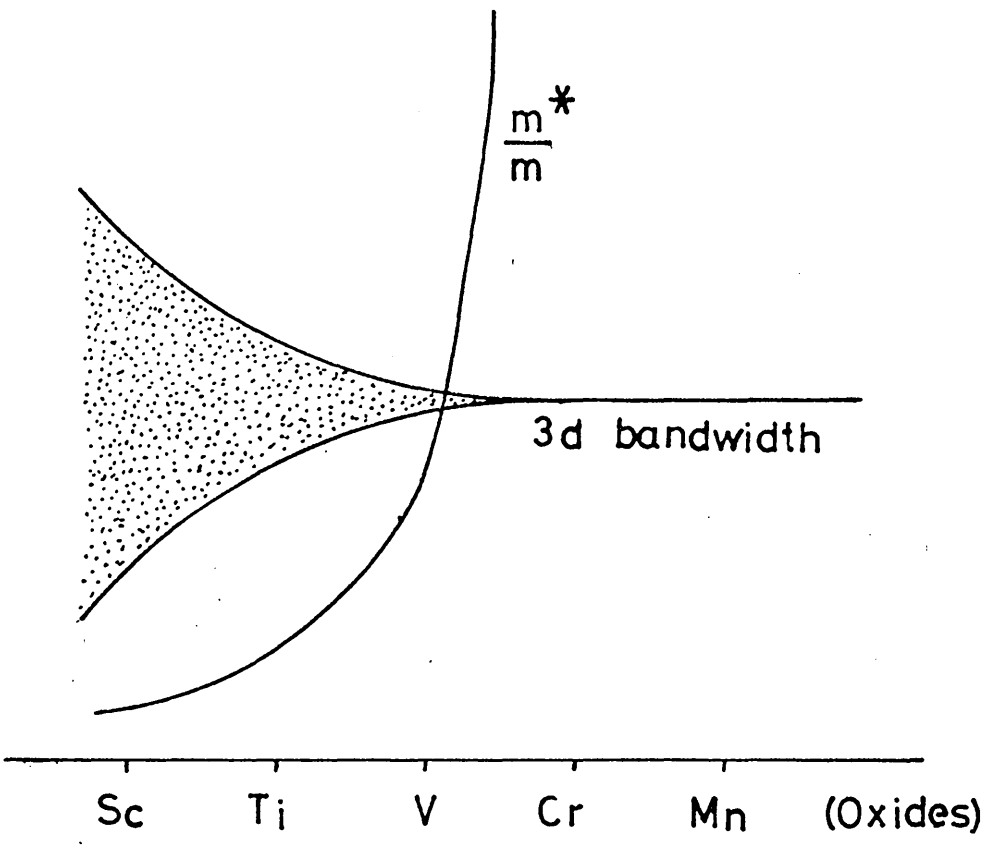

Fig. 2.1 Schematic representation of the decrease in 3d bandwidth and increase in effective mass (m*) with increasing atomic number (after Morin, Ref. 10).

but at normal temperatures this cannot occur because of the large energy required (≃4eV), hence NiO is an insulator.

To render NiO conducting, Ni^{3+} ions can be introduced by deviations from stoichometry, or it can be doped with an oxide of a mono-valent metal such as lithum. The singly charged lithium ions (Li^{+}) are compensated by tri-valent nickel ions (Ni^{3+}). Conduction in lithium doped nickel oxide is more fully discussed in section 2.3.

Pure, single crystal, vanadium pentoxide (V_2O_5) has empty d-bands and is expected to be an insulator. In practice, when grown from the melt, it is found to be an N-type semiconductor with a conduction activation energy of around 0.28eV. It is not clear, at present, whether this is caused by a doping arising from impurities as in Li doped NiO, or a loss of oxygen from the melt. Unless V_2O_5 is melted under strongly oxidising conditions small quantities of oxygen are evolved thus:

$$2\ V_2O_5 \rightarrow 2\ V_2O_4 + O_2$$

On cooling and crystallisation the four valent vanadium remains and conduction proceeds by transfer of electrons from V^{4+} sites to V^{5+} sites,

$$V^{4+} + V^{5+} \rightarrow V^{5+} + V^{4+}$$

2.3 ENERGY BAND SCHEMES FOR SOME CRYSTALLINE TRANSITION METAL OXIDES

Band structures have been derived for some of the simpler oxides but generally information in the literature is scanty. The compounds studied in most detail are VO_2 and NiO. Considerable attention has

been given to the former because it exhibits a transition from a semi-conducting to an apparently metallic phase as the temperature is raised through 68°C.

2.3.1 Band Structure of NiO

The band structure of NiO has been deduced by Morin[10] and Van Houten[14] by considering measurements on lithium doped NiO. The following table shows how charge carriers can be formed in lithium doped nickel oxide, a typical lattice of which is shown in Figure 2.2 (after Morin)[10].

Electronic Process Producing Carriers	
(a) $O^{--}(2p^6)+Ni^{++}(3d^8)\rightarrow O^{-}(2p^5)+Ni^{+}(3d^9)$	$2p^5$ hole + $3d^9$ electron
(b) $Ni^{++}(3d^8)+Ni^{++}(3d^8)\rightarrow Ni^{+}(3d^9)+Ni^{+++}(3d^7)$	3d hole + $3d^9$ electron
(c) $Ni^{++}(3d^8)\rightarrow Ni^{++}(3d^7 4S)\rightarrow Ni^{+++}(3d^7)$+4S electron	4S electron
(d) Vac-$Ni^{+++}(3d^7)+Ni^{++}(3d^8)\rightarrow$Vac-$Ni^{++}(3d^8)+Ni^{+++}(3d^7)$	3d hole
(e) $Li^{+}Ni^{+++}(3d^7)+Ni^{++}(3d^8)\rightarrow Li^{+}Ni^{++}(3d^8)+Ni^{+++}(3d^7)$	3d hole

The carriers formed are 2p holes, 4S electrons and 3d holes and electrons. Morin[10] plots these levels with respect to the free electron energies, using the ionisation potential (18.2 eV) of $Ni^{+}(3d^9)$ and spectrographic data from the National Bureau of Standards Circular 467[15] to give the energy difference between the $(3d^8)$ and $(3d^9)$ levels. When the lattice is formed the energy of the oxygen ion $(2p^6)$ is reduced by the Madelung potential while those of the

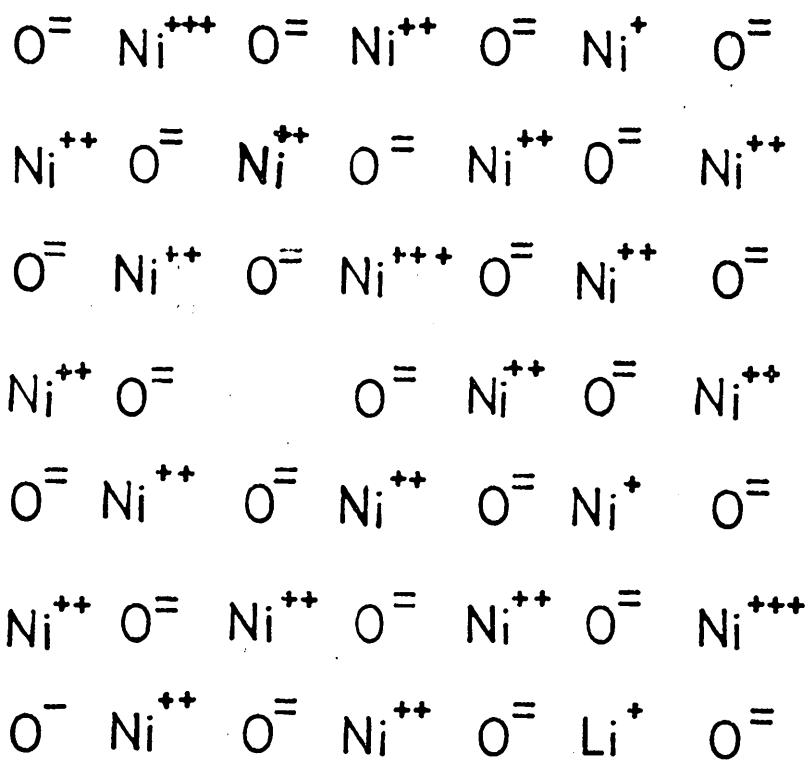

Fig. 2.2 A NiO lattice with Ni^{+++} acceptors near a cation vacancy and a substituted Li^{+}, Ni^{+} electron and a Ni^{+++} hole and a O^{-} hole in the 2p band (After Morin, Ref. 10).

Ni^{+} and Ni^{++} are raised by the same amount. This is shown in Figure 2.3. Corrections to these energy levels must be made, however, to allow for the polarisation of the lattice by the nickel and oxygen ions. Two approaches have been used to solve this problem. Morin considered the lattice as a dielectric, thus the energies of the ions must be divided by the dielectric constant of NiO to allow for the lattice polarisation. On the other hand, Van Houten suggests that it is more realistic to calculate the polarisation energy by considering the dipoles induced on the lattice sites by an excess charge, as indicated by Mott and Littleton[16].

In addition, Van Houten[14] introduces a correction for the crystal field stabilisation of the Ni^{+} level based on the data of Tanabe and Sugano[17]. The Ni^{+} ($3d^{9}$) level is raised by 0.9 eV and the energy level scheme thus arrived at is shown in Figure 2.4. The level Ea (acceptor levels) is produced by the ($3d^{7}$) vacancy formed in process (d). Morin's calaculation for the energy level scheme agrees qualitatively with those of Van Houten but quantitatively the two are different.

2.3.2 Band Structure of VO_2

Much effort has been devoted to the study of the electrical and optical properties of VO_2 both above and below its transition temperature. Below $68^{o}C$, VO_2 has a monoclinic crystal structure and behaves as a semiconductor. Above $68^{o}C$ it has a tetragonal rutile structure and a metallic conductivity. At the transition temperature there is a discontinuous change in electrical conductivity of several orders of magnitude.

Verleur[18] et al considered as an analogy the Ti site in strontium

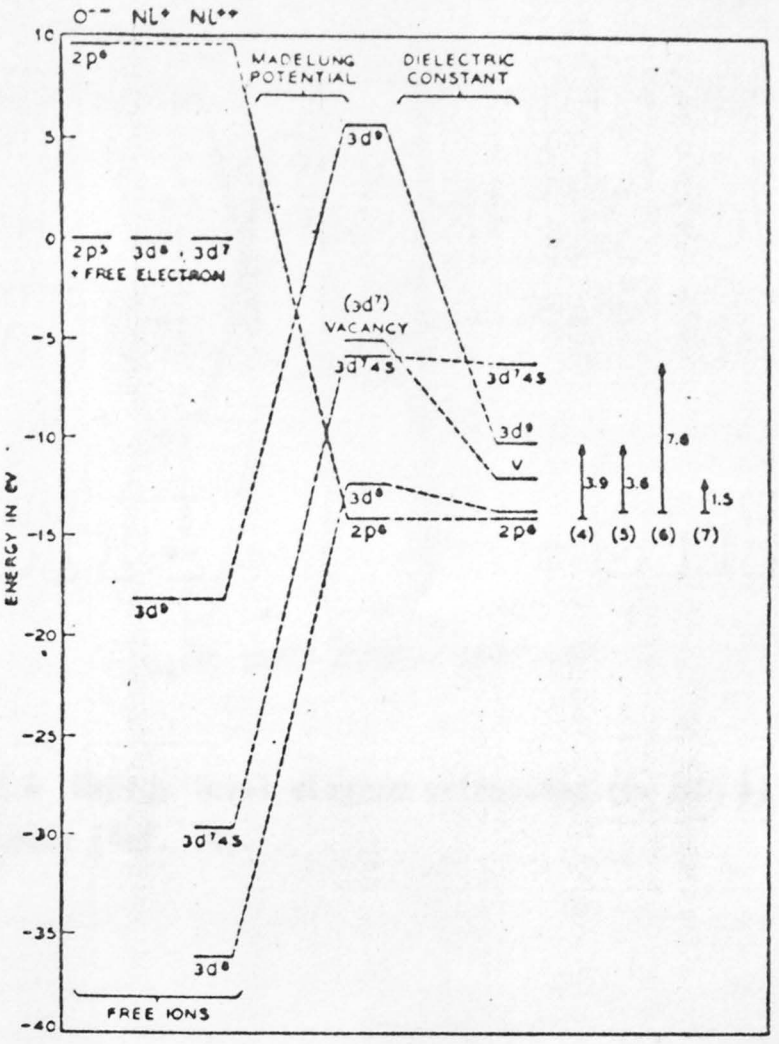

Fig. 2.3 Energy level diagram calculated for NiO, showing the energy required for reactions (a) to (e) (After Morin, Ref. 10).

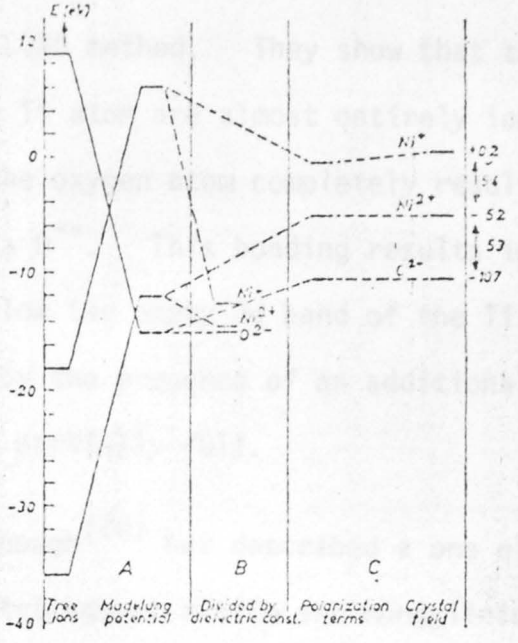

Fig. 2.4 Energy level diagram calculated for NiO by Van Houten (Ref. 14).

doped titanium oxide (Sr TiO_3) which has a similar environment to that of the vanadium ion in VO_2 in the metallic (rutile) phase. Sr TiO_3 has been studied by Kahn and Leyendecker[19] who have deduced its band structure using the LCAO method. They show that the four electrons in the outer shell of the Ti atom are almost entirely ionised and fill the outer shell of the oxygen atom completely resulting in a Ti^{4+} ionically bonded to a O^{--}. This bonding results in a filled oxygen 2p band 3.25 eV below the empty 3d band of the Ti. In VO_2 the situation is altered by the presence of an additional 3d electron hence the 3d band becomes partially full.

More recently, Goodenough[20] has described a one electron energy band scheme for both the tetragonal rutile and monoclinic crystalline forms of VO_2. This is shown in Figure 2.5a and b. To account for the semiconductor-metal transition at 68^oC it is necessary that below this temperature the crystal field is distorted in such a way as to cause splitting of the d-bands. This will give rise to a semiconductor if the lower of the bands are filled and the upper are empty; optical data shows that they are separated from the higher energy unfilled bands by about 0.7 eV.

2.4 ELECTRONIC TRANSPORT

2.4.1 Conduction in Narrow-band Semiconductors

The electronic transport properties of wide-band semiconductors are well described by band theory, but unfortunately this is not the case for narrow-band materials where the theoretical treatment is at present rather incomplete because of difficulties in describing the details of the motion of the carriers. The term "narrow-band

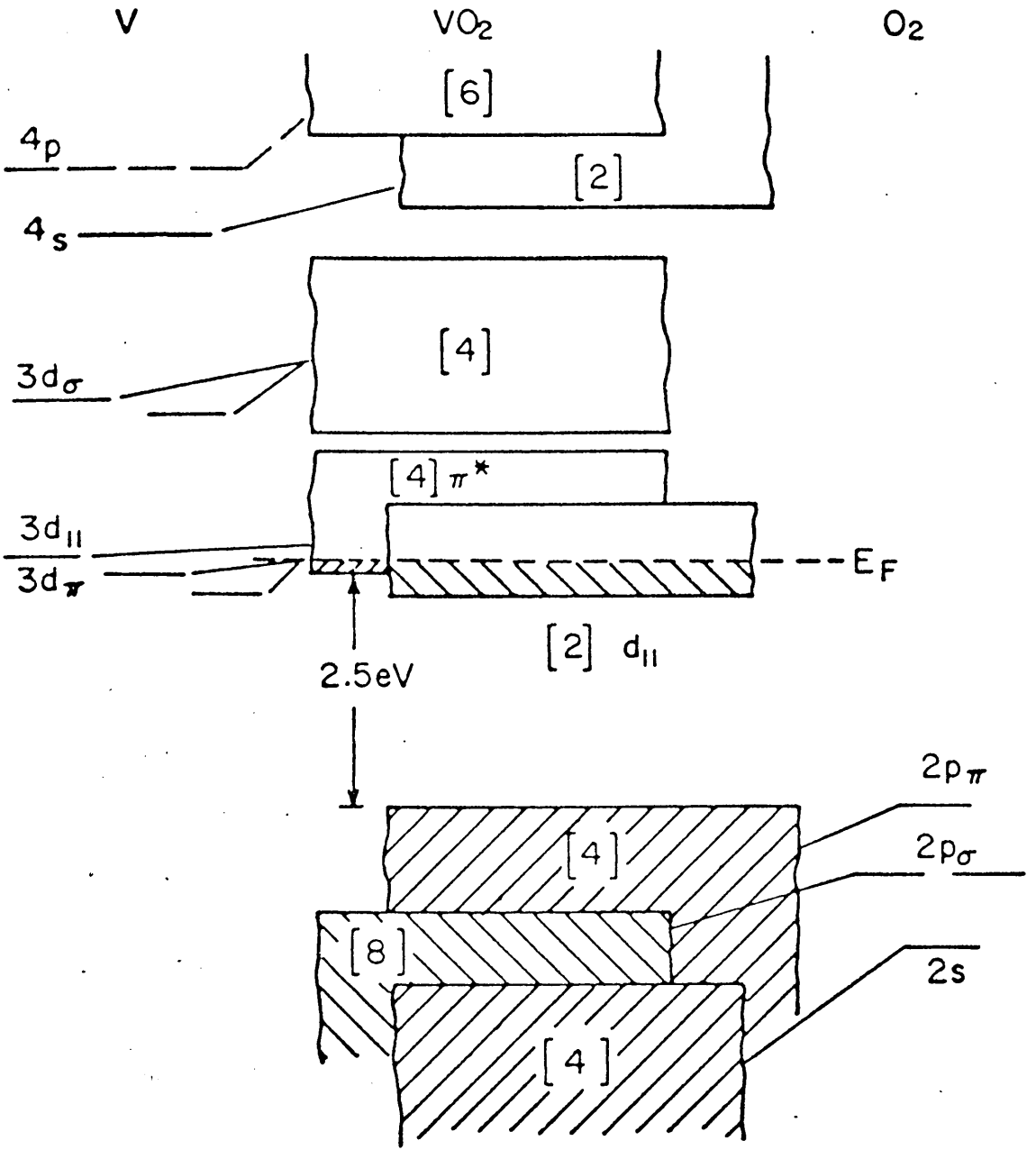

Fig. 2.5 (a) One electron band structure for metallic VO_2 (After Goodenough, Ref. 20).

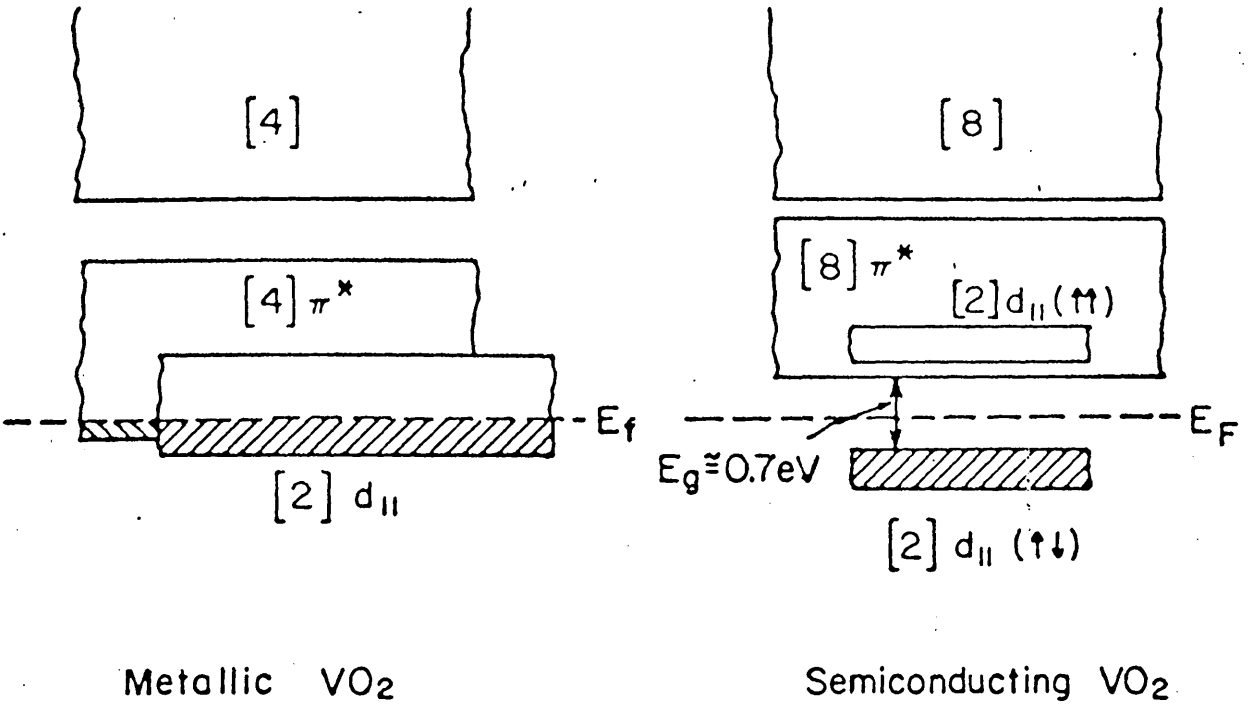

Fig. 2.5 (b) Modification of the d band structure of VO_2 on passing from the metallic to the semiconducting phase (after Goodenough, Ref. 20).

semiconductors" covers a variety of materials ranging from the transition-metal oxides to organic materials the common feature being that their charge carriers have such a high effective mass that they become localised on lattice sites. Under such conditions the carriers may be regarded as classical particles with site quantum numbers and their motion treated as a "jump" from site to site.

As for wide-band semiconductors, the carrier concentration in narrow-band semiconductors can be controlled by doping, but because of localisation a very high carrier concentration (10^{28} m^{-3}) does not give rise to degeneracy of the carriers. An appreciable thermal activation energy is usually required to free these carriers since they tend to remain tightly bound in the vicinity of the impurity centre.

Heikes[21] derives an expression for hopping conductivity of a narrow-band semiconductor by considering the transition probability for a carrier, ie,

$$\tau^{-1} = M.\nu.\ \mathrm{Exp}\ \frac{-W_H}{kT} \qquad \ldots (2.1)$$

where τ^{-1} = the transition probability

M = number of possible sites for carrier to jump to

ν = a phonon frequency

W_H = an activation energy for hopping

Since the carriers are localised, conduction can be treated on the basis of a classical diffusion model as follows :

$$\sigma = \frac{n\ e^2 D}{kT} \qquad \ldots (2.2)$$

where σ = electrical conductivity

n = carrier concentration

e = electronic charge

D = diffusion coefficient

k = Boltzmann's constant

T = absolute temperature

and $$D = \beta a^2 \tau^{-1} \quad \ldots (2.3)$$

In the above expression 'a' is the site spacing and β is a constructure dependent parameter equal to 1/6 for a cubic lattice and equivalent to half the probability that a given transition will cause a carrier to leave its original plane.

Therefore $$\sigma = \frac{n\, e^2 a^2}{6kT} \cdot \tau^{-1}$$

but $n = cN$

where N = concentration of lattice sites.

Therefore, $$\sigma = N \frac{e^2 a^2}{6kT} \cdot c \cdot \tau^{-1} \quad \ldots (2.4)$$

or $$\sigma = N \frac{e^2 a^2}{6kT} \cdot c \cdot \nu M \exp\left(\frac{-W_H}{kT}\right) \quad \ldots (2.5)$$

In a simple cubic lattice M is the number of the six nearest neighbour sites to which the carrier can hop, ie,

$$M = 6(1 - c)$$

Therefore, from (2.5)

$$\sigma = N \frac{e^2 a^2}{kT} \cdot c(1 - c)\, \nu \exp\left(\frac{-W_H}{kT}\right) \quad \ldots (2.6)$$

In the case of a mixed valence semiconductor 'c' would be interpreted as the mole fraction ($0 \leqslant c \leqslant 1$) or reduced ions and hence

(1-c) would be the concentration of the oxidised species, e.g. V^{4+} respectively, in a vanadate-based material. Thus according to (2.6) the conductivity of such a material would increase linearly with c, at small c, go through a maximum at the ratio

$$c = \left(\frac{\text{concentration of reduced ions}}{\text{total ion concentration}}\right) = 0.5$$

and then decrease linearly with c at large c. This is illustrated schematically in Figure 2.6.

2.4.2 Thermo-electric Power of Narrow-band Semiconductors

Heikes and Ure[21] have developed an expression for the thermo-electric power of a narrow-band semiconductor by considering the addition of a charge carrier to the lattice. They obtain,

$$\alpha = \frac{k}{e} \left\{\frac{\Delta Sr}{k} + \ln\left(\frac{c}{1-c}\right)\right\}$$

where α = thermoelectric power

k = Boltzmann's constant

e = electronic charge

c = fraction of occupied lattice sites

ΔSr = change in entropy of an ion due to the presence of a carrier

This expression assumes that at the carriers are free to hop and that all of the lattice sites have the same energy. Austin and Mott[22] estimate that the entropy term is small and that $\frac{\Delta Sr}{k}$ has a value of approximately 0.1. Studies made by Nester and Kingery [23] of the thermoelectric power of vanadate glasses confirm this view, as good agreement is obtained between measured values and estimates made from wet chemical analysis data. Nester and Kingery[23] make no attmept to include a value for $\frac{\Delta Sr}{k}$ in their calculated values. 'c' is the molar

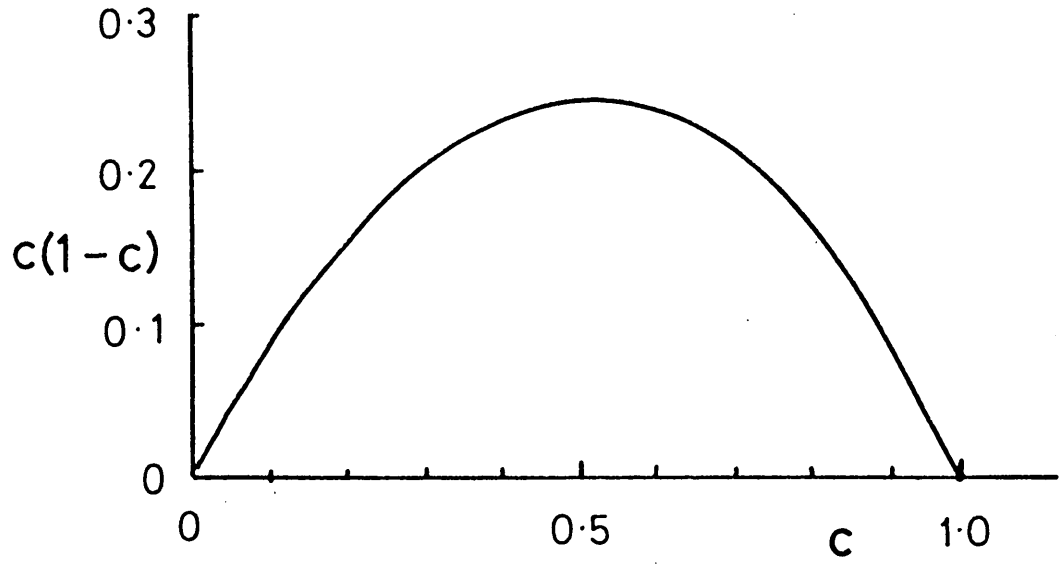

Fig. 2.6 Variation of c(1 - c) as c varies from 0 to 1.

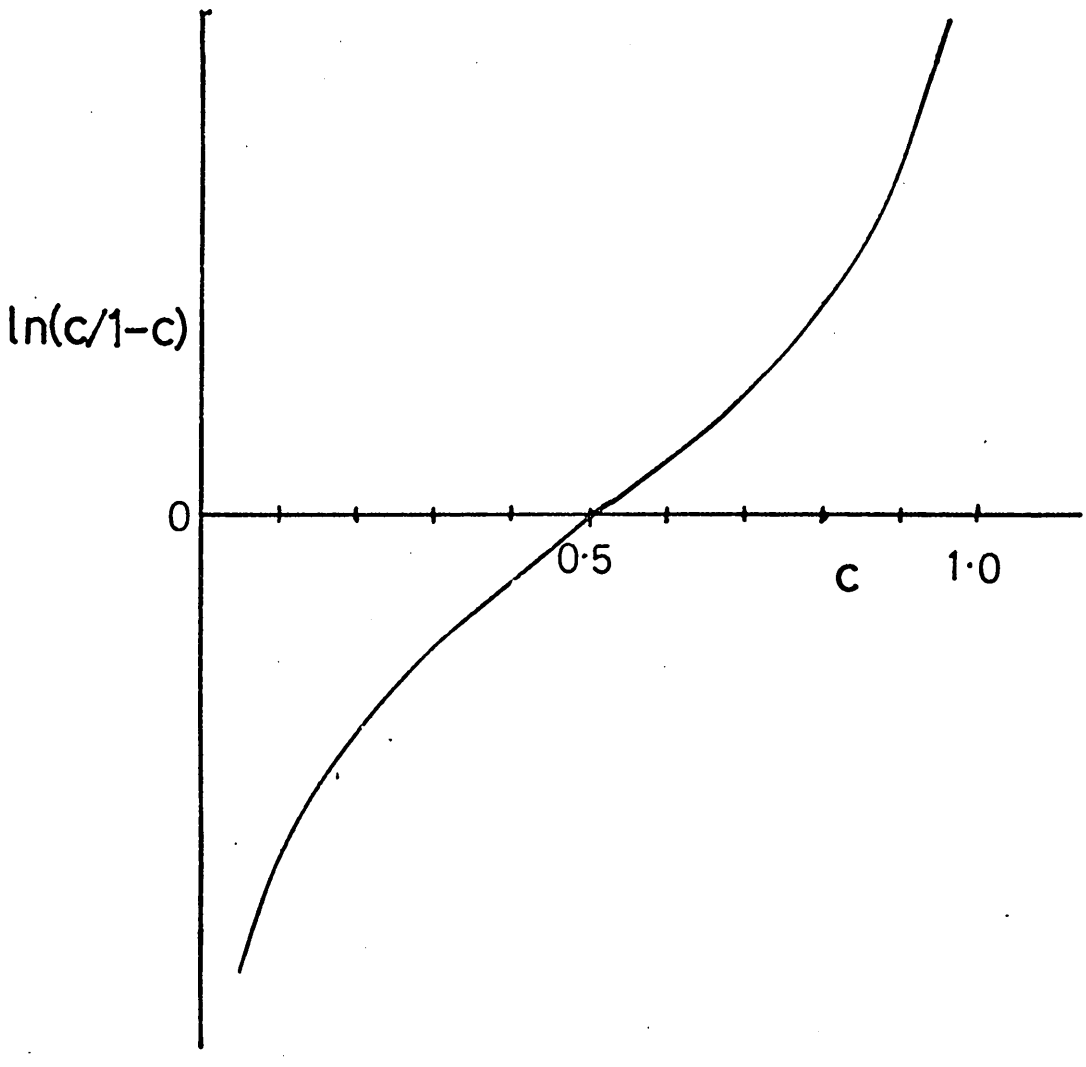

Fig. 2.7 Variation of ln (c/1 - c) as c varies from 0 to 1.

fraction of reduced ions and (1-c) is the concentration of the oxidised species. Thus according to expression 2.7 the thermopower of such a system would be large and negative at small values of c reducing to zero at $c=\frac{1}{2}$ and increasing positively to large values when c is close to unity. This is illustrated in Figure. 2.7.

Eqn. 2.7 is derived for the case where none of the carriers are localised i.e. at a sufficiently high temperature for all of the carriers to be able to hop from one site to another by thermal activation. Heikes and Ure[21] point out that it should be equally valid at lower tempteratures if c is interpreted as the fraction of lattice sites that have carriers which are free to hop.

2.5 POLARON FORMATION AND TRANSPORT

Polaron formation occurs when the time that a carrier resides on each lattice site is sufficiently long in relation to the lattice vibrational period for the lattice to relax under the influence of the electrostatic potential of the carrier. Figure (2.8a) shows a simple ionic lattice and Figure (2.8b) shows the same lattice with the addition of an electron to a positive site. The surrounding atoms tend to displace in response to the presence of the electron and the electron with its surrounding "cloud" of displaced atoms is known as a "polaron". The carrier is self-trapped within its own potential well and behaves as a particle consisting of an electron and a phonon combined.

Polarons are usually classified as being "large" or "small". A large polaron is one where the electron overlap is large compared to its binding energy, resulting in a lattice distortion which extends

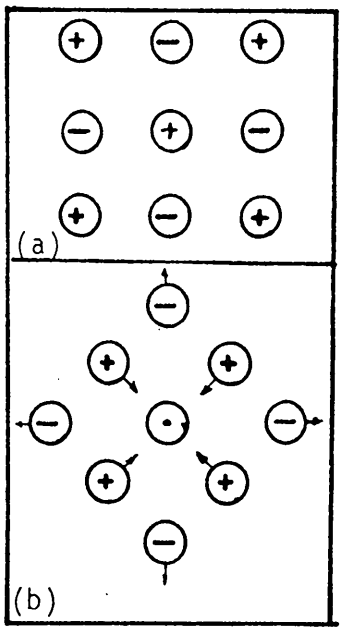

Fig. 2.8 (a) shows a section of an ionic lattice, while (b) shows the readjustment of the positions of the ions in response to an excess electron present on the central positive ion (after Emin, Ref. 60).

over several lattice sites. When the opposite conditions occur the polaron is tightly bound and the extent of the lattice distortion becomes comparable to a lattice spacing resulting in a small polaron. The formation of small polarons can occur in materials where there are strong electron-lattice interactions and also when carriers are strongly localised.

In materials where polarons are formed two mechanisms of conduction are possible. Firstly consider that charge carriers and their associated lattice deformations may reside on any site. These configurations are degenerate with each other and the proper states of the system are linear combinations of Bloch waves, consequently they may form a "polaron conduction band". In this case carriers are free to move through the lattice with exact conservation of lattice energy; thus conductivity will be independent of temperature. Secondly the interaction between lattice waves and the deformation potential of the polaron can give rise to a "hopping" mechanism of charge transfer. Figures 2.9 a,b and c show this schematically. Figure 2.9a illustrates an excess charge on a lattice site; the length of the vertical line represents the strength of the deformation potential round the carrier. If a lattice wave interacts with this deformation potential causing the wave function of the occupied site and the adjacent one to become the same (Figure 2.9b) the carrier can transfer to the next site as they are momentarily degenerate with each other (Figure 2.9c) shows the carrier in equilibrium on the next site. This second method of charge transport can only occur when the lattice vibrations are of sufficient amplitude, i.e. at temperatures above one half the Debye temperature. Holstein[24] makes detailed calculations of this

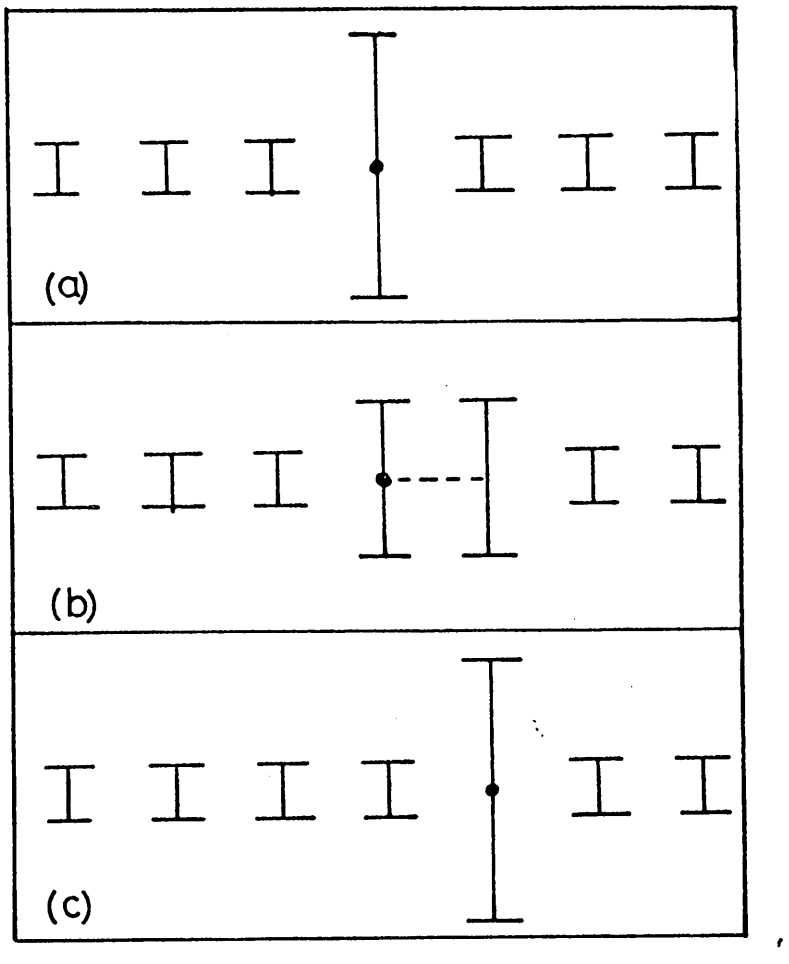

Fig. 2.9 The small-polaron jump process (after Emin, Ref. 60).

behaviour in a one-dimensional molecular crystal consisting of a linear chain of diatomic molecules with the electron orbitals centred on these molecules. The separation between the nuclei of the molecules is allowed to vary but the distances between the centres of gravity of the molecules is fixed. The temperature dependence of the mobility as predicted from Holstein's small polaron treatment is shown in Figure 2.10. A minimium occurs at approximately half the Debye temperature ($\frac{\theta_D}{2}$), the transition temperature between the two different conduction mechanisms. Above this temperature the main mechanism of charge transport is that of electron hopping induced by interchange of phonon energy between the carrier and the lattice. Below this temperature charge transport occurs within a polaron band characterised by exact conservation of the lattice energy. The conductivity of a crystalline material where charge transport occurs by the motion of small polarons will have an activation energy (W_H), the hopping activation energy above $\frac{\theta_D}{2}$, while below this temperature the conductivity will be un-activated as conduction occurs within a polaron band.

It should be noted at this point that the concept of polaron formation is applicable to a wide range of materials, not just the transition-metal oxides. The name "polaron" arises from the early consideration by Mott and Gurney[25] of self-trapping of a carrier in ionic (or polar) materials but the concept is applicable to other materials. In fact the best experimental evidence for the existance of self-trapped carriers is to be found in the data on ortho-rhombic sulphur obtained by Gibbons and Spear[26]. Other examples are found in realgar (As_4S_4)[27] and solid N_2 and O_2[28]. Of the transition

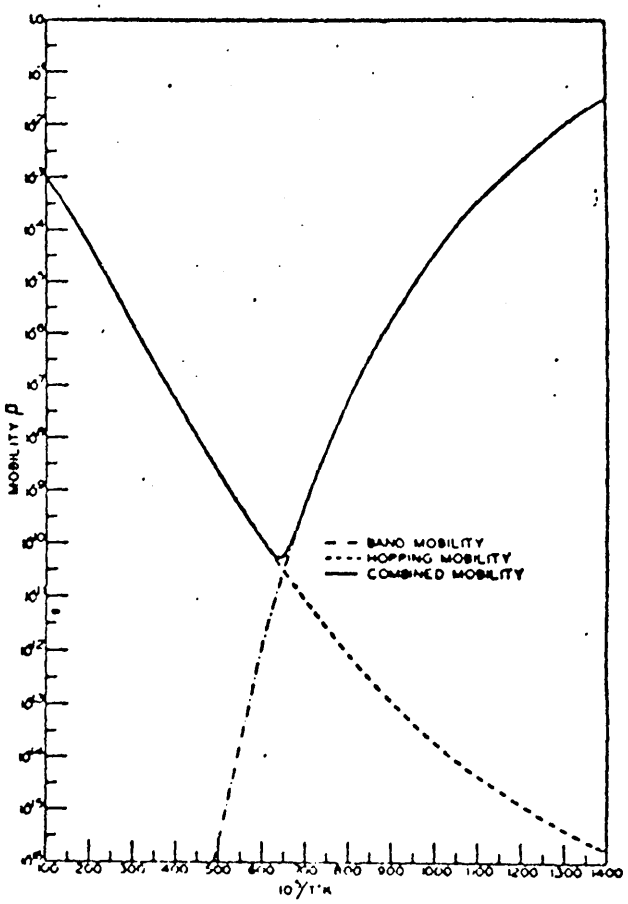

Fig. 2.10 Behaviour of Mobility as a function of temperature for a small polaron (after Holstein, Ref. 24).

metal oxides, p-type MnO and TiO_2 are most likely small polaron conductors.

2.6 EXPERIMENTAL DATA ON CONDUCTION IN TRANSITION-METAL OXIDE CRYSTALS

Austin and Mott[22] show data on the variation of resistivity with temperature in crystalline lithium doped NiO. This is reproduced in Figure 2.11. At temperatures above 100K the resistivity has a constant activation energy of 0.2 to 0.4 eV, dependent upon the doping level; while below 100K the octivation energy drops slowly from $\sim$ 0.05 eV to $\sim$ 0.004 eV at 10K. Austin and Mott[22] interpret the transition to the lower activation energy on the onset of impurity conduction arising from the presence of compensating donor centres (possibly oxygen vacancies) which give up electrons to the Li^+ Ni^{3+} acceptors. It is suggested that the continuous decrease in activation energy to the lowest temperatures is due to the occurence of variable range hopping in the impurity states.

Bosman and van Daal[29] report data on the variation of resistivity with temperature in a number of crystalline transition-metal oxides. Figure 2.12 illustrates their data on lithium doped CoO, MnO, NiO and Fe_2O_3. The samples of MnO and CoO show a constant activation energy to very high resistivity values while the NiO and Fe_2O_3 show a decrease in activation energy with temperature, which Bosman and van Daal[29] attribute to impurity conduction. This different behaviour stems from the dissimiliar properties of the impurity centres. In CoO and MnO dielectric loss measurements have shown that the bound hole around the Li ion has a high activation energy for movement (CoO $\simeq$ 0.2 eV; MnO $\simeq$ 0.3 eV) resulting in very small bound-carrier

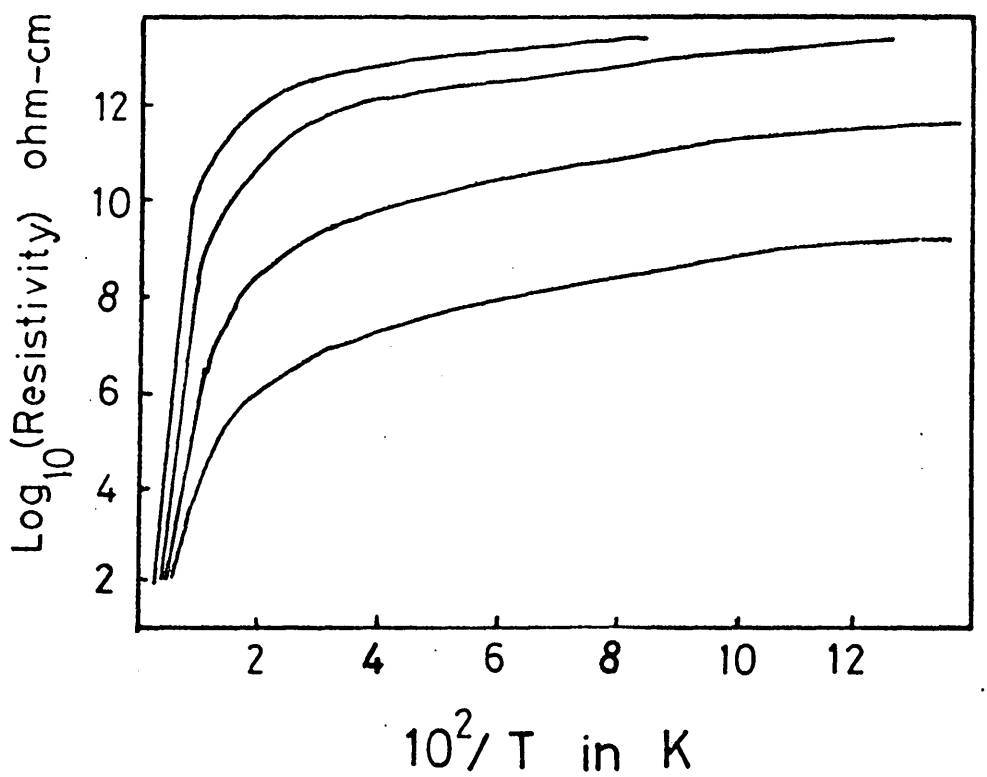

Fig. 2.11 Temperature dependence of conductivity for Li doped NiO (after Austin and Mott, Ref. 22).

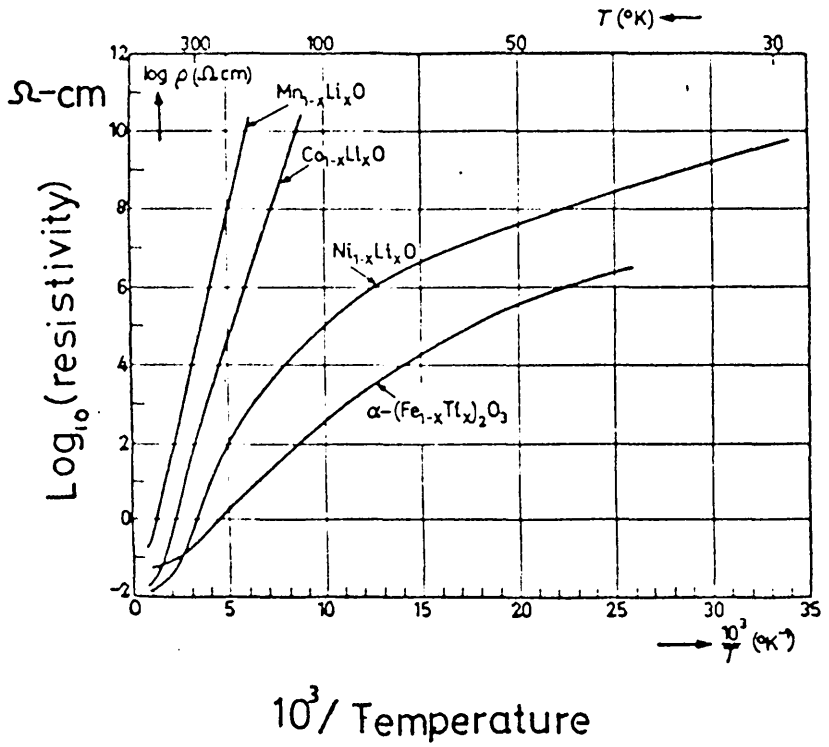

Fig. 2.12 Temperature dependence of conductivity in Li doped CoO, MnO, NiO and Fe_2O_3 (after Bosman and van Daal, Ref. 29).

mobilities at low temperatures, compared to those of NiO and Fe_2O_3. As a result it is expected that impurity conduction will be severely limited in CoO and MnO compared with NiO and Fe_2O_3.

van Daal[30] concludes that free charge carriers in NiO and CoO can be successfully described on the basis of a large polaron band model; i.e. one where the extent of the lattice deformation is greater than one lattice spacing, while bound carriers can be described as small polarons. van Daal[30] discounts the possibility of charge transport in NiO and CoO by small polarons on the basis of the behaviour of thermopower at high temperatures ($\simeq$ 1000K). In the low temperature regime, he suggests that small polaron band transport is impossible because of the energy fluctuations between adjacent sites. Such fluctuations arise from the random distribution of charged majority and minority centres and effectively prevent the formation of a polaron band.

Recent arguments by Emin[31] have raised the question of whether or not a small polaron hopping mechanism can occur at high temperatures In NiO and CoO. Previously the drift mobilities of NiO and CoO were considered to be too large to be attributed to the hopping of polarons. Emin[31] shows that the mobility of small polarons is greatly increased if account is taken of the correlation between successive hops of the polaron.

CHAPTER III : PREPARATION AND STRUCTURE OF TRANSITION METAL OXIDE GLASSES

3.1 AMORPHOUS TRANSITION METAL OXIDES

Pure transition metal oxides will not form a glass under normal quenching conditions, e.g. casting onto a chilled metal slab, but amorphous films of VO_2, V_2O_3 and V_2O_5 have been prepared by, for example, R.F. sputtering and vapour phase deposition. Kennedy et al [32] have reported unsuccessful attempts to prepare V_2O_5 glass by casting the melt onto a copper slab cooled to liquid nitrogen temperature, but thin films of V_2O_5 were prepared by condensing the vapour onto cold substrates in vacuum and the absence of crystallinity was confirmed by microscopic examination in polarised light and by electron diffraction. The conductivity at room temperature was about $10^{-4}\Omega^{-1}m^{-1}$ but no information was given about the variation of conductivity with temperature. The value of conductivity was surprisingly low compared to estimates of around $1.6 \times 10^{-2}\Omega^{-1}.m^{-1}$, based on the extrapolation of the conductivity-composition curves of various glass systems (See later). Kennedy et al, attribute this to the closely stoichometric composition of their films but state that they did not carry out chemical analysis of the films because of the small amounts of material available.

Kennedy and Mackenzie[33] have reported the preparation of amorphous films of VO_2 and V_2O_3 by R.F. sputtering onto cold substrates but these films did not exhibit the metal-semiconductor transition

found in their crystalline counterparts. Figures 1(a) and (b) show the variation of resistivity with temperature for amorphous V_2O_3 and VO_2 respectively. For VO_2 at temperatures below 68°C the resistivity of the amorphous film is three orders of magnitude lower than that of the crystalline solid. The observed resistivity corresponds more closely to that of the high temperature metallic phase although the temperature coefficient is not metallic.

For amorphous V_2O_3, (Figure 1(b)) the resistivity corresponds more closely to that of the high temperature crystalline phase. It is suggested that this is because the films were formed by rapid quenching onto substrates above the transition temperature and consequently retain the short range structural order of the high temperature phase. The electrical conductivity is probably governed primarily by the short range order of the films, thus very low resistivity amorphous films are formed.

3.2 TRANSITION METAL OXIDE GLASS SYSTEMS

3.2.1 Classification of Transition Metal Oxide Glasses

It was mentioned in Section 3.1 that pure transition metal oxides will not form glass by normal quenching. Never the less, many transition metal oxides are capable of forming glasses when combined with "glass-forming" oxides and in some cases the glass-forming oxide need only be present in small quantities (e.g. a few mole percent) so that the transition metal oxide is the predominant constituent. The oxides TiO_2, V_2O_3, Fe_2O_3 and CuO are known for example to form glasses over a wide range of composition when combined with oxides such as P_2O_5, TeO_2 B_2O_3 and GeO_2. Mixtures of V_2O_5 - BaO and V_2O_5 - PbO are known[34] to

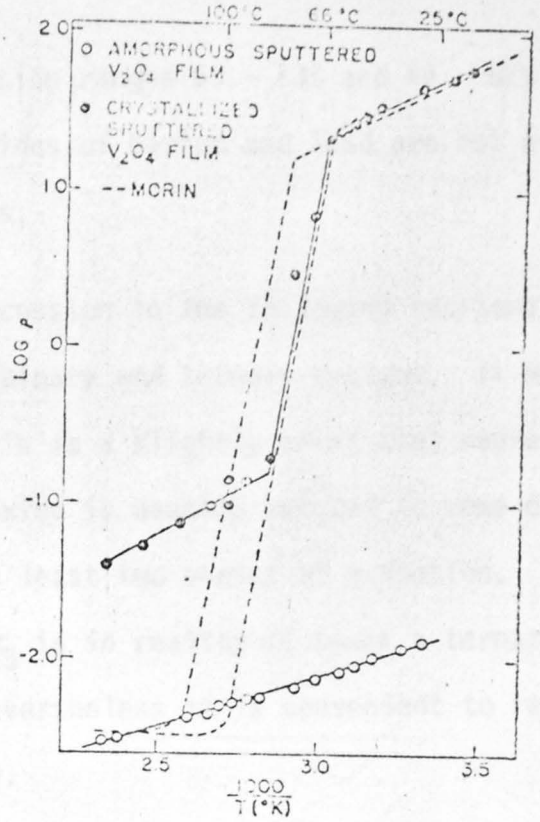

Log resistivity versus reciprocal temperature for crystalline and amorphous V_2O_4.

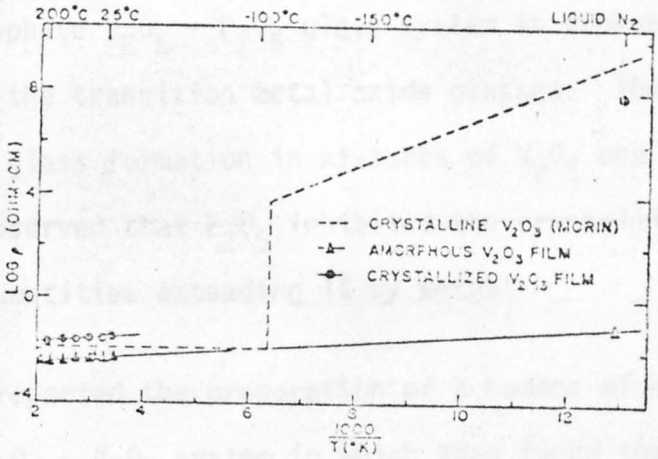

Log resistivity versus reciprocal temperature for crystalline and amorphous V_2O_3.

Fig. 3.1 Temperature dependence of conductivity for both crystalline and amorphous V_2O_3 and V_2O_4 (after Kennedy and Mackenzie, Ref. 33).

form glasses, in the composition ranges 63 - 73% and 46 - 62% V_2O_5 respectively although the oxides of barium and lead are not normally considered to be glassformers.

For the purposes of discussion in the following sections the glasses are classified into binary and ternary systems. It must be remembered, however, that this is a slightly artificial representation since the transition metal oxide is usually reduced to some extent and is present, therefore, in at least two states of oxidation. Thus the "binary" system $V_2O_{(5-x)}$ P_2O_5 is in reality *at least* a ternary system, i.e. V_2O_5 - V_2O_4 - P_2O_5. Nevertheless it is convenient to regard such systems notionally as binary.

3.2.2 Binary Glass Systems Containing Transition Metal Ions

The vanadium-phosphate V_2O_5 - P_2O_5 glass system is probably the most closely studied of the transition metal oxide glasses. The first recorded observation of glass formation in mixtures of V_2O_5 and P_2O_5 was by Roscoe[35] who observed that P_2O_5 inhibited the crystallisation of V_2O_5 if present in quantities exceeding 1% by weight

Denton[34] et al reported the preparation of a number of vanadate glasses including the V_2O_5 - P_2O_5 system in which they found that glasses are readily formed over the range 0 to 95 mole percent V_2O_5. They also reported making vanadate glasses with the glass formers GeO_2, TeO_2 and As_2O_3. Table 3.1 shows the approximate composition ranges of glass formation for each of the systems investigated by Denton et al . Included in this table are data on glass formation with the oxides BaO and PbO which, as mentioned earlier, are normally considered to be intermediate rather than glass-forming oxides.

Glass System	Approximate range of V_2O_5 content forming glass
V_2O_5 - P_2O_5	< 95%
V_2O_5 - GeO_2	10% - 75%
V_2O_5 - TeO_2	10% - 60%
V_2O_5 - As_2O_3	> 50%
V_2O_5 - BaO	63% - 73%
V_2O_5 - PbO	46% - 62%

Table 3.1 Composition range for glass formation of various vanadate glasses as determined by Denton et. al. (Ref. 34).

Magnetite (Fe_2O_3) will form a glass when combined with a glass-former such as P_2O_5. The preparation of phosphate glasses containing 55 molar percent FeOx was reported by Hansen[36], Hansen and Splann[37] and by Kinser[38].

Sayer and Mansingh[39] have described the preparation of phosphate glasses containing 50 molar per cent of each of the 3d transition metal oxides except chromium, ie, TiO_2. V_2O_5, Mn_3O_4, Fe_2O_3, CoO, NiO and CuO. They also prepared phosphate glasses containing molybdenum and tungsten oxides, ie, MoO_3 and WO_3, the existence of which was noted earlier by Linsley[40].

3.2.3 Ternary Glass Systems Containing Transition-Metal Ions

A wide variety of three component glasses containing a transition-metal oxide as one component have been prepared. A typical ternary system would be one containing a transition-metal oxide, a glass-forming oxide and a modifier or an intermediate oxide, eg, V_2O_5 - P_2O_5 - Na_2O and V_2O_5 - P_2O_5 - CaO respectively.

Denton et al[34] investigated the preparation of a V_2O_5 - TeO_2 - BaO glass and outlined its physical properties. Kennedy and Mackenzie[41] have prepared glasses in the systems V_2O_5 - B_2O_3 - CaO and V_2O_5 - P_2O_5 - CaO and have investigated the effect of the network forming oxide on the conductivity of the glass. The alkaline earth oxide CaO was included since glass formation is difficult in the binary system V_2O_5 - B_2O_3.

The work of Dimitriev et al[42] illustrates the wide range of glass formation in the system V_2O_5 - TeO_2 - CdO. Figure 3.2 shows

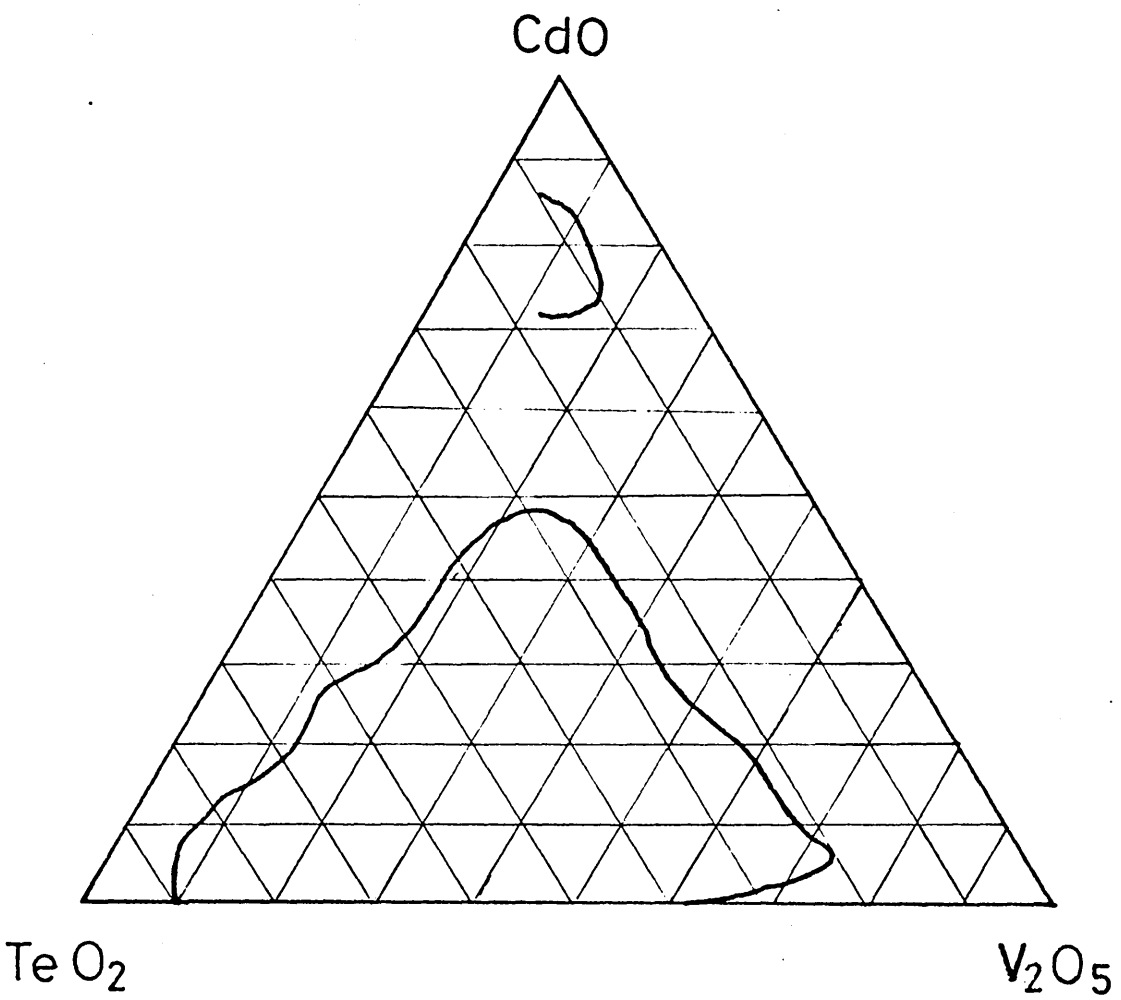

Fig. 3.2 Ternary phase diagram showing glass formation in the V_2O_5 - TeO_2 - CdO system (after Dimitriev et. al., Ref. 42).

the glass forming regions as determined by quenchingbatches of two grams. Two regions of glass formation can be distinguished, the first at lower (<50 m.p.c.) CdO contents and the second at high (>75 m.p.c.) CdO contents. This is attributed to the CdO acting as a network modifier when present in low concentrations, leading to the break up of the glass network as the proportion of CdO is increased. As an explanation of the glass forming region at high concentrations of CdO Dimitriev[42] et al postulate that CdO can act as a glass former when present in sufficient concentration.

Glass formation in the system V_2O_5 - TeO_2 - CaO has been reported by Dimitriev[43] et al . Glasses were made in the range 20 to 65 percent V_2O_5 and incorporating up to 25 molar percent CaO; beyond that concentration of CaO the glasses devitrified.

Drake[44] et al have reported the preparation of copper-calcium phosphate (CuO - CaO - P_2O_5) and copper calcium borate (CuO - CaO - B_2O_3) glasses in their studies of electrical switching behaviour. Certain compositions including 35 CuO - 5CaO - 60 P_2O_5 and xCuO - (45 - x) CaO - 55 B_2O_3 were prepared for electrical measurements but the glass forming properties of the systems are not reported *per se*.

Nester and Kingery[23] described the preparation and electrical properties of glasses in the system V_2O_5 - P_2O_5 - NaO. These materials were prepared in approximately twenty gram batches using V_2O_5, H_3PO_4 and Na_2CO_3 as the starting materials and quenched onto steel plates heated to 200°C prior to being annealed.

Munakata[45] has reported the preparation of glasses in the system

V_2O_5 - P_2O_5 - BaO and this was perhaps the first systematic study of the effect of variations in the ratio of oxidised to reduced transition metal ions. Munakata found that by melting under normal atmospheric conditions the ratio of V^{4+}: V total could be varied by changing the concentration of BaO.

3.3 THE TRANSITION METAL ION VALENCE STATE

3.3.1 The Valence State of Transition-Metal Ions in Glass

In transition-metal oxide glasses a proportion of the transition-metal ions are normally reduced to lower valence states during the melting process. The degree of reduction can be controlled either by incorporating an oxidising or reducing agent to the melt or by controlling the furnace atmosphere.

In Chapter II it was pointed out that electrical conduction in transition-metal oxide crystals is thought to occur by the hopping of carriers between high and low valence transition-metal ions. The same is true for transition-metal oxide glasses and obviously an exact measurement of the number, and valence state of the transition-metal ions in the glass is necessary to enable an estimate of the carrier concentration in the glass to be made. Methods by which this can be done are described later in this chapter.

Electron spin resonance (E.S.R.) data on vanadium phosphate glasses shown by Lynch[46] et al suggest that the concentration of vanadium valence states lower than four is small. E.S.R. was used to measure the concentration of V^{4+} ions in a 80 molar percent V_2O_5 - 20 molar percent P_2O_5 glass by a comparison of the intensity of the resonance

due to the V^{4+} ions with that of a sample of anhydrous copper sulphate of known spin concentration. The predominately single line resonances observed suggest that the concentration of valence states below the first reduced state is low, since V^{3+}, V^{2+} and V^{1+} are expected to give signals with appreciable fine structure. Lynch[46] et al also found that the ratio of high to low vanadium valence states measured by E.S.R. agreed reasonably well with that obtained from wet chemical analysis, which, assuming that the wet chemical analysis data is a measure of the total reduced vanadium content, regardless of valence state, suggests that little vanadium is in valence states other than four and five. It is also worth noting that according to Kitaigorodskii[47] the similaneous presence of V^{3+} and V^{5+} states is unlikely at high vanadium concentrations and at high temperatures, such as those used for glass melting, since the auto-oxidation reaction

$$V_2O_5 + V_2O_3 \rightarrow 2V_2O_4$$

is likely to occur under such conditions.

3.3.2 The Influence of Vanadium Valence State on Glass Formation

In the V_2O_5 - P_2O_5 system the range of glass formation, by normal quenching techniques, is usually quoted as 0 to $\sim$ 95 mole percent V_2O_5. The degree of reduction of the vanadium does, however, affect the glass-forming ability of a particular composition and thus is best illustrated by considering the ternary system V_2O_5 - V_2O_4 - P_2O_5. The approximate glass-forming region, in the appropriate ternary diagram, is shown in Figure (3.3). This was constructed from data given by Linsley[40] and it corresponds to the preparation of glass in quantities of several grams by normal quenching of the melt. Figure (3.3) shows

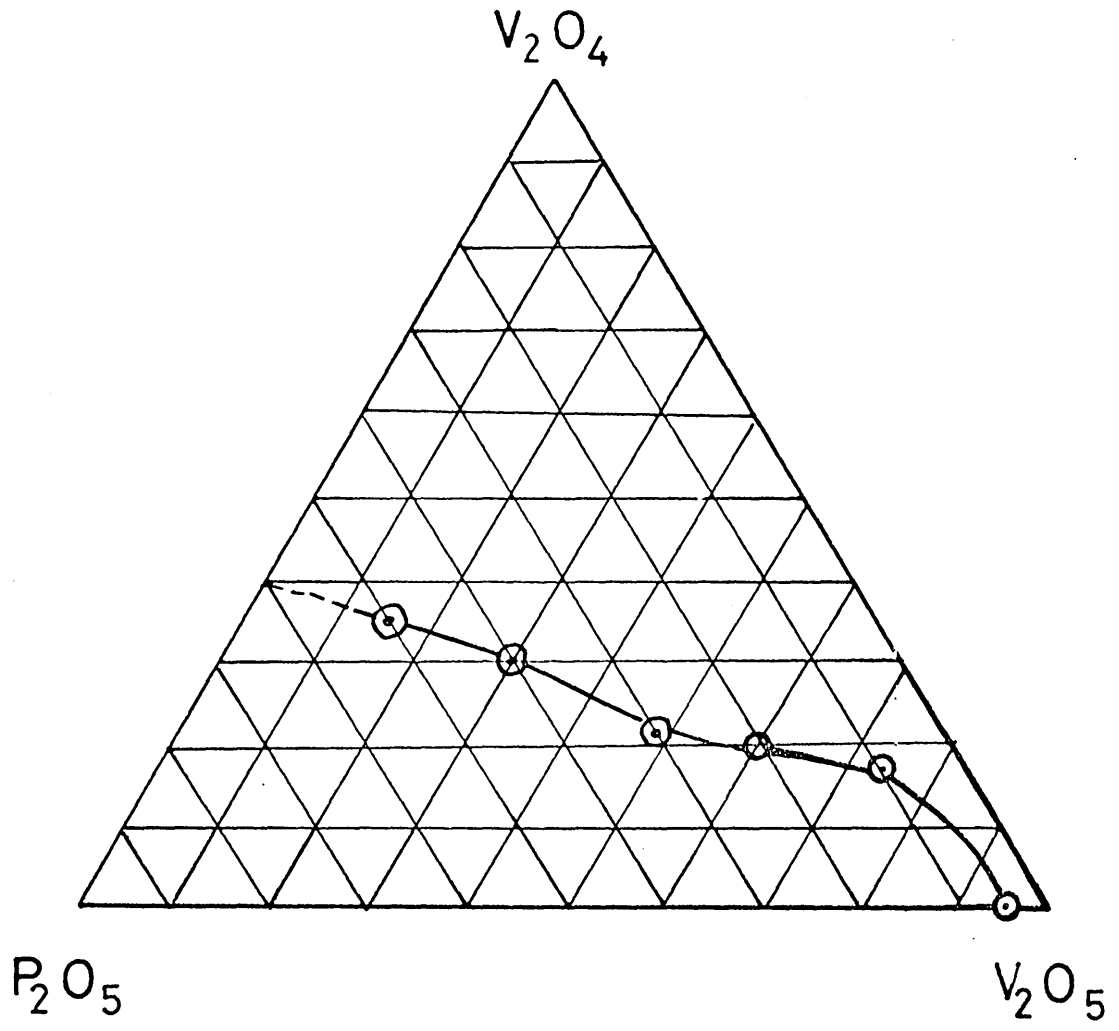

Fig. 3.3 Ternary phase diagram showing glass formation in the V_2O_5 - V_2O_4 - P_2O_5 system using data given by Linsley, (Ref. 40).

clearly that the greater the total vanadium concentration the smaller the degree of reduction which can be incorporated in the glass. Linsley's data is based on the probably justifiable assumption that all the reduced vanadium occurs as V^{4+}; the presence of lower valence states might be expected to limit glass formation even more. There is insufficient information to construct diagrams similar to Figure (3.3) for other vanadate systems but it is almost certainly reasonable to generalise and conclude that in all cases the greater the total vanadium content the smaller the degree of reduction which can be incorporated without devitrification. In fact, the generalization can probably be broadened to encompass all transition-metal oxide glasses.

3.4 PREPARATION AND CHEMICAL ANALYSIS

3.4.1 Valence Ratio Control

The vanadate glasses are prepared by melting weighed amounts of powdered vanadium pentoxide (V_2O_5) and a glass forming oxide which have been intimately mixed together. After the melt has received any chemical treatment required to control the oxidation-reduction ratio it is quenched by some means, such as casting on cold metal plates, to form glass.

The major difficulty is *control* of the oxidation-reduction ratio in the glass. This can be done in two ways, either by controlling the furnace atmosphere or by adding an oxidising or reducing agent to the melt. To oxidise the melt, i.e. prevent reduction when V_2O_5 is being melted, oxygen is bubbled through the melt. In practice the problem is usually one of reducing the melt since V_2O_5 is normally used as the starting material for glass preparation. Munakata[45] controlled

the proportion of reduced-vanadium by altering the proportion of BaO and P_2O_5 in the ternary system 60% V_2O_5 .x BaO. (40 - x) P_2O_5. This method has the disadvantage of introducing a third oxide (BaO in this case), which will affect glass-forming properties of the V_2O_5 - P_2O_5 system and possibly complicate the conduction mechanism in the glass.

To overcome this problem Linsley[40] added powdered sucrose to the starting materials. On melting this reacts with a proportion of the oxygen in the V_2O_5 to give V_2O_4, carbon dioxide and water. Reduction could also be achieved, of course, by adding metallic vanadium to the melt and Linsley sometimes used this procedure in addition to reduction with sucrose. Few other systematic studies have been made of the effect of varying the vanadium valence ratio while not altering the composition in any other way. Another method of valence ratio control which does not introduce any additional components to the melt, and is applicable to glass systems such as V_2O_5 - TeO_2, is to add the element which on oxidation gives the glass forming oxide. In the case of tellurium the raction

$$2\ V_2O_5 + Te \rightarrow 2\ V_2O_4 + TeO_2$$

occurs resulting in a proportion of the vanadium in the glass being reduced and the formation of additional TeO_2. This method was used for valence state control in the present work and is described in greater detail in Chapter V.

3.4.2 Valence Ratio Determination

Accurate determination of the concentrations of different valence transition-metal ions in a transition-metal oxide glass is

important for two reasons; firstly, the concentration of the reduced ion has an effect on the glass-forming properties (See section 3.3.2). Secondly, theories of mixed valence semiconduction require a knowledge of the ratio occupied to unoccupied transition-metal ion sites if comparison is to be made between theoretical analyses and experimental data.

A number of different methods can be used for the determination of the redox ratio including wet chemical analysis, electron spin resonance and magnetic susceptibility.

3.4.2.1 Wet Chemical Analysis

The method most commonly used for the measurement of valence ratio is titration of a solution prepared from the powdered glass, against standardised acidified potassium permanganate ($KMn\ O_4$). In a vanadate glass for instance the four-valent vanadium undergoes the reaction:-

$$5V^{4+} + Mn^{7+} \rightarrow 5V^{5+} + Mn^{2+}$$

resulting in the decolorisation of the permanganate solution. This permanganate titre gives an estimate of the reduced vanadium content of the solution. To measure the total vanadium content all of the vanadium is reduced to the V^{4+} state by bubbling SO_2 gas through the solution and then titrating against $KMnO_4$ as before. This titre gives the total vanadium content of the solution.

3.4.2.2 Spectro-photometric Analysis

In glasses containing the glassformer TeO_2 it is not possible

to use chemical analysis techniques based on oxidation and reduction of the transition-metal ions, because it is known that tellurium can also exist in different valency states in glass. On titration with $KMnO_4$ the lower valency states of tellurium are oxidised along with those of vanadium and interfere with the end-point of the titration. To avoid this difficulty a spectro-photometric method has been used in the present work.

Solutions which contain V^{5+} ions have an absorption peak at 380 nm while those containing V^{4+} ions have an absorption peak at 790 nm. The two peaks do not interfere with each other in solutions containing mixtures of the ions. By measuring the optical absorption of a solution containing V^{4+} and V^{5+} ions at 380 nm and 790 nm respectively, and comparing these with the absorptions of standard solutions of the ions it is possible to determine the concentration of V^{4+} and V^{5+} ions in the solution prepared from the glass. This method has the disadvantage, common to all of the wet chemical analysis methods, of requiring dissolution of the glass in dilute acid with the attendent danger of altering the transition-metal ion valence state, but it has the advantage that the colourless and insoluble tellurium oxide does not interfere with the final result. This method of vanadium valence ratio analysis is described in more detail in Chapter V.

3.4.2.3 Electron Spin Resonance

Methods of analysis based on electron spin resonance (E.S.R.) have the advantage of measuring, in situ, the reduced transition-metal ion content of the glass, without altering the structure in any way.

In the case of a vanadate glass for example, V^{4+} ions are paramagnetic and give strong E.S.R. signals while V^{5+} ions are diamagnetic. Measurement of the intensity of the resonance peak gives an indication of the concentration of V^{4+} ions. The technique used by Lynch *et al*[46] was to compare the area under the resonance peak due to the V^{4+} ions with the area under a similar peak due to a known concentration of Cu^{2+} ions in hydrated copper sulphate $CuSO_4\ 5H_2O$.

E.S.R. methods can be used at low temperature. Lynch[46] *et al* find that the paramagnetic spin concentration is independent of temperature and conclude that the temperature defendence of conductivity arises from variation of the mobility with temperature. Landsberger and Bray[48] have used E.S.R. analysis to estimate the valence ratio in V_2O_5-P_2O_5 glasses and find reasonable agreement with wet chemical analysis data obtained by Mackenzie[49] on glasses of similar compositions. It should be noted, however, that Landsberger and Bray[48] did not carry out wet chemical analysis on their own glasses and since they used different glass preparation conditions from Mackenzie, the assumption that their glasses have the same vanadium valence ratios is questionable.

E.S.R. analysis has the disadvantage over wet chemical analysis in that it is not as accurate in its estimation of the valence ratio. Landsberger and Bray[48] quote an accuracy of $\pm$ 20% for their results which is surprisingly good since they used powdered glass samples for the analysis. To estimate the spin concentration in a powdered glass sample a packing factor must also be determined for the powder. This is difficult to do accurately since it will be strongly dependent upon the degree to which the sample is compacted into the tube.

E.S.R. is probably the only method to use when a measure of the valence ratio is required on a solid sample without destroying it, but if accuracy is the prime consideration wet chemical analysis is probably the best method.

3.5 STRUCTURE OF VANADATE GLASSES

3.5.1 Local Structure (S.R.O.)

It was pointed out in Chapter I that glasses retain features of crystalline structure in their short range order (S.R.O.). This local structure can be determined by X-ray absorption spectroscopy and X-ray diffraction infra-red absorption spectroscopy, E.S.R. or N.M.R. data either independently or in conjunction with each other. Studies of this kind show that vanadium ions in glass have the five fold coordinated structure characteristic of crystalline V_2O_5, as illustrated in Figure (3.4).

3.5.1.1 X-ray Absorption Edge Spectroscopy

Harper and McMillan[50] report X-ray absorption data on V_2O_5 glasses with V_2O_5 contents ranging from 10 to 90 m.p.c. They conclude that the V^{4+} ions in these glasses are assymetrically coordinated and suggest that at lower vanadium oxide contents a structural modification occurs involving a change in the coordination of the vanadium. It is noted that this coincides with a change in the E.S.R. spectra of the glasses when the V_2O_5 content falls below 50 m.p.c.

3.5.1.2 Infra-red Absorption

Infra-red absorption spectra give information on the local

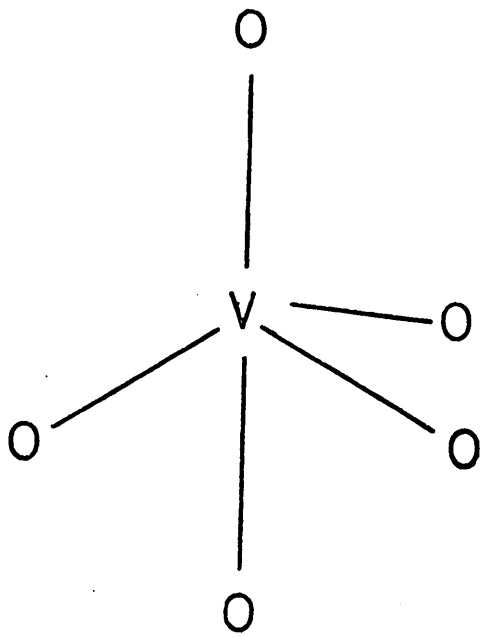

Fig. 3.4 Coordination diagram for crystalline V_2O_5 (after Landsberger and Bray, Ref. 48).

differences between electron site energies, i.e. $W_D < kT$ ($T \simeq 77k$) or electrons are localised on sites which differ in energy from the average by an amount such that $W_D > kT$ ($T \simeq 400k$). In the first case the site energies must be identical within 0.008eV (kT at 77k) and for the second case the amount of redistribution of site energies over the temperature range 77 to 400k is small. Because of the inherent disordered nature of the glass Lynch et al conclude that the second interpretation is more valid and point out that this is consistent with the observed behaviour of the temperature dependence of the low-temperature a.c. and d.c. conductivities.

Lynch[46] et al also note that the absence of any long range order in the glass is confirmed by the lack of orientation dependence of the E.S.R. signals.

3.5.2 The Macrostructure of Vanadate Glass

3.5.2.1 The Chemical Structure of Vanadate Glasses

The oxides of vanadium and phosphorous are known to form long chain polymeric compounds, both individually and in mixtures, and there is evidence that in V_2O_5 - P_2O_5 glasses long chain polymeric vanadophosphate complexes are formed. Ohashi[53] reports the use of paper chromatography to study nature of the structural complexes formed in the Na - V - P - O glass system.

The vanadium is regarded as being mostly in the V^{5+} state but with some V^{4+} present. Only the V^{5+} ions can form structural complexes and Ohashi suggests that the V^{4+} acts as a network modifier in the form of the vanadyl ion VO^{2+}. The chromatographic data show that

the quantity of long chain phosphates increases as the phosphate content of the glass increases. On the assumption that five valent vanadium replaces phosphorous in the phosphate chain, the structure shown in Figure (3.5) is postulated for the long chain molecules in the V_2O_5 - P_2O_5 glass system.

3.5.2.2 Phase separation

Phase separation has been reported in many vanadate glasses where systematic studies have been made of macrostructure. Scanning electron microscopy was used by Kinser and Wilson[54] to study the macrostructural features of the vanadium phosphate glass system and indicated extensive separation into two glassy phases, with maximum phase separation occuring at the extremes of the glass-forming region. It also appears that glasses may be structurally more homogeneous near the conductivity maximum while those removed from the conductivity maximum are more heterogenous. This observation could be the result of a maximum miscibility of V^{4+} and V^{5+} along the maximum conductivity line in the Gibbs triangle.

According to Bogomolova[55] et al, their E.S.R. and scanning electron microscopy data can be interpreted to show the V_2O_5 - P_2O_5 - CuO glasses are phase separated into regions of high and low conductivity. Scanning electron micrographs reveal two phases which correspond to the high and low conductivity regions. When paramagnetic V^{4+} ions appear in more than one phase of an inhomogeneous glass a complex E.S.R. spectrum is expected consisting of the superposition of the spectra of the V^{4+} ions in the different phases. No such complex spectrum is observed

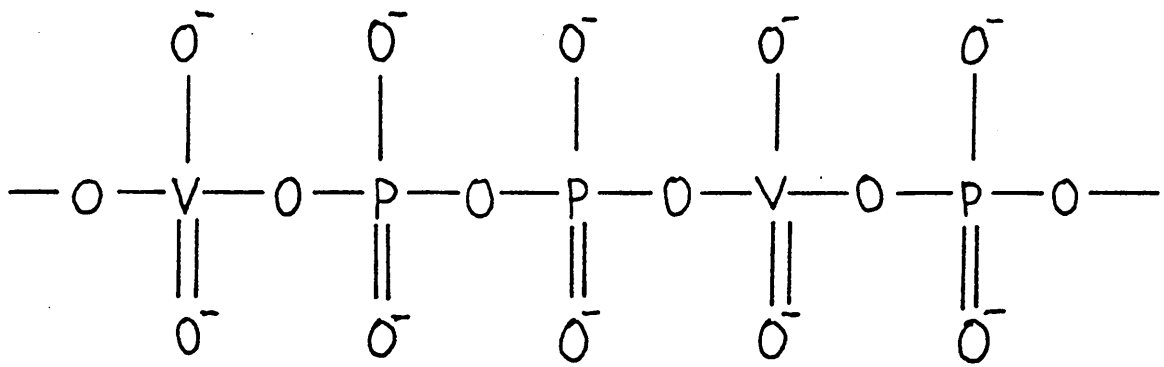

Fig. 3.5 Chain structure postulated by Ohashi for V_2O_5 - P_2O_5 glasses with up to 50% V_2O_5.

and the conclusion is that all the V^{4+} ions are contained in only one phase which is solely responsible for electronic conduction.

and the conclusion is that all the V^{4+} ions are contained in only one phase which is solely responsible for electronic conduction.

CHAPTER IV : REVIEW OF ELECTRONIC PROPERTIES OF TRANSITION-METAL OXIDE GLASSES

4.1 CONDUCTION IN TRANSITION-METAL OXIDE GLASSES

In Chapters I and II the elctronic properties of crystalline transition-metal oxides were discussed. This Chapter is concerned with the electronic properties of disordered transition-metal oxides systems, in particular, glasses containing the oxides of vanadium. These materials are narrow-band semiconductors and even when crystalline carrier localisation is an important feature. The effect of structural disorder is to increase localisation and to produce a spread in energy levels corresponding to the different site energies within the glassy network. Mott[56] likens the conduction process in such materials to that of impurity conduction in doped and compensated semiconductors. Figure 4.1 is a schematic representation of the energy band structure for this situation. The activation energy for a carrier to hop from site to site is $W = W_H + 1/2\ W_D$ where W_H is the energy required for the hop and W_D is the"disorder energy". Thus the effect of disorder is to require additional energy for carrier transfer from site to site.

Structural disorder has a direct effect on the temperature dependence of conductivity because of its influence on the activation energy, thus allowing for disorder the activation energy term, W, in equation 2.6 must be modified

$$\sigma = N \frac{e^2 a^2}{kT}\ c(1 - c)\,\nu\,\mathrm{Exp}\left(\frac{- W_H - \tfrac{1}{2}W_D}{kT}\right) \quad \ldots (4.1)$$

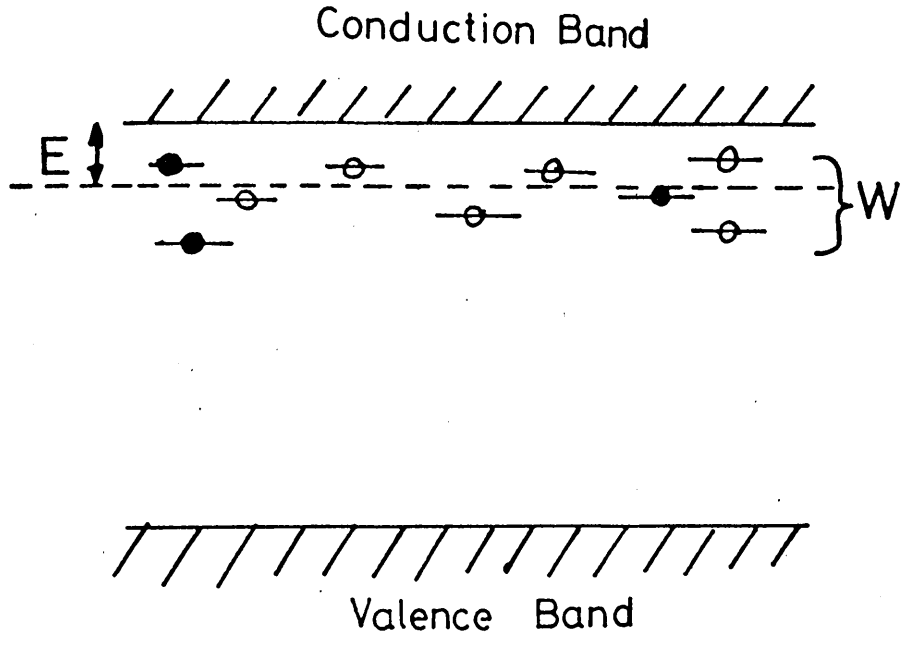

Fig. 4.1 Energy band model for transition metal oxide glasses (after Mott, Ref. 56).

Structural disorder does not appear to directly affect the dependence of conductivity on the ratio of high to low valence ions (c : 1-c) predicted from equation 2.6 although the position of the maximum in the conductivity-valence ratio relationship is displaced from the theoretically predicted value. Possible reasons for this are discussed in Section 4.2.2.1.

In section 2.5 it was seen that in a crystalline material, hopping only occurs at temperatures in excess of one half the Debye temperature, while at lower temperatures a transition occurred to a 'polaron band' conduction mechanism. In glasses, Schnakenberg[57] argues that band processes are impossible because of structural disorder ($W_D > kT$), hence the conductivity remains activated down to the lowest temperatures. Austin and Mott[22] show that in a glass containing transition-metal ions the conductivity is activated thus

$$W = W_H = 1/2\ W_D \qquad T > \frac{\theta}{2} \qquad \ldots (4.2)$$

$$W = W_D \qquad T < \frac{\theta_D}{4}$$

The experimental data on the oxide glasses show that this can only be partly true. At temperatures above $\frac{\theta_D}{2}$ the conductivity shows a constant activation energy, while below this temperature the activiation energy for conduction shows a continuous decrease down to the lowest temperatures for which data is available ($\triangleq$50k). Figure 4.2, for example, shows the data of Schmid[58] on V_2O_5 - P_2O_5 glasses. This type of behaviour is widely observed in transition-metal oxide glasses.

On the basis of the following assumptions Killias[59] predicted

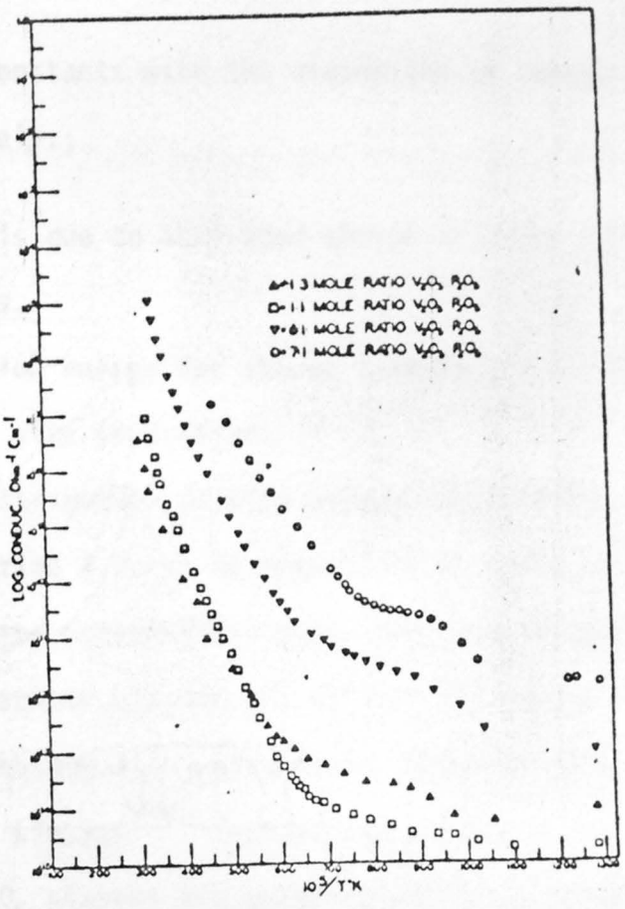

Fig. 4.2 Temperature dependence of conductivity in various V_2O_5 - P_2O_5 glasses as determined by Schmid (Ref. 58).

a temperature dependent activation energy of the form

$$W = \varepsilon_o \left(1 - \frac{\theta_R}{T}\right) \qquad \ldots (4.3)$$

where ε_o and θ_R are constants with the dimensions of energy and temperature respectively.;

a. conduction is due to activated charge transfer between atomic sites,

b. the activation energy for charge transfer is a linear function of site separation,

c. a random distribution of site separations exists.

The constants in equation 4.3 can be determined by means of a least squares fit to the experimental data. Killias fitted Hansen's[36] data on 40% Fe_2O_3 phosphate glasses and data of his own on 10% Fe_2O_3 phosphate glass to equation 4.3 and obtained values of 150k and 185k respectively for θ_R. Linsley[40] carried out a similar analysis on his data on V_2O_5 - P_2O_5 glasses and obtained values of around 50k for θ_R. Killias does not comment on the range of valadity for equation 4.3, but obviously it must be limited since it predicts a negative activiation energy when $T < \theta_R$.

Recent work by Emin[60] predicts a much less rapid decrease in the hopping activation energy with decreasing temperature and a W_H which is virtually constant down to $\frac{\theta_D}{3}$. The phonon assisted, two site, jump rate of carriers is calculated as a function of the Debye temperature. The jump rate (R) is related to the d.c. conductivity by the expression

$$\sigma = \frac{n e^2 a^2}{kT} \cdot R \qquad \ldots (4.4)$$

By comparison with equation 4.1 it is seen that the temperature dependence of the jump rate determines the conductivity temperature dependence. The graphical solution for the jump rate (given by Emin[60]) as a function of the Debye temperature (θ_D) is shown in Figure 4.3. This shows a high temperature region of constant activation energy down to a temperature of $T = \frac{\theta_D}{2}$ and a gradual decrease in slope as the temperature is reduced, caused by progressive phonon "freeze-out", down to temperatures of around $T = \frac{\theta_D}{8}$. This suggests that there is still an appreciable hopping contribution to conduction down to temperatures of 60 - 70k (if $\theta_D \simeq 500k$).

Schmid[58] presents arguments for small polaron conduction in glasses containing tansition-metal oxides and concludes that in the high temperarure region ($T > \frac{\theta_D}{2}$) carriers transfer from one site to another by means of simultaneous exchange of energy with the lattice, while in the low temperature region ($T < \frac{\theta_D}{4}$) carriers can transfer with exact conservation of the lattice energy. Schmid suggests that at low temperatures the individual energy levels resulting from disorder are sufficiently close to each other, in energy terms, for the very small amounts of thermal energy available to bring sites into coincidence with each other, allowing carriers to transfer with conservation of lattice energy. This arguement is difficult to accept because the random potential fluctuations produced by structural disorder are most likely to be greater than kT in the low temperature regime, effectively preventing band conduction from occuring. Other objections to Schmid's interpretation of the small polaron theory arise, in the high temperature regime, because it predicts a temperature dependent carrier concentration. This is contrary to experimental

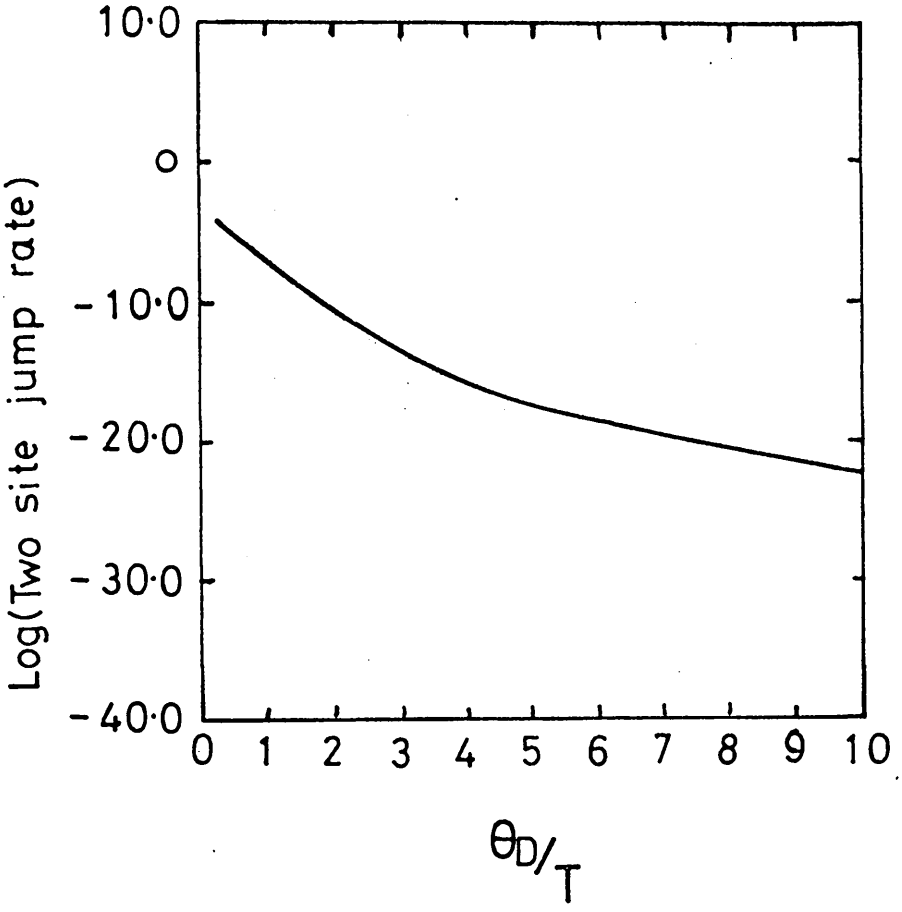

Fig. 4.3 Two site jump rate for carriers as a function of temperature (after Emin, Ref. 60).

evidence from thermopower and E.S.R., which indicate that the carrier concentration is constant with temperature.

4.2 BINARY VANADATE GLASS SYSTEMS

4.2.1 Temperature Dependence of d.c. Conductivity

Of all transition-metal oxide glasses investigated the electrical properties of the vanadates have probably been most widely studied, with the vanadium phosphates having received a large proportion of this attention. This is probably largely because of the good glass-forming properties of the system and the ease with which glasses with widely varying vanadium contents can be prepared. The first reported observations of the electrical properties of vanadate glasses are by Denton et al[34] who measured the temperature dependence of the d.c. conductivity and the thermopower of vanadate glasses containing P_2O_5, GeO_2, TeO_2, As_2O_3, BaO and PbO. Denton et al [34] concluded that they are all n-type semiconductors. The conductivity was measured over the range 300 to 400k and showed a temperature dependence of the form

$$\sigma = \sigma_o \text{ Exp } \frac{-W}{kT} \qquad \ldots (4.5)$$

where σ_o is a pre-exponential constant and W is an activation energy.

Nester and Kingery[23] report on the variation of conductivity of V_2O_5 - P_2O_5 glasses as a function of temperature over the range 100 to 300k and find a change in slope in the reciprical temperature variation of long-conductivity at temperatures below 250k. They attributed this to a change in conduction mechanism, but did not comment farther. Their data show a continuous decrease in activation

energy as temperature decreases from 250k to 100k.

Linsley[61] et al show data on the conductivity variation with temperature of V_2O_5 - P_2O_5 glasses with differing V_2O_5 contents. The data are approximately linear above 250k on an Arrhenius-type plot but below this temperature show a decreasing slope (activation energy) as the temperature is reduced. Strictly if an expression of the form 4.5 is used to describe the temperature variation of conductivity the pre-exponential factor has a recipricol temperature dependence and log σT should plot as a straight line against recipricol temperature. Linsley[40] made plots of his data in this way but found that the reduction of activation energy, at low temperatures, was not significantly affected.

Sayer and Mansingh[39] made an extensive study of the electrical properties of vanadium phosphate glasses and found the temperature dependence of the d.c. conductivity to be in agreement with the examples cited earlier with activation energies in the range 0.3 to 0.42 eV. Estimates of the disorder energy (W_D) were made by measuring the activation energy for conduction at 77k. The validity of this procedure is questionable since the conductivity data still shows curvature at these temperatures. A general trend observed by Sayer and Mansingh is that glasses with high conductivities have low activation energies, while those with low conductivities have high activation energies. The logarithm of the conductivity is found to plot as a linear function of activation energy, with a slope of $(-\frac{1}{kT})$, for a number of vanadium phosphate glasses, and indeed, phosphate glasses containing other 3d transition-metal ions. The conclusion drawn from this is that the

pre-exparential term in the Arrhenius-type conductivity expression is constant and independent of composition for phosphate glasses containing transition metal oxides.

Sayer and Mansingh[39] use an expression similar to equation 2.6 to describe conduction in vanadate glasses but include a factor $\exp(-2\alpha a)$ to allow for tunnelling of electrons between sites, i.e.

$$\sigma = \nu_o N \cdot \frac{e^2 a^2}{kT} c(1 - c) \text{ Exp } (-2\alpha a) \text{ Exp } \left(\frac{-W}{kT} \right) \quad \ldots (4.6)$$

where α is a tunnelling probability.

The conclusions drawn by Sayer and Mansingh are that for a phosphate glass the activation energy is the main factor determining the conductivity and that the tunnelling factor does not vary very rapidly and is close to[62] unity.

4.2.2 Composition Dependence of Conductivity

Munakata[45] found that the conductivity of vanadium phosphate glasses maximises as the ratio of high to low valent vanadium ions in the glass is altered. The maxima for different glasses with different total vanadium contents were found to occur at $V^{4+}: V_{Total} = 0.15$ instead of the predicted value of 0.5. No attempt was made to explain this discrepancy..

Linsley et al [61] made an extensive study of the valence ratio dependence of conductivity in the V_2O_5 - P_2O_5 glass system, by varying the valence ratio in glasses of fixed total vanadium and phosphorous

contents. Again a discrepancey between the measured and predicted values was observed, with the measured maximum occuring at $V^{4+}:V_{Total}$ = 0.1. To explain this difference between theory and experiment it is suggested that a portion of the V^{5+} sites are unable to participate in the conduction process because they are complexed into macrostructural units within the glass. This explanation is based on the known [53] tendency for vanadates and vanado-phosphates to form large polymeric ions. The wet chemical analysis methods normally used to measure the V^{4+}: V_{Total} ratio do not of course give any information on the local environment of the individual ion species. They give an overall ratio for the glass as a whole, which is not necessarily the effective value for conduction, if one of the different vanadium valence states is preferentially complexed into the large polymeric ions and effectively isolated from the conduction paths.

The explanation of the position of the conductivity maximum proposed by Bogomolova et al[55] is similar to that of Linsley et al[61] except that they suggest that phase separation instead of chemical complexing is responsible for isolating a portion of the V^{5+} ions from the conduction process. Scanning electron micrographs were made of a V_2O_5 - P_2O_5 - CuO glass showing two phases, one of which occupied 35% of the total volume. E.S.R. was used to look for V^{4+} ions in the two different phases, but only one type of signal was detected for the glass as a whole. The conclusion drawn from this was that the V^{4+} ions are located in one phase only and that the V^{5+} ions are distributed in both phases, hence conduction occurs in one phase only. This accounts for the displacement of the conductivity maximum from the theoretically predicted value. As support for this idea, the V^{4+} : V^{5+} ion ratio in

the conducting phase, at the conductivity maximum, is estimated to be 1.13 i.e. reasonably close to the value expected on the basis of mixed valence semiconduction theory.

Kinser and Wilson[54] show a ternary phase diagram (Gibbs triangle) for the system P_2O_5 - VO_2 - V_2O_5 (i.e. reduced V_2O_5 - P_2O_5 glass) which has constant resistivity contours based on the data of Linsley[40], Brown[63], Sayer [46][51][64] and Kennedy[32] plus some data of data of their own. This is reproduced in Figure 4.4. A conductivity maximum is located along a line parallel to the V_2O_5 - P_2O_5 side of the triangle at compositions with $V^{4+}:V_{Total} \simeq 0.1 \rightarrow 0.2$.

Scanning electron micrographs of glasses of different compositions indicate that there is greater structural heterogeneity at the extremes of the glass-forming region and the conclusion drawn is that the conductivity maximum is due to the formation of a nearly homogeneous glass at the centre of the glass-forming region. Kinser and Wilson also note that a second maximum *may* exist at the theoretically predicted V^{4+}: $V_{Total} = 0.5$ position. Unfortunately there is no data on glasses in this region, because they are difficult to prepare, but there is evidence from the shape of the conductivity contours that there may be a second maximum at the limits of glass-formation.

Harper and McMillan[50] show E.S.R. data on V_2O_5 - P_2O_5 glasses in the composition range 40 - 90 molar percent V_2O_5. The fine structure of their E.S.R. reveals the presence of oxidation states of vanadium lower V^{4+} in glasses containing less than 30 molar percent V_2O_5. On the basis of evidence from X-ray absorption edge spectroscopy that V^{5+} ions are in assymetrically coordinated sites, they suggest that

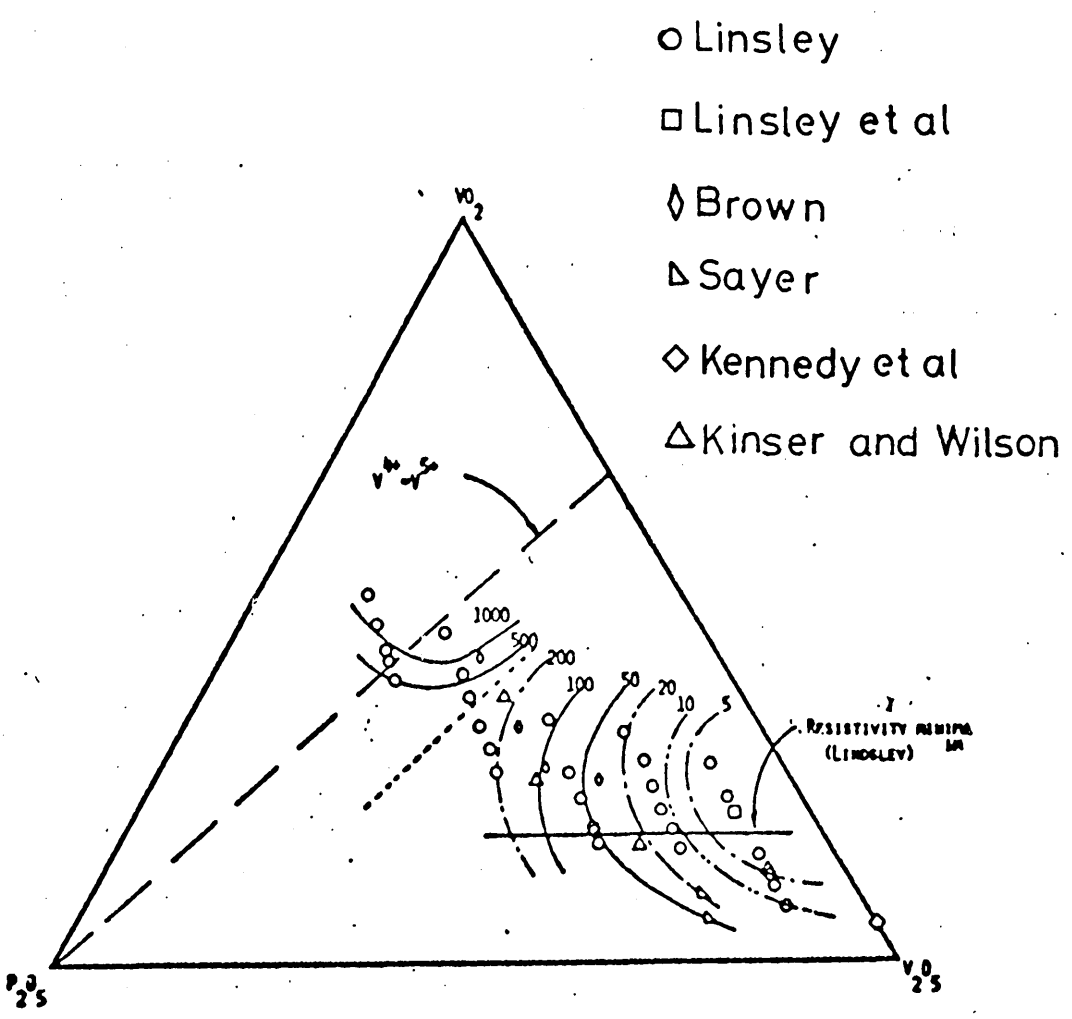

Fig. 4.4 Ternary phase diagram of the V_2O_5 - VO_2 - P_2O_5 system constructed by Kinser and Wilson using data from the literature. Shown on the diagram are constant conductivity contours.

the presence of some V^{4+} and V^{3+} ions in symmetrically coordinated sites leads to the shift in the position of the conductivity maximum to lower $V^{4+}:V^{5+}$ ratios. This suggestion is made on the assumption that the assymetrically coordinated ions cannot participate in the conduction process because of the higher activation energy required for an electron to hop to one of these sites.

4.2.3 Thermo-electric Power of Vanadate Glasses

Measurements have been made of the thermo-electric power of vanadate glasses as a function of composition, but in general there is a lack of reliable data on the temperature dependence below 250K. This is presumably because of difficulty in measuring the small thermo-electric voltages from the high source resistances presented by the glasses at low temperatures. In the room temperature region the data of different workers are in general agreement that the vanadates are n-type semiconductors with a temperature-independent thermopower.

Nester and Kingery[23] report measurements on V_2O_5- P_2O_5 glasses in the composition range 50 to 90 molar percent V_2O_5 which show an increasing thermopower with increasing V_2O_5 content. The data fit the expression of Heikes and Ure[21] for the thermopower of narrow-band semiconductors (Equation 2.7) remarkably well when the entropy term is assumed to be negligibly small. In addition to the room temperature measurements Nester and Kingery[23] report measurements at temperatures of 200K and 125K on a V_2O_5 - P_2O_5 - Na_2O glass and find it reduced from a temperature-independent value of 200μV/K to 135μV/K and 65μV/K respectively. They suggest that it decreases linearly towards zero at zero temperature and note that the change in behaviour from the temperature-independent to a temperature-dependent regime is indicative of

a change in conduction mechanism, supporting statements by Heikes and Ure that charge transport at low temperatures *may* be by means of band conduction.

Brown[63] shows thermopower data on vanadium phosphate glasses containing 87.5, 80.0 and 70.0 molar percent V_2O_5 over the temperature range 90K to 470K. His data also show a temperature independent region at temperatures above 250K but below this point there is a rapid increase to values of around 1.0mV/K at 120K. This contrasts with the behaviour reported by Nester and Kingery[23]. Brown draws comparisons with his results and those of Heikes[65] et al on lithium doped NiO and states that his data are similar in that they rise at low temperatures. No farther interpretation of the data is offered.

Chaudari and Li[66] have measured the thermopower in a V_2O_5 - KPO_3 glass and note that it reduces linearly with inverse temperature over the range 200K to 400K with a thermal activiation energy of 0.22eV. This is contrary to data obtained by other workers [23],[61],[63] who found thermopower to be temperature independent in this region. Chaudari and Li offer no explanation, but a possible explanation of this observation is that the transition from a hopping conduction mechanism occurs at a much higher temperature, possibly because the disorder energy (W_D) of the potassium containing vanadium phosphate glass is greater than that of vanadium phosphate glass.

Extensive observations were made by Linsley[40] of thermopower in the V_2O_5 - P_2O_5 glass system as a function of total vanadium content and vanadium valence ratio at temperatures in the range 300K to 400K. The thermopower was independent of temperature, as

predicted by Heikes and Ure[21], but was strongly dependent on the vanadium valence ratio. The valence ratio dependence is found to follow the general form of that predicted by Heikes and Ure for a narrow-band semiconductor

$$S = \frac{k}{e} \left(\frac{V^{4+}}{V^{5+}}\right) \qquad - \qquad (4.7)$$

but there is no exact numerical correspondence. Equation (4.7) predicts that the thermopower should go to zero when there are equal numbers of high and low valence ions present. In the vanadate glasses studied by Linsley[40] this happened when $\frac{V^{4+}}{V^{5+}} = 0.2$, roughly the same value at which the conductivity was observed to minimise.

Kennedy and Mackenzie[67] have carried out measurements of thermopower as a function of valence ratio in V_2O_5 - CaO - P_2O_5 and V_2O_5 - CaO - B_2O_3 glasses and find that it is independent of the glass-forming oxide used and follows the behaviour predicted by the Heikes and Ure formula as the valence ratio is varied.

4.2.4 The a.c. Properties of Vanadate Glasses

The vanadate glasses have a frequency dependent a.c. conductivity of the form predicted by Pollak[68],[69] for hopping conduction

$$\sigma(\omega) \propto \omega^{n} \qquad - \qquad (4.8)$$

where $\sigma(\omega)$ is the a.c. conductivity, ω is the radian frequency and n is a numberical factor with a value close to 0.85.

Sayer et al [64] have studied the behaviour of a.c. conductivity as a function of frequency and temperature in 80% V_2O_5 - 20% P_2O_5 glasses

with different V^{4+} : V^{5+} ratios and find it is virtually temperature independent at high frequencies. When plotted as a function of frequency the data show a frequency dependence of the form

$$\sigma(\omega) \propto \omega^{0.85} \quad - \quad (4.9)$$

over almost eight decades of frequency. Sayer et al[64] also measured the dielectric constants of their glasses as a function of temperature and frequency and found peaks in dielectric loss which occur at progressively higher temperatures as the measurement frequency is increased, suggesting that the dielectric behaviour is best described by a Debye-type relaxation process with a broad distribution of relaxation times in these materials. The data is shown to be well described by a model of a.c. conduction developed by Schnakenberg[57] which is normally applied to doped broad-band semiconductors. Differences between the temperature dependence of the a.c. and d.c. conductivities are attributed to a distribution of site energies within the glass. The real part of the dielectric constant (ε^*) is estimated to change by a factor of two between 77K and 300K and it is suggested that this must affect values calculated for both the polaron binding energy and the disorder energy. The implication that the polaron hopping energy and disorder energy are temperature dependent has far reaching effects since most theories [57],[58] assume them constant, and may go some way towards explaining the gradual decrease seen in activation energy at low temperatures. It is pointed out by Sayer et al that comment on this point is difficult because of the lack of reliable experimental data on thermopower in the low temperature region where the disorder energy should predominate.

Sayer and Mansingh[39] made farther studies of the a.c. properties of some vanadium phosphate glasses and find the a.c. conductivity is again of the form

$$\sigma(\omega) \propto \omega^n \qquad \text{where} \qquad n \doteq 0.85$$

The dielectric loss calculated from the a.c. conductivity at a fixed frequency peaks as the temperature is varied. As the frequency of measurement is increased the maximum in dielectric loss moves to higher temperatures. This behaviour is indicative of a Debye-type dielectric dispersion process. The temperature dependence of the relaxation time is deduced from the temperature at which the loss peak occurs and the measurement frequency used. The relaxation time is found to be thermally activated with a similar activation energy to that of the d.c. conductivity. The conclusion is that the same hopping mechanism is responsible for both the d.c. and the a.c. conductivity.

Linsley, Owen and Hayatee[61] studied a.c. conductivity and dielectric constant in a 70% V_2O_5 - 30% P_2O_5 glass as a function of temperature and vanadium valence state. They observed no frequency dependence of the position of the maxima in conductivity versus valence ratio, as espected on the basis of the "inactive sites" model proposed to explain the anomolous position of the maxima. The a.c. conductivity was also measured as a function of frequency and temperature. The general features are that in each glass the d.c. conductivity predominates at low frequencies and is strongly dependent on composition; the a.c. conductivity dominates at high frequencies and is much less composition dependent. At low temperatures (77K) the d.c. conductivity is suppressed and the low frequency a.c. conductivity (10^2 - 10^5 Hz) depends

strongly on the vanadium valence ratio. The dielectric dispersion is found to be dependent on the vanadium valence ratio at higher temperatures while at 77K the dependence is reduced.

Hayatee[70] suggests that the a.c. properties of the vanadium phosphate glasses can be explained in terms of Maxwell-Wagner polarisation arising between regions of high and low conductivity. The exact nature of these regions was not discussed but there is also some evidence from d.c. conductivity data of regions of different conductivity. Kinser has studied $NaPO_3$ - V_2O_5 [38] and P_2O_5 - FeO[38] glasses and concludes that the a.c. loss and dielectric dispersion in the audio-frequency range are due to the separation of a crystalline phase in the glass matrix. By means of transmission electron microscopy Kinser[38] was able to detect the presence of the crystalline phase within the glass and farther showed that the dielectric properties were strongly dependent on thermal history, which suggests that the a.c. properties are dependent on structural factors.

Mansingh[72] et al have carried out annealing experiments to determine whether or not the a.c. conductivity was the result of the presence of crystallites in the glass. The electrical properties of V_2O_5 - P_2O_5 glasses in the composition range 60 → 80 molar percent V_2O_5 were found to be unaltered by annealing at temperatures up to 300°C and the conclusion was that the a.c. conductivity is an intrinsic property of the glass and not a result of polarisation effects arising from phase separation or crystallisation. They suggest that many of the changes in dielectric properties observed by other workers are the result of phase separation induced by annealing at excessive temperatures.

4.2.5 High Field Conduction Properties

Austin and Sayer[73] report conductivity measurements on vanadium, iron, copper and tungsten phosphate glasses at fields of up to 6×10^7 Vm^{-1}. The samples were sections of glass film, in the thickness range 0.5 - 15 μm, taken from bubbles blown from the melt. At fields below 10^6 Vm^{-1} the conductivity was ohmic while at high fields the conductivity increased with field. The behaviour was found to be well described by Poole's Law, ie -

$$\sigma(E) = \sigma(0) \frac{\text{Sinh } \frac{eaE}{2kT}}{\frac{eaE}{2kT}} \qquad \ldots (4.10)$$

where $\sigma(E)$ is the high field conductivity, $\sigma(0)$ the low field conductivity, E the applied field and is a length parameter. This behaviour is typical of hopping conduction where carriers hop between parabolic potential wells separated by distance a. On the basis of this simple model the site spacing, a, should be the transition-metal ion spacing which is readily calculable from the composition. When calculated from the high field data, however, a is found to be too large to be interpreted in this way.

Austin and Sayer explain this anomaly by assuming that the local field is not uniformly distributed throughout the material, because of the presence of "hard hops", at which it is more difficult for the carriers to hop from one site to the next. In this situation the potential drop across the "hard hops" is increased giving a higher local field there, than throughout the bulk of the glass. A conductivity enhancement factor (p) is postulated where

$$a_j = p\,a \qquad \ldots (4.11)$$

and a is the site spacing between adjacent transition metal ion sites. This factor relates the local enhanced field at the energetically less favourable "hard hops" to the average field throughout the glass. The "hard hops" are thought to arise through structural features in the glass or long range Coulombic potentials due to donor defects. If the extent of these areas is large enough, spatial variations will occur in the Fermi level resulting in regions of differing conductivities. It is also noted that the accumulation of space charge in the regions of lower conductivity will also tend to increase the local field across the "hard hop" regions. The overall effect of this behaviour will be a field dependent conductivity dominated by the "hard hops", resulting in an increased field dependence at lower fields than predicted by a simple Poole's Law approach. Austin and Sayer interpret their data on the field dependent behaviour of phosphate glasses using this model and, in general, obtain good agreement between experiment and theory.

Slight deviations from Equation 4.10 were observed whereby the onset of non-ohmic conduction is more rapid at low fields and the increase in conductivity at high fields ($10^8 V.m^{-1}$) is less rapid than predicted. This latter effect is most pronounced in 80% V_2O_5 - 20% P_2O_5 and the iron phosphate glasses. Analysis of the "hard hop" model by Austin and Sayer[73] predicts a reduction in the enhancement factor (p) at high fields, so accounting for this behaviour.

4.2.6 Optical Properties of Vanadate Glasses

Nester and Kingery[23] report optical absorption data on thin films of V_2O_5 - P_2O_5 glasses produced by bubble blowing from the melt. A fundamental absorption edge is reported which increases from 455nm

to 550nm as the V_2O_5 content is increased from 50 to 90 m.p.c. The shift in absorption edge is found to be related to the refractive index and hence the high frequency dielectric constant. The energy of the absorption edge (Ea) is inversely proportional to the square of the high frequency dielectric constant i.e.

$$Ea = \frac{K}{\varepsilon^2_\infty} \qquad \ldots (4.12)$$

The energy of the absorption edge is found to vary from 2.2 to 2.7eV and it is suggested that this is due to the trapping of charge carriers. Nester and Kingery[23] also report attempts to measure photoconduction in their glasses, but none was observed. This was attributed to carriers in optically excited states having a shorter lifetime than a lattice vibrational period, effectively preventing the carrier from transferring from its initial site.

Anderson[74] has reported optical absorption measurements in the range 330 to 2600nm on 50%V_2O_5 - 50% P_2O_5 glasses with varying degrees of reduction. A fundamental absorption edge was found at 2.67eV with a broad tail that extended into the lattice vibration absorption bands at about 7μm. The reduction of the glass resulted in an increase in the absorption tail along with the introduction of an absorption band at 2.41eV. Both are attributed to the presence of V^4 ions in the glass, more particularly to electronic transitions within the d states. The tail is suggested to occur as a result of the broadening, by structural disorder, of a number of absorption bands due to d-d type electronic transitions which merge together.

Austin and Garbett[75] present data on 70% V_2O_5 - 30% P_2O_5 glasses,

with different fractions of reduced vanadium present, which show absorption bands at energies below the fundamental absorption edge. These are attributed to optically excited charge transfer between V^{4+} and V^{5+} sites. The intensity of these absorption peaks is found to be dependent on the concentration of V^{4+} ions in the glass and attempts were made to relate the optical and conduction activation energies on the basis of small polaron theory. This predicts a Gaussian absorption band when $h\nu = 2$ Wp i.e. when the incident photon energy ($h\nu$) is twice the polaron binding energy (Wp). The energy for thermal charge transfer of the carrier i.e. the hopping activation energy $W_H \geqslant 1/2$ Wp; thus W opt $\leqslant 4\ W_H$. This is found to give good agreement with experiment in materials such as nickel ferrites and yttrium iron garnet (Y.I.G.).

It is pointed out by Austin and Garbett[75] that problems could arise in interpreting such spectra if the absorption band arose from an internal excitation within the d-levels on one site rather than an optically excited charge transfer from one site to another. One method of overcoming this difficulty of distinguishing between absorption bands due charge transfer and those due to internal d-d excitation is to electromodulate the absorption spectrum.

Reik[76] has analysed the optical behaviour of small polarons at high electric fields by considering an electric field which has both a.c. and d.c. components being applied to a medium in which the hopping conductivity is dependent upon frequency, field and temperature. By means of the Kubo procedure it is found that the a.c. conductivity, at optical frequencies, due to small polarons is field dependent, in other words, there is a field dependence of optical absorption.

Experimentally this shows up as a shift in energy of the position of the optical absorption peak, due to polaronic hopping, when a high field is applied. A farther result of Reik's analysis is that optical absorption due to other causes is not affected significantly by high fields, thus providing a means of distinguishing polaron absorption bands from absorption bands due to other causes.

Austin, Sayer and Sussman[77] predict a symetrical broadening of the charge transfer bands if a carrier can hop up and down the externally applied field with equal probability, but if the probabilities up and down the field are altered by the application of a high electric field a shift occurs in the position of the charge transfer bands. The internal d-d excitation bands remain unaffected since they do not involve a spatial movement of charge carriers.

By this means it is possible to ascertain the origin of the absorption bands in vanadate glasses. Austin[77]et al report two broad absorption bands occuring in V_2O_5 - P_2O_5 glasses at 2.2 - 2.4 eV and at 1.9 eV which increase in intensity as the V^4 content increases. Of these only the one at 1.9 eV is modulated by the application of an electric field. The conclusion drawn from this is that the absorption centred on 2.3 eV arises from an internal field transition within the V^{4+} ion.

4.2.7 Switching Phenomenon in Vanadate Glasses

Gaman et al [78] report studies of the electrical switching behaviour of V_2O_5 - TeO_2 glasses. The compositions 50% V_2O_5 - 50% TeO_2 and 25% V_2O_5 - 75% TeO_2 were used to make "bead" structures by dipping wires into the melt. Before switching behaviour could be

observed the samples had to be "formed" by the application of a high a.c. voltage until a sudden increase in conductivity occurred. After forming threshold switching behaviour was observed. It is suggested that this behaviour is the result of formation of polycrystalline VO_2, produced by the forming process. Crystalline VO_2 is known to undergo a semiconductor-metal transition at $68^{o}C$, one property of which is a discontinuous increase in conductivity of several orders of magnitude. As evidence for this interpretation of the behaviour it is noted that the threshold voltage for switching appears to extrapolate to zero at the VO_2 transition temperature.

Kalygina and Gaman[79],[80] made similar studies of the switching properties of V_2O_5 - P_2O_5 glasses and also conclude that switching behaviour is due to the formation of crystalline VO_2 in a filament between the elctrodes after the switch has been "formed" by the application of an initial high power pulse.

Rhee et al[81] report observations of the switching behaviour of 50 molar percent V_2O_5 - 50 molar percent TeO_2 glass. On the first cycle the I - V characteristic is ohmic at fields below $\sim 10^6$ Vm^{-1}, while at higher fields it becomes increasingly nonohmic until a threshold voltage is reached where it switches to the "on" state. In the on state the switches show a differential resistance with a holding voltage of approximately ten percent of the initial threshold voltage. On subsequent operations the threshold voltage is reduced from the initial value and is not much greater than the holding voltage.

This behaviour is interpreted as being due to the heating of the sample on the first cycle leading to the formation of a devitrified

filament in the glass. On subsequent cycles the devitrified filament dominates the I-V characteristic, but no explanation is offered for the shape of the curve. It is likely that in the process of devitrification polycrystalline VO_2 is formed in the filament and the switching action is at least partially due to the phase transition occuring as it is heated through 68^oC.

4.3 CONDUCTION IN TERNARY VANADATE GLASS SYSTEMS

Of many different possible compositions of ternary vanadate glasses, those based on the V_2O_5 - P_2O_5 system have received the most attention. The third oxide can be either a modifying oxide e.g. V_2O_5 - P_2O_5 - Na_2O, on an intermediate oxide e.g. V_2O_5 - P_2O_5 - PbO. In general, however, ternary vanadate systems have received less systematic study than the simpler binary systems upon which they are based, presumably because of the complicating factor of the third oxide. Additionally there is poor agreement between the results on conductivity of different workers.

The third oxide can affect the conductivity in three ways. Firstly it can affect the glass forming properties of the system resulting in either a more or less homogeneous glass, secondly it can act as a diluent affecting the transition metal ion spacing and finally can alter the transition-metal ion valence ratio by changing the partial pressure of oxygen during melting. Ioffe[82] et al claimed that the only important factor is the ratio of V_2O_5 to P_2O_5. Mackenzie[83] replotted resistivity data of Ioffe[82], Baynton[84] et al and Hamblen[85] et al on vanadium phosphate glasses containing BaO, Na_2O and CdO as a function of V_2O_5 - P_2O_5 ratio and showed that there is no direct relation between these factors. The V_2O_5 - P_2O_5 ratio is undoubtably an important

parameter in controlling the conductivity but only insofar as it affects the $V^{4+}:V^{5+}$ ratio, the transition metal ion spacing and the glass-forming properties.

Munakata[45] used varying amounts of BaO in the system V_2O_5 - P_2O_5 - BaO to alter the vanadium valence ratio in what was probably the first attempt to make a systematic study of the influence of valence ratio on conductivity. The conductivity maximised around $V^{4+}:V_{Total}$ = 0.2. Later work by Linsley[40] dispensed with the need for the third oxide by using organic reducing agents which "burnt-off" during glass melting, leaving a reduced glass without altering the molar percentage of vanadium or glass-forming ions.

In general theories of conduction for binary vanadate glasses are applicable to ternary systems and the additional oxide is not considered to participate directly in the conduction process, but influences the conductivity by acting as a diluent, influencing the transition metal ion valence state and affecting the glass-forming properties of the system.

The foregoing discussion has assumed that the third oxide is either another glass-former or modifier and not a different transition-metal oxide. The presence of a second transition-metal would presumably affect the conductivity by changing the transition-metal ion spacing, valence ratio and glass-forming properties of the system. The conduction process will be complicated by the additional factor that charge transfer can occur between high and low valence ions of the different transition-metal ion species as well as between high and low valence ions of the same species. At present no information on such systems is available in the literature.

4.4 IRON PHOSPHATE GLASSES

Magnetite(Fe_2O_3) will form a glass when combined with a glass-forming oxide such as P_2O_5. The electrical properties of the system 55 m.p.c. FeO - 45 m.p.c. P_2O_5 have been studied by Hansen,[36] Kinser[38] and Hansen and Splann[37]. Hansen reports that the d.c. conductivity obeys the general relationship

$$\sigma = \sigma o \quad \text{Exp} \left(\frac{-W}{kT}\right) \qquad \ldots (4.13)$$

where the activation energy, W, is approximately 1.6eV. Between 110°C and 150°C there is, however, a change in slope of the log σ versus $\frac{I}{T}$ plot and the reasons for this behaviour are not completely understood. Several tentative explanations are offered including: conduction in different phases above and below the break; charge transfer between iron ions in similar positions at low temperatures while at high temperatures conduction occurs between different sites; and ionic conduction in one temperature range and electronic conduction in the other. This latter possibility is dismissed as being unlikely since no time dependence, attributable to ionic drift, is observed in either region..

On varying the Fe^{3+}: Fe_{Total} ratio in glasses containing 55 m.p.c. FeO - 45 m.p.c. P_2O_5 the conductivity is found to maximise at Fe^{3+}: Fe_{Total} = 0.5 as predicted for a mixed valence semiconductor and the thermopower is observed to change from n-type to p-type as Fe^{3+}: Fe_{Total} decreased below 0.38. In general terms the behaviour of the thermopower with valence ratio followed that predicted by Heikes and Ure[21] for narrow band semiconductors

$$\propto = \frac{k}{e} \ln \left(\frac{c}{1-c}\right) \qquad \ldots (4.14)$$

where k is Boltzmann's constant

e is electronic charge

c is the fraction of T.M.I. sites in the low valence states. Additionally, Hansen[36] found that thermopower was independent of temperature over the range 125°C to 400°C implying that the carrier concentration is independent of temperature over this range.

4.5 COPPER PHOSPHATE GLASSES

Drake[44] et al have studied the elctrical properties of the copper phosphate glass 30 CuO - 10 CaO - 60 P_2O_5. In this material the conduction mechanism seems to be different from that in V_2O_5 and Fe_2O_3 because the conductivity is many orders of magnitude lower (3×10^{-15} $\Omega^{-1}m^{-1}$ at 300K) and the activation energy of $\simeq$ 0.95eV much higher than for glasses containing equivelent amounts of iron or vanadium.

Drake[44] et al regard conduction in copper phosphate glass as charge transfer between neighbouring Cu^+ and Cu^{++} ions in substantially different environments. For an electron to transfer between a Cu^+ and a Cu^{++} site, energy is required to overcome the energy difference between the sites. It follows from the high conduction activation energies observed experimentally that there must be a considerable energy difference between Cu^+ and Cu^{++} sites implying that they are in very different configurations. The mechanism of charge transport proposed by Drake[44] involves the production of electronic dipoles on Cu^+ sites. These are thought to be bound electron-hole pairs. When an electric field is applied the dipoles will align with the field and charge transport proceeds by successive production and destruction of dipoles as electrons are thermally activated from the Coulombic attraction of their dipolar sites.

This conduction mechanism was developed by Drake et al to explain the switching behaviour observed in copper phosphate glasses whereby simple two-terminal bead structures showed a transition from a high resistance "off" state to a low resistance "on" state as the voltage across the switch increases. The field in the glass increases the ordering of the structure, as the dipoles align with the field. The increasing order reduces the energy difference between the two types of site and delocalisation of the excess electron on the cuprous ion produces a semimetallic condition. This state is maintained even in the absence of an electric field until sufficient energy is dis-sapated within the lattice to raise its temperature sufficiently to disorder it thereby returning it to the "off" state.

CHAPTER V : APPARATUS AND EXPERIMENTAL TECHNIQUES

5.1 GLASS PREPARATION

Glasses from the V_2O_5 - TeO_2 system were prepared in 20 g batches at intervals of 10 molecular percent between 10% V_2O_5 and 50% V_2O_5 by melting at 900^{o}C and quenching on a metal plate at room temperature. In the composition range 50% V_2O_5 to 90% V_2O_5 microscopic examination showed that polycrystalline regions were formed in the glass but more rapid cooling techniques, such as hot-pressing between mica sheets glassy solids could be produced with up to 70% V_2O_5. However, it was considered advisable from the viewpoint of sample reproducibility to standardise on one technique of sample preparation and to this end only those compositions which could be preapred as glasses by quenching on a metal plate at room temperature were studied. The glasses were subsequently annealed at about 250^{o}C to improve their mechanical properties.

The glass melts were prepared by melting together weighed amounts of vanadium pentoxide and tellurium oxide using reagent grade chemicals as supplied by B.D.H. Appropriate amounts of the oxides were intimately mixed and melted, for 30 minutes, in small Vitreosil silica crucibles heated to 900^{o}C in an electric furnace. After melting and pouring the melt the crucibles were checked for signs of corrosion and slight pitting was observed with glasses of high TeO_2 content but estimates of the amount of SiO_2 dissolved by the melt showed that it was small enough to have negligible effect on the properties of the glass.

The glasses were melted in a small platinium-wound tube furnace (Figure 5.1) installed in a fume cupboard. The extraction of any waste gases was considered advisable in view of the toxic nature of tellurium oxide. Provision was made to control the furnace atmosphere by introducing nitrogen or oxygen but this facility was never used since it was possible to vary the valence ratio of the vanadium in the glass over the full range permitted by the bounds of the glass-forming region by other means.

5.2 VANADIUM VALENCE STATE CONTROL

To control the valence ratio of the vanadium it is necessary to reduce a proportion of the total vanadium content from the V^{5+} state to V^{4+}. Thus

$$2\ V_2O_5 \rightarrow 2\ V_2O_4 + O_2$$

This process occurs to a limited extent when glasses are melted in air because the partial pressure of oxygen in the equilibrium reaction $2\ V_2O_5 \rightleftharpoons 2\ V_2O_4 + O_2$ is less than the vapour pressure of oxygen in the atmosphere above the melt. As melting proceeds it is possible to observe slight effervescence of the melt as oxygen is liberated from the V_2O_5. Simply melting mixtures of V_2O_5 and TeO_2 in air does not, however, give any control over the valence ratio and only a very limited proportion of the total vanadium is reduced. Typical $V^{4+} : V^{5+}$ ratios were, for example, around 0.05. Experience showed that to promote further reduction in a controllable fashion it was most convenient to add elemental tellurium to the oxides and allow this to reduce the V_2O_5 by forming TeO_2 in the melt. Thus-:

$$2\ V_2O_5 + Te \rightarrow TeO_2 + 2\ V_2O_4$$

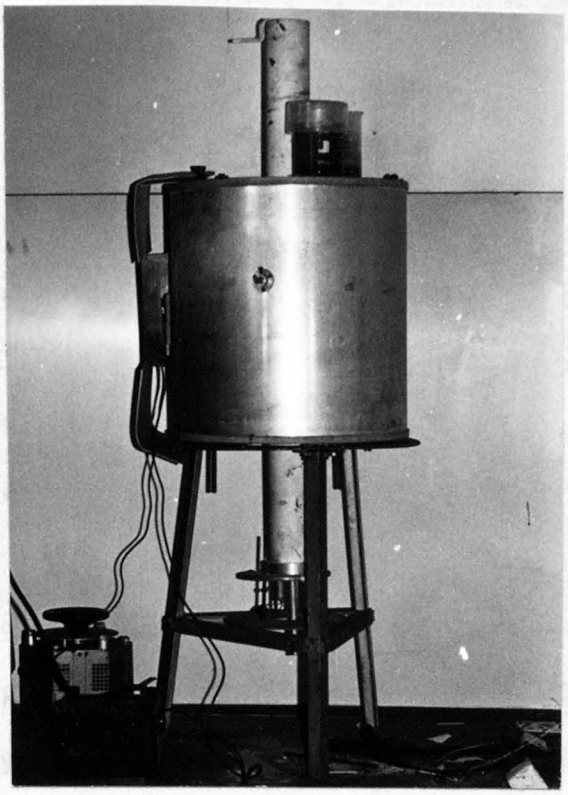

Fig. 5.1 Photograph showing the furnace used for glass melting.

This procedure has the advantage over other methods, such as the addition of carbon, in that it produces a glass which contains no elements in appreciable quantity other than vanadium, oxygen and tellurium. The powdered tellurium was added before melting and carefully ground and mixed into the batch. Reduction of the glass was progressively increased with each batch until no farther tellurium could be assimilated by the melt. This condition was indicated by the presence of a shiny metallic globule of molten tellurium at the bottom of the crucible after melting and pouring the glass. After quenching onto a steel plate at room temperature the samples were annealed at 250^{o}C for 2 hours by placing the steel sheet on a hot plate. This process was found necessary to relieve the mechanical stress in the glass and hence to enable the handling of samples without breakage.

5.3 SAMPLE PREPARATION

On completion of the melting schedule the crucible was removed from the furnace and the glass was poured onto a horizontal metal plate so as to form small "pools" about 1 cm in diameter. If the melt was of a suitable viscosity, and the metal plate horizontal, the pieces of glass produced were reasonably circular and about 2 - 3 mm thick with a flat lower surface and a slightly convex upper surface. The top and bottom surfaces were ground flat and parallel on a glass sheet using 10μm alumina grinding powder in a medium of methanol so as to avoid water absorption. The samples were cleaned in methanol and then transferred to a Birvac electron beam vacuum coating plant and the flat surfaces were coated with gold. Each sample was masked

using strips of cellulose adhesive tape around the circumference. Gold was chosen as the electrode material since it was found by Linsley[40] to give ohmic contacts to oxide glasses.

The thickness of the discs was measured with a micrometer and was usually around 1 mm. Since the samples were not always perfectly circular the areas were measured by placing on squared millimeter graph paper and drawing around the perimeter with a sharp pencil and subsequently counting the squares enclosed. The thickness and areas were then recorded and the samples allocated a reference number. This type of sample was used for experiments which needed bulk samples, e.g. d.c. conductivity, dielectric and thermopower measurements.

For optical and high field work very thin sections of glass were required. Thin-film preparation by R.F. sputtering of a crushed glass was attempted in atmosphere of 80% Argon- 20% oxygen at a pressure of 8×10^{-3} Torr. Deposition rates were very slow ($\sim$ 100 nm/Hour) and to obtain useful film thicknesses it was necessary to sputter for very long periods. Checks made by comparing the film resistivity with bulk values indicated that there was considerably less V_2O_5 in the films than the starting materials. Tests made by sputtering the two oxides separately showed that the TeO_2 sputtered at approximately ten times the rate of V_2O_5. After evaluation R.F. sputtering was not considered to be a suitable technique for the production of thin sections of glass in the present work where chemical composition is a parameter which must be known accurately.

Where thin sections were required, therefore, pieces of glass bubbles were used. These were produced from the molten material by

withdrawing a blob on the end of a 2 mm bore quartz tube. The other end of the tube was attached to a pipette bulb and by squeezing the bulb when the viscosity was in a suitable range, sausage-shaped bubbles of glass, about 10 cm long and 3 cms in diameter could be blown after some practice. These bubbles were used to give glass films in the thickness range 2 to 20μm.

Small sections were broken from the bubbles and either used directly for optical work or gold electrodes were applied to opposite faces for high field measurements. For the application of the gold electrodes the bubble sections were clamped between copper foil "out-of-contact" masks which served to hold the samples and also to define the electrode areas. Great care had to be exercised when handling pieces of the bubbles to obtain a reasonable yield of workable samples. After deposition of gold electrodes, as described, for the bulk samples, the bubble film samples were mounted on glass slides with pads of conducting silver paint to provide connections to the external circuitry.

Figures 5.2 shows (l to r) a piece of V_2O_5 - TeO_2 glass after quenching and annealing, a piece of glass after grinding and electrode deposition and a bubble of V_2O_5 - TeO_2 glass.

5.4 CHEMICAL ANALYSIS OF THE V_2O_5 - TeO_2 GLASSES

Analysis of the ratio V^{4+} : V^{5+} was carried out using colorimetry methods. Dilute solutions of V_2O_5 and V_2O_4 in 0.2 M sulpuric acid are coloured yellow and blue respectively and this fact was used to determine the ratio of the two valence states of vanadium present in the glasses.

Fig. 5.2 Photograph showing (l to r) (i) a piece of vanadate glass produced by quenching onto a cold metal plate, (ii) one of the disc samples with gold electrodes on opposite faces, and (iii) a piece of V_2O_5 - TeO_2 glass bubble. (a 1 pence coin is included as an indication of scale).

Samples of the glass which were unsuitable for electrical measurements because of their size and shape were used for the chemical analysis. They were crushed and powdered in a percussion mortar and dissolved in 0.2 M sulphuric acid. The optical absorption of the solution was measured at 790 nm for the relative V^{4+} concentration and at 380 nm for the relative V^{5+} concentration. The ratio of the number of V^{4+} ions to V^{5+} ions was calculated by comparison with a graph of vanadium ion concentration versus optical absorption determined from standard solutions of Johnson Matthey "Specpure" ammonium metavanadate ($NH_4 VO_3$) to which:

(a) Ammonium persulphate was added to ensure that all the vanadium was in the V^{5+} state.

(b) Sulphur dioxide was added to ensure all the vanadium was in the V^{4+} state.

A Pye-Unican SP 500 spectrophotometer was used for these measurements and checks were made for cross-interference between the V^{4+} at 790 nm and V^{5+} at 380 nm. Even at concentrations of 440 mg/ml, V^{4+} had no effect at 380 nm nor did V^{5+} at 790 nm. No cross-interference could be detected.

5.4.1 Discussion of Method

The colormetric analysic method was chosen because tellurium is known to exist in two different valence states and hence could interfere with the endpoint of a titration involving vanadium only. Linsley[40] used such a titration method for vanadium phosphate glasses but was unable to obtain a well-defined endpoint when this method was applied to the vanadium tellurite glasses.

From the outset of the present work it was considered necessary to find a method of chemical analysis which could distinguish the amounts of V^{4+} and V^{5+} and yet be unaffected by the TeO_2 present in the glass. Polarographic analysis was attempted but it was found difficult to obtain consistant results probably because of dissolved oxygen in the solutions. Colorimetry was chosen because it required a minimum of chemical work and gave a direct measure of the V^{4+} and V^{5+} present.

This method assumes that the glass goes into solution without any change in the vanadium valence ratio, i.e., on dissolution no oxidation or reduction takes place. General evidence suggest that this is the case. For instance when the glasses were progressively reduced in the melt and the valence ratios and conductivities were measured, the three parameters varied correspondingly, i.e., the degree of reduction of the melt determined the valence ratio which in turn determined the conductivity. As a more rigorous check of this the following two tests were made.

(1) A solution of known concentration of vanadium in 0.4 M H_2SO_4 was divided into three parts. The first was heated for 72 hours, the second for 144 hours while the third received no heat treatment. No significant change was observed in the V^{4+}:V^{5+} ratios indicating that little oxidation took place once the oxides were dissolved.

(2) A 0.4 M H_2SO_4 solution containing only vanadium in the V^{4+} state was divided into two parts and one part heated near boiling for 72 hours while the other was similarly treated for 144 hours. When these solutions were checked

for V^{5+} none could be found, again indicating that the acidic solutions containing the vanadium did not tend to oxidise the lower valence state.

Checks were also made on the V^{4+} content of some samples using electron spin resonance. This method has the advantage of measuring the amount of V^{4+} without altering the physical state of the glass and although it did not achieve the same degree of accuracy as wet chemical analysis, rough agreement was observed. Errors arose because of the necessity to use powdered glass samples, resulting in errors estimating a packing factor for the powdered sample.

5.4.2 Lower Oxidation States of Vanadium

The inability of the chemical analysis to identify valence states of vanadium other than V^{4+} and V^{5+} could have serious consequences for the interpretation of the results if states other than V^{4+} and V^{5+} were formed in significant quantities, According to Kitaigorodskii[47], however, the similtaneous presence of V^{4+} and V^{5+} in a glass is unlikely at high temperatures, (i.e. in the melt) the reaction

$$V_2O_5 + V_2O_3 \rightarrow 2\ V_2O_4$$

takes place.

Munakata[45] points out that V_2O_3 is not as soluble in dilute acid as V_2O_4 and suggests that any analysis method involving the dissolution of the glass in dilute acid will not readily detect V_2O_4.

Lynch[46] et al used both E.S.R. and chemical analysis to determine the reduced ion concentration in a 80% V_2O_5 - 20% P_2O_5. glass. E.S.R.

cannot detect any diamagnetic V^{3+} ions present, but good agreement was obtained between the methods suggesting that only a small proportion of the vanadium was reduced farther than V^{4+}.

5.5 D.C. CONDUCTIVITY

The D.C. conductivity was measured as a function of temperature, composition and $V^{4+}:V^{5+}$ ratio. The samples used for this work were of the disc-type described earlier in this chapter. The measurements were carried out in an Oxford Instruments CF 100 continuous flow cryostat using liquid nitrogen as the refrigerent. The cryostat operates on the principle of a controlled continuous flow of coolant (liquid nitrogen) from a storage dewar to a vacuum insulated, radiation shielded sample block. The temperature of the sample block may be maintained at any temperature between 77K and room temperature to within 0.1K by controlling the heat flow into the cryostat. For control an Oxford Instruments Harwell temperature controller was used with an iron-gold thermocouple at 77K as the reference junction. The controller worked by comparing a set voltage corresponding to the required temperature with the thermocouple e.m.f. and deriving the corresponding error signal which was used to control the heater power level to obtain a balance. The controller could be used in three-term or proportional mode. Normally the three-term mode was selected as it gave the most rapid temperature stabilisation. Figure 5.3 shows the cryostat with a sample mounted ready for D.C. conductivity measurements.

The conductance of the samples was measured using a Keithley 640 vibrating capacitor electrometer. This instrument has an input

Fig. 5.3 Photograph showing the sample mounting arrangements in the Oxford Instruments C.F.100 cryostat.

impedance of $10^{16}\Omega$ making it suitable for measuring resistances of around $10^{14}\ \Omega$. The voltage source used was a Fluke 412B switchable power supply. The circuit is shown in Figure 5.4. The entire system was carefully screened and earthed to avoid pickup from stray electromagnetic fields. With this apparatus it was possible to measure conductances of $10^{-14}\ ^{-1}$.

The measurement of room temperature conductance of all the samples as a function of composition and $V^{4+}:V^{5+}$ ratio was carried out using a Keithley 160 digital multimeter. These measurements were made on the complete range of samples in one session to eliminate the effects of room temperature variation.

5.6 THERMOELECTRIC POWER MEASUREMENTS

To measure thermoelectric power, a thermal gradient is applied to a sample and the resulting e.m.f. measured in the direction of this gradient. For this work the disc-type samples described earlier in this chapter were used. Samples were held between large copper electrodes which had been ground and lapped to give good thermal and electrical contact to the sample, (Figure 5.5). Each electrode was provided with a heater and a chromel-alumel thermocouple. The "top" electrode was a copper bar overwound with P.T.F.E. tape and upon which was wound a heater coil of cupron resistance wire embedded in epoxy resin. The bottom electrode was placed on an aluminium block from which it was electrically insulated with a 0.1 mm P.T.F.E. sheet. A heater element was wound around the block embedded in aluminium loaded epoxy resin. The aluminium block was attached to a copper flange (See Figure 5.5) which was cooled to liquid nitrogen temperature through

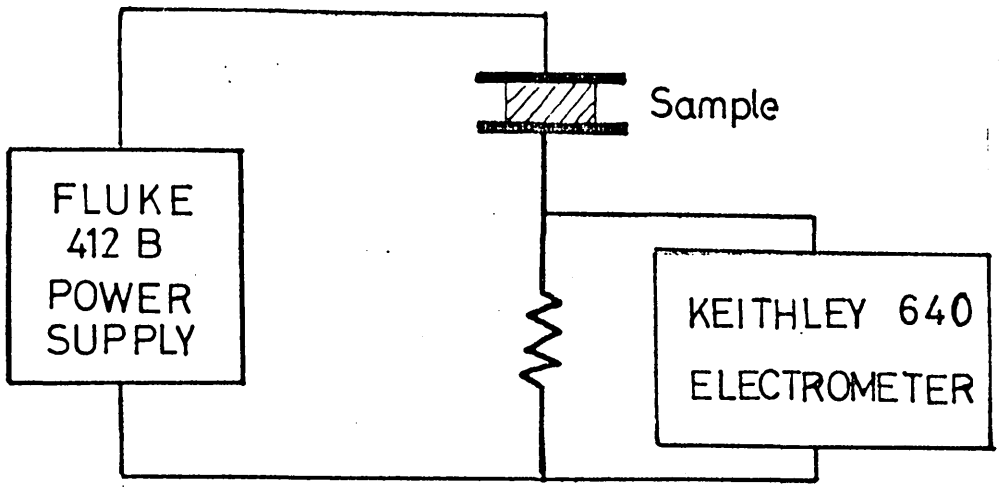

Fig. 5.4 Circuit used for d.c. conductivity measurements.

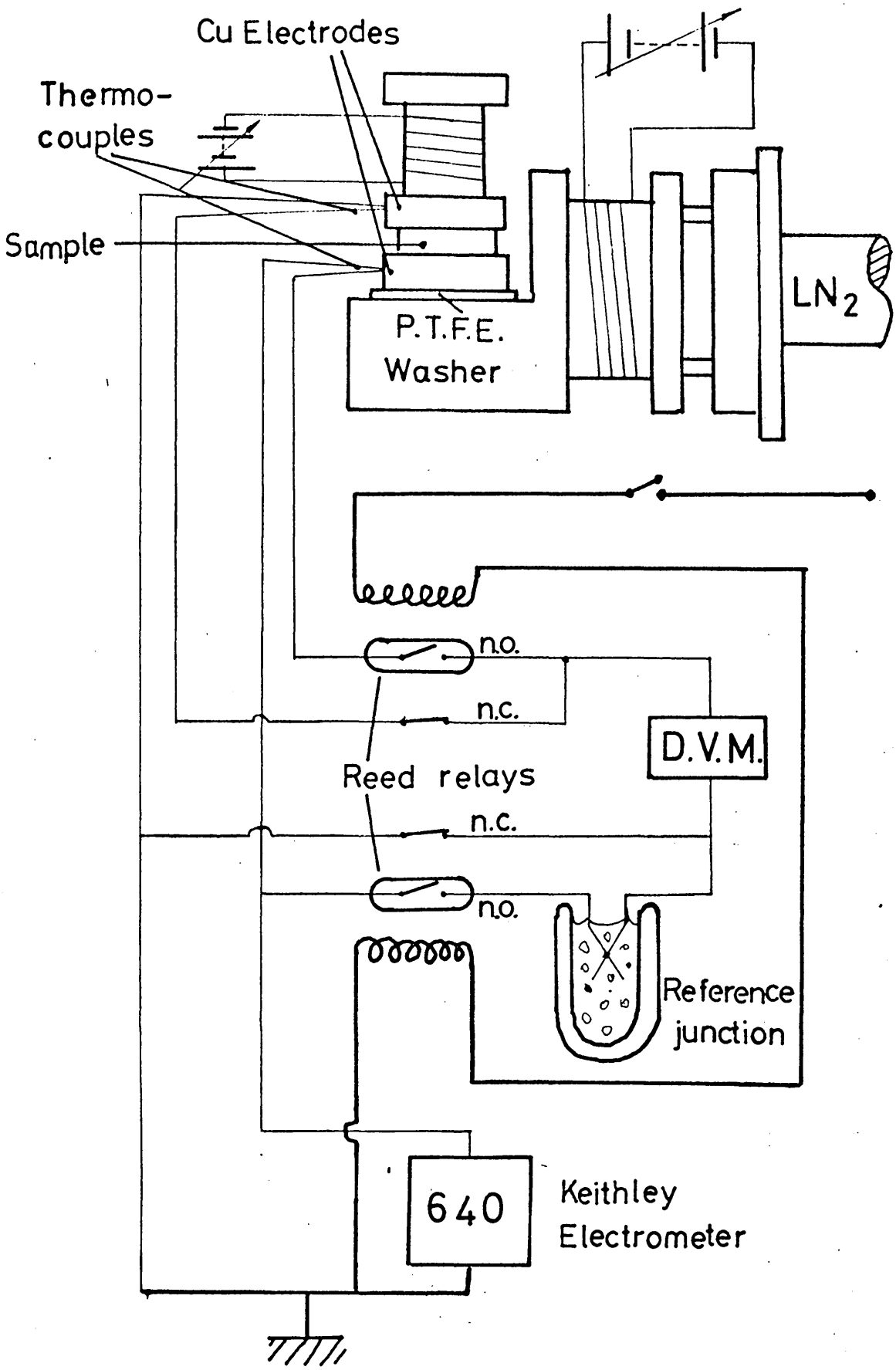

Fig. 5.5a Schematic of the apparatus for the thermoelectric power measurements.

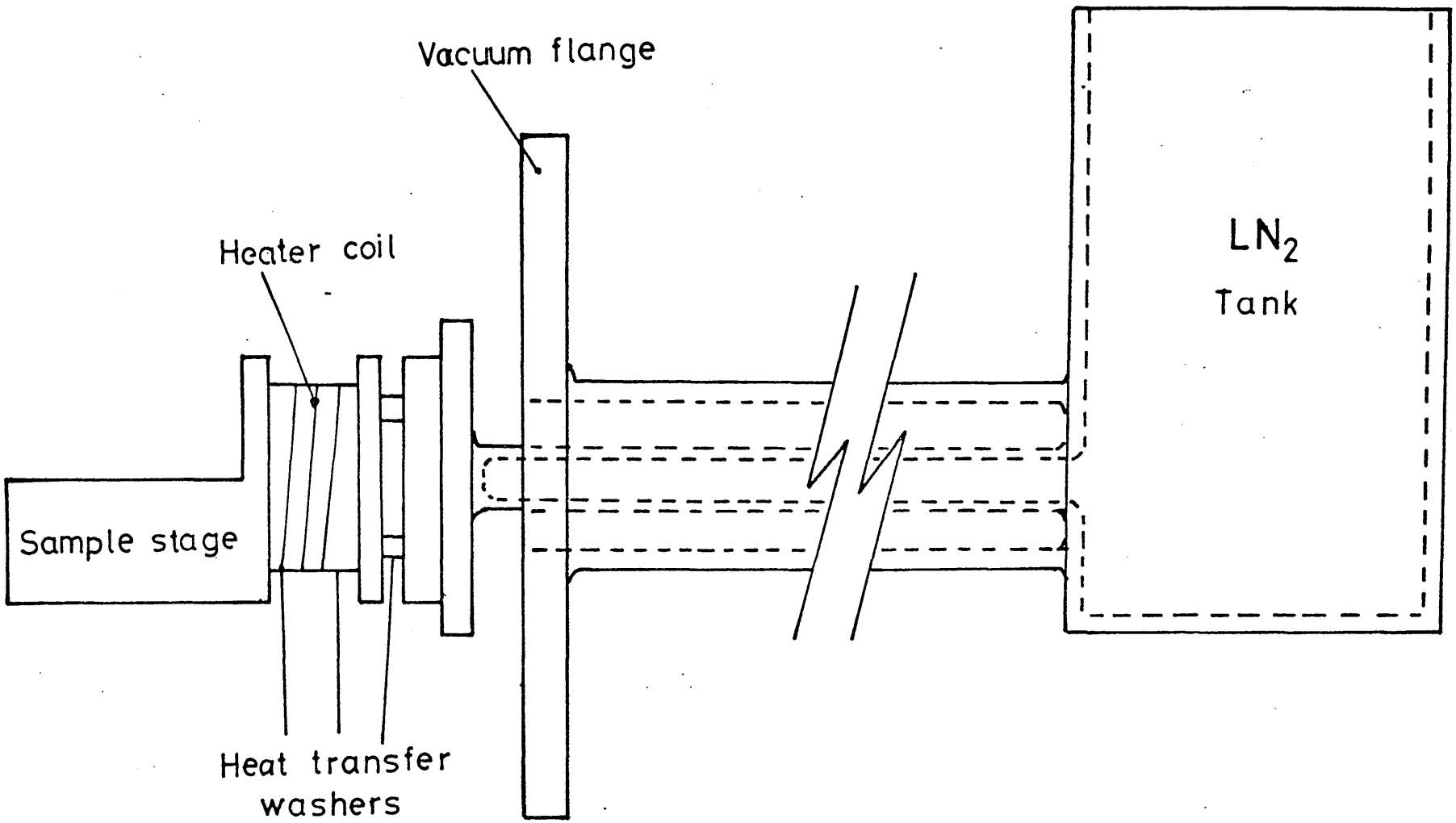

Fig. 5.5b Drawing of cold-finger used for the thermoelectric power measurements.

four small heat transfer washers. The flange was coupled to a liquid nitrogen container by a hollow vacuum jacketed copper rod. With this arrangement the temperature of the block could be adjusted between 100K and 400K by balancing the input power against the heat loss to the nitrogen resevoir. At low temperatures it was not found necessary to apply power to the top electrode to establish a thermal gradient across the sample. The thermal resistance of the sample was sufficient to cause the top electrode to equilibriate about 15K above the bottom one.

Electrical connections to the measurement circuitry were made via the four leads to the thermocouples which were led through the vacuum flange in ceramic tubes set in epoxy resin. The heater elements were powered via vacuum "barb" feed-through insulators. The whole assembly was then placed in a brass box and evacuated with a rotary pump.

The thermo-electric e.m.f. from the sample was measured across the chromel branches of the thermocouples, with the bottom, well insulated electrode, connected to the electrometer "Hi" input while the chromel banch of the top electrode thermocouple was connected to the electrometer input earth to minimise leakage effects. The thermocouples were run with a common reference junction at $0^{o}C$ in ice-water and a common output to a Computing Techniques digital millivoltmeter. The two junctions mounted in the copper electrodes were selected by means of a double-pole change-over configuration of reed relay inserts. These were chosen because of their high insulation resistance in the off state. Normally the millivoltmeter monitored the temperature of the top ("Lo") electrode and only when it was necessary to take a reading of the bottom electrode temperature were the reed relays energised.

This arrangement was necessary to avoid having a reference junction connected permanently to the electrometer "Hi" terminal, which would result in pick-up interfering with the small (typically 5mV), high source impedance (typically $10^{10}\Omega$) thermoelectric e.m.f.s. Figure 5.6(a) and (b) are photographs of the apparatus.

With this apparatus it was possible to measure the thermopower over the temperature range 120 K to 400 K. The temperature gradient (ΔT) along the sample is $(T_1 - T_2)$. The sample temperature is taken to be the average temperature, ie, T sample $=[(T_1 + T_2)/2]$, assuming that $\Delta T \ll$ T sample and there is a linear temperature gradient across the sample. The temperature difference ΔT was kept as small as possible to minimise errors in measuring the average temperature; it was usually around $10^{o}C$.

In a semiconductor the sign of the thermopower gives information on the dominant carrier in the transport process. For a semiconductor in which the dominant carriers are electrons the cold electrode is negative with respect to the hot electrode and vice versa for holes.

5.7 A.C. CONDUCTIVITY AND DIELECTRIC MEASUREMENTS

Measurements of the A.C. conductivity were made on some glass compositions over the frequency range 3 Hz to 100 MHz. A modified Lynch bridge was used in the range 3 Hz to 100 kHz and a Marconi Instruments TF1245 Q-bridge was used in the 100 kHz to 100 MHz range.

5.7.1 Lynch Bridge

The circuit of the modified Lynch bridge was shown in Figure 5.7.

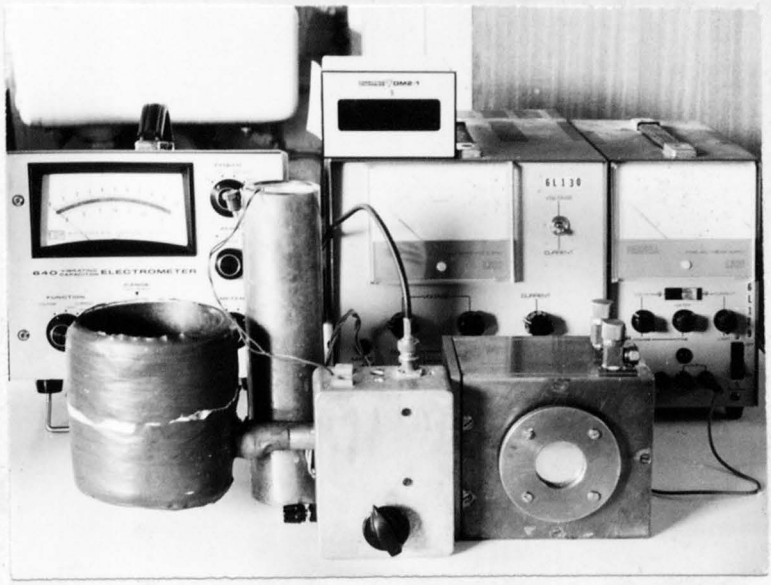

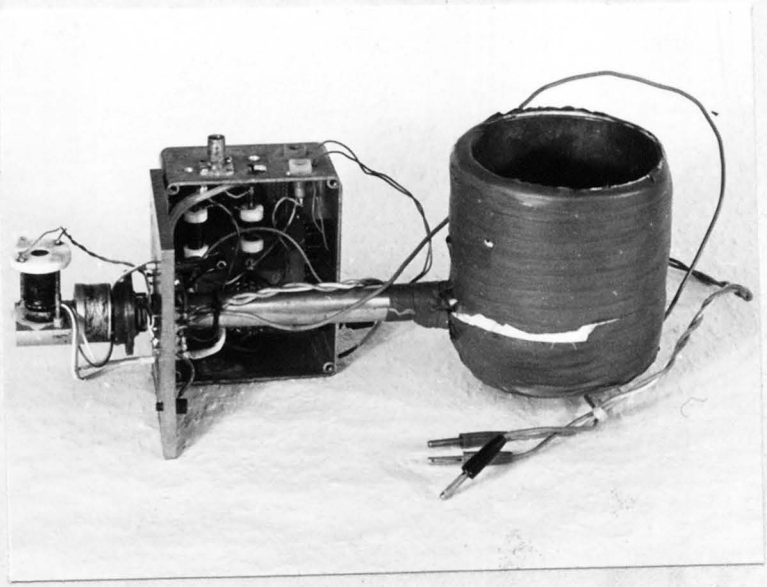

Fig. 5.6 Photographs showing apparatus used for thermoelectric power measurements.

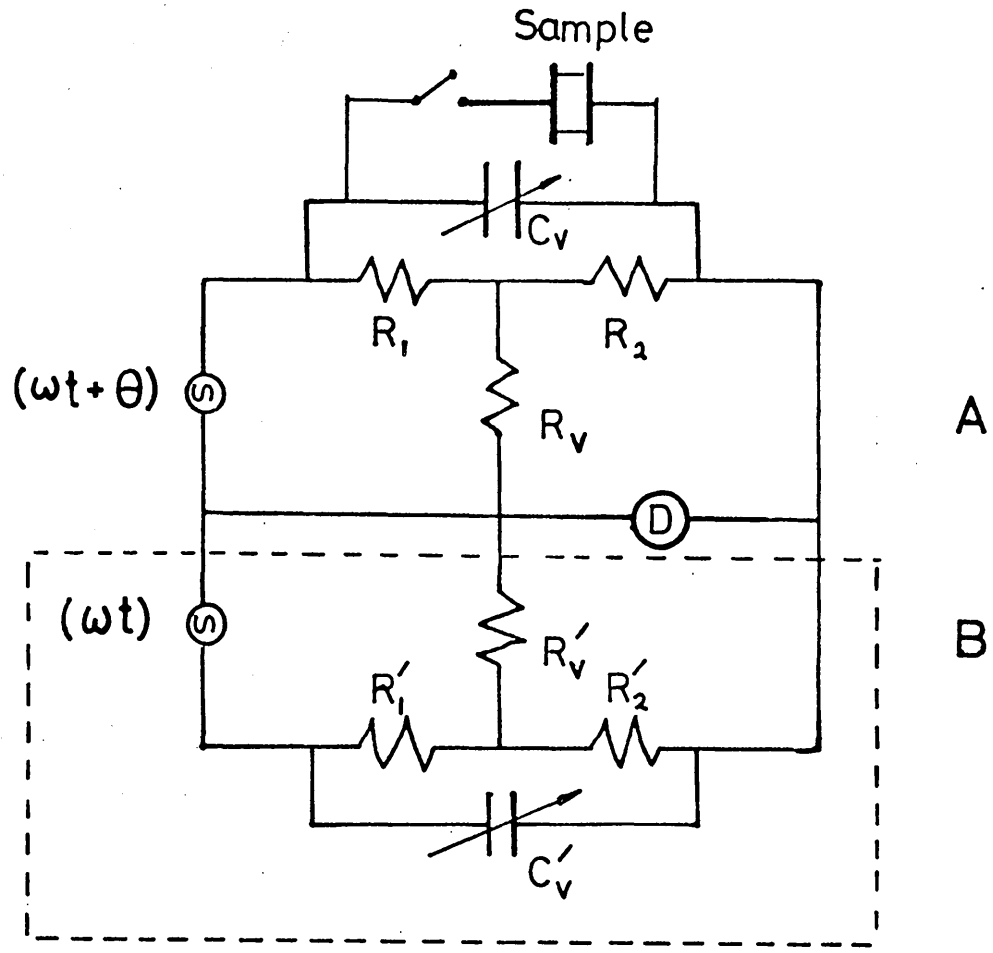

Fig. 5.7 Circuit of modified Lynch bridge used in present work.

The arms A and B are fed from two voltage generators 180^{o} out of phase with each other. In the original bridge described by Lynch[86] this facility was provided by a transformer with the two halves of a bifilar secondary winding connected in series. The bandwidth of this component limited the low frequency capability of the bridge. In this work the two arms of the bridge were fed from the "A" and the"-A" outputs of a Hewlett-Packard 3300 A Function Generator. This provides two waveforms 180^{o} out of phase by electronically inverting one to produce the other. This method is not subject to the phase errors and frequency restrictions imposed by the use of a transformer.

The Lynch bridge is operated by obtaining a null with Rv' and Cv' while Rv and Cv are set to some convenient arbitrary value with the sample in circuit. The sample is then disconnected and a null obtained on Rv and Cv with Rv' and Cv' left unchanged. The conductance and capacitance of the sample are then given by

$$Gs = \frac{\Delta Rv}{R_1 R_2} \qquad \ldots (5.1)$$

$$Cs = \Delta Cv \qquad \ldots (5.2)$$

where Δ Rv and ΔCv are the adjustments to Rv and Cv, respectively, required to obtain the null.

The Lynch bridge operates by providing signals from each arm of the bridge, at the detector which are complex conjugates of each other. The result is a complete cancellation of the signals when the bridge is balanced. Before use, the bridge was checked using "dummy" samples made up of silver mica capacitors and carbon resistors of known values.

5.7.2 The Marconi Q-bridge

The Lynch bridge was unsuitable at high frequencies because of stray capacitance and other spurious effects. In the M.F., H.F. and low V.H.F. range (100K → 100MHz) conventional a.c. bridges are normally replaced by resonant circuits. One such instrument is the Marconi TF 1245 Q-bridge (See Figure 5.8). This instrument measures the detuning produced in a resonant circuit by the addition of a sample of material in parallel with the resonating capacitor. The bridge is a series-tuned circuit consisting of a fixed inductor and precision variable capacitor which is accurately calibrated in pico-Farads.

The material conductivity is measured by noting the change in circuit Q value caused by the addition of the sample to the circuit. The procedure used was as follows:-

(i) The circuit was detuned to its half-power points on either side of the peak. Let these capacitance values by Ct and Ct_2.

(ii) The sample was removed after retuning the calibrated capacitor to its resonance position. The circuit is then re-resonated by adjusting the electrode seperation.

(iii) The circuit is then detuned as in (i) and the half power capacitances duly noted Ct_1^1 and Ct_2^1.

(iv) The conductivity of the sample is calculated from

$$\sigma = f. \frac{d}{A} (\Delta C_t' - \Delta C_t) \qquad \ldots (5.3)$$

where $\Delta C_t' = \Delta Ct_2' - \Delta Ct_1'$ and $\Delta C_t = \Delta Ct_2 - \Delta Ct_1$

d = sample thickness, A = sample area

f = resonance frequency.

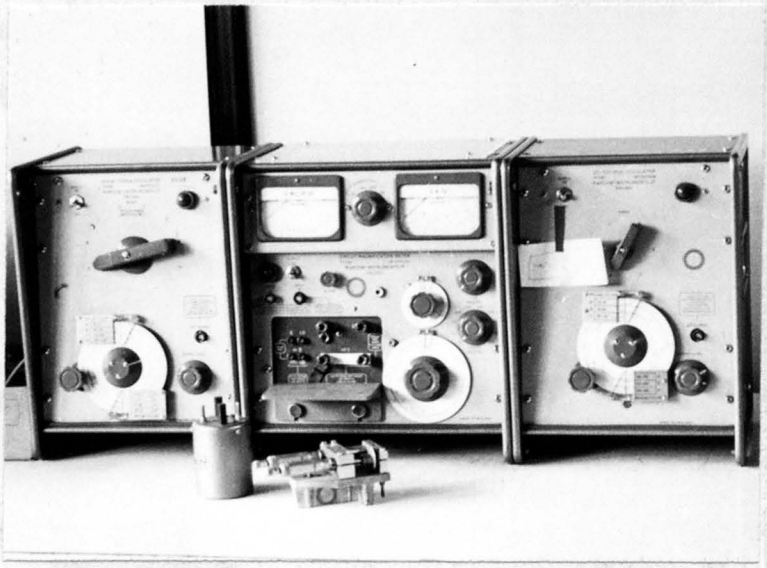

Fig. 5.8 Photograph showing Marconi Q-bridge type TF 1245.

The dielectric constant of the material is calculated by noting the amount of additional capacitance (Δ C) required when the sample was removed from the electrodes, while the electrode spacing was kept constant and using the formula

$$\varepsilon r = \frac{\Delta C}{\varepsilon o} \cdot \frac{d}{A} + 1 \qquad \ldots (5.4)$$

where Er is the relative dielectric constant.

The measurements were not extended beyond 100MHz because this technique becomes less accurate in the high V.H.F. range. Errors arise from the low Q of the inductors and from skin effects at the electrode surfaces caused by incomplete contact with the sample holder. The effects of fringing capacitance are also difficult to evaluate because of their frequency dependence.

The A.C. measurements at low temperatures were not made because of the necessity to place the sample in a temperature controlled container which would have to be physically removed from the instrument The Q-bridge method would not have been suitable for this type of measurement since it involved removing the sample from the holder in the course of the measurements.

The measurements made on the Q-bridge and the Lynch bridge were always overlapped in frequency range as a check on each other.

5.8 HIGH FIELD MEASUREMENTS

Measurements were carried out on the V_2O_5 - TeO_2 glasses to fields of 10^7 to 10^8 Vm^{-1}. To make these measurements with readily attainable voltages, bubble samples in the thickness range 1 to 10 μm

must be used. Samples were prepared as described in section 5.3. A typical bubble sample with an electrode area of 1 mm^2 will have a resistance around $10^6\ \Omega$ and consequently a low duty cycle pulse train is required to limit power dissapation.

For these measurements a pulse generator capable of producing pulse voltages of up to 1 kV was required. This was achieved by the use of two mercury-wetted contact relays controlled by suitable timing pulses. The connections to the relay contacts are shown in Figure 5.9. The first relay RL1 is normally open and is closed by the leading edge of the first control pulse. This switches the power supply directly onto the sample. The second relay (RL2) is normally closed and is opened by the leading edge of a second delayed control pulse. The second relay is normally closed and is held open until the first re-opens then it is released until the next timing cycle starts.

The advantage of this system over others using valves, transistors or thyristors is that the output pulse height corresponds exactly to the input voltage and has a sub-nanosecond rise-time. The disadvantage is that jitter appears on the pulse width and consequently the minimum pulse width obtainable is about 5 μS.

The control pulse generator circuit is shown in Figure 5.10. Tr_1 and Tr_2 form an astable multivibrator producing clock pulses which determine the pulse repetition frequency of the output pulse train. Tr_3 is a buffer amplifier whose output drives the first 74121 T.T.L. monostable ($I.C._1$). The output from this stage is buffered by Tr_4 to drive RL1. R_1 and C_1 determine the length of this pulse and 2 mS was found to give good bounce-free relay operation:

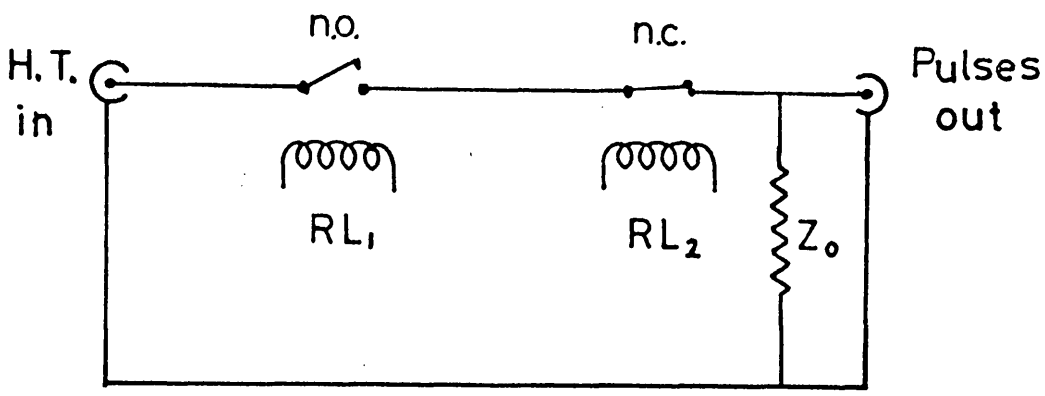

Fig. 5.9 Relay configuration for pulsed high-field conductivity measurements.

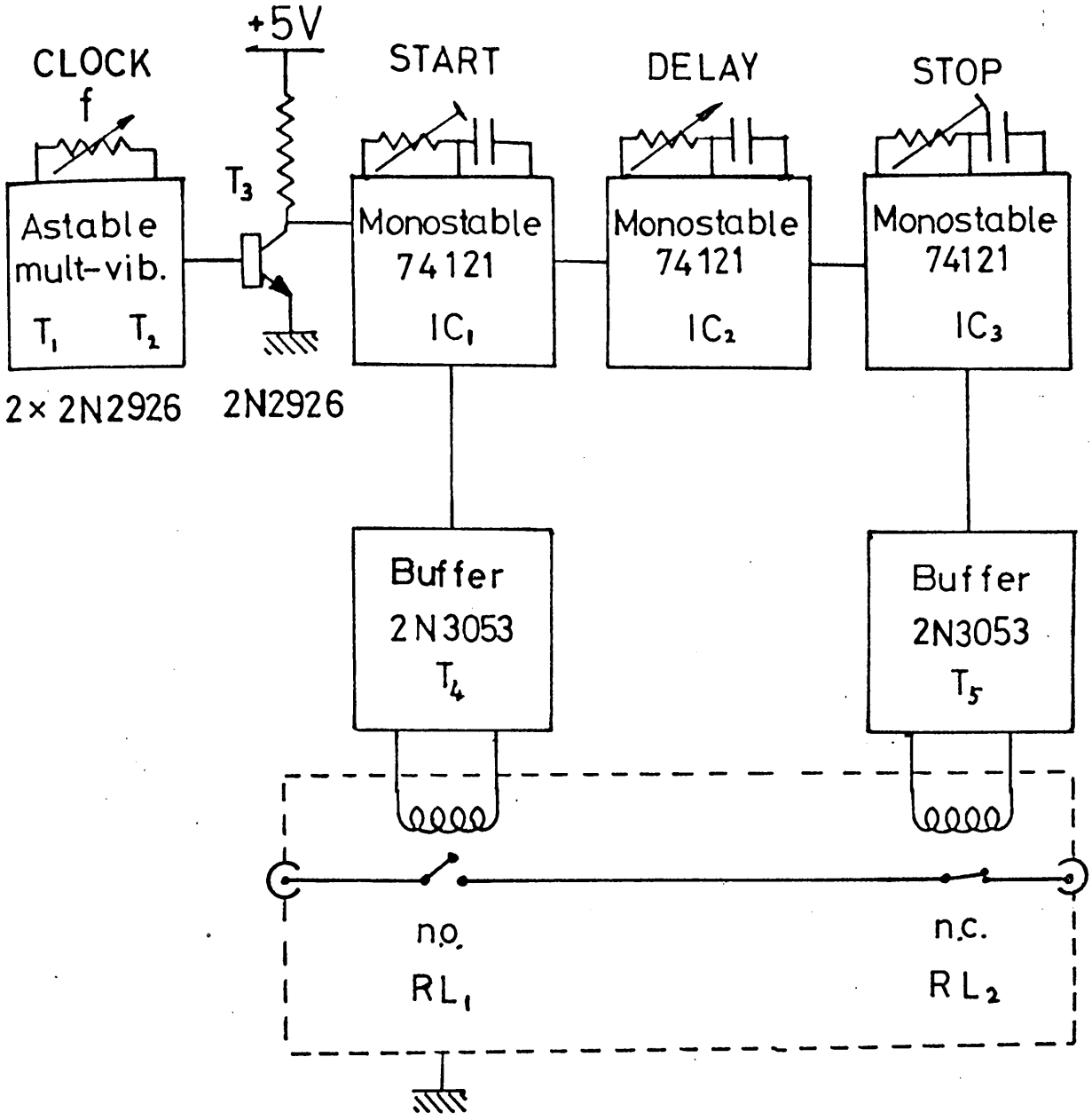

Fig. 5.10 Block diagram showing the timing circuitry for driving the relay pulse generator for the high-field pulse measurements.

$I.C._2$ is also driven from the astable multivibrator and is used to generate a delay pulse of slightly greater length than that from $I.C._1$. This pulse is used to trigger $I.C._3$ which is used to open RL2. By controlling the length of the delay pulse it is possible to control the H.V. pulse width.

The pulse unit was constructed in two separate metal boxes, one containing a stabilised 5V supply, to run the T.T.L. integrated circuits, along with the timing pulse generator. The other box held the H.V. relay switching circuitry. This was found necessary to minimise transients from the relay contacts interfering with the control circuitry. It was also necessary to decouple the feeds to the relay coils with R.F. chokes and capacitors.

To use the pulse unit a high voltage power supply was required with an oscilloscope to check the voltage pulse shape and to measure current pulse amplitude. A typical set-up for voltage-current plotting is shown in Figure 5.11. The pulse amplitude to be applied to the sample is set by adjusting the output from the power supply to the required voltage, and the width and frequency of pulses is controlled by the pulse generator.

The current pulse amplitude was measured using a 1 k sampling resistor in series with the sample under test as shown in Figure 5.11. The current pulse amplitude was measured from the leading edge of the current pulse before heating occurred.

5.9 OPTICAL MEASUREMENTS

Optical absorption measurements were carried out on the

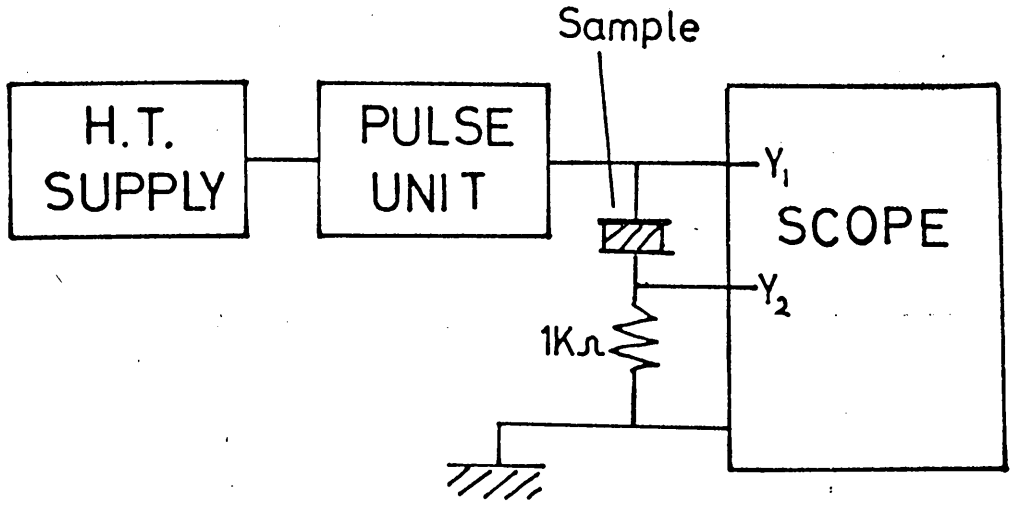

Fig. 5.11 Measuring setup for high field conductivity measurements.

V_2O_5 - TeO_2 glasses at room temperature and 77K. Sections of bubble films were used for these measurements. Samples were enclosed in an evacuated cold-finger box, similar to that used for the thermo-electric experiments. The sample mount had two identical holes in it; one hole had a thin section of the V_2O_5 - TeO_2 glass mounted over it and held in place with silicone grease, while the other was left uncovered. The cold-finger box had quartz windows such that the two holes in the metal flange could be viewed in transmission. The box was then mounted in a moveable carriage in combination with a Zeiss MM12d monochromator so that the sample or the open hole could be moved into the light beam. Figure 5.12 shows the box in position in the Zeiss MM12d. The open hole was used as a reference for 100% transmission and the proportion of light transmitted through the sample taken as the transmission coefficient T. From T the absorption coefficient α was calculated by using the relationship :-

$$T = (r - 1)^2 e^{-\alpha d} \frac{1}{1 - r^2 e^{-2\alpha d}} \qquad \ldots (5.5)$$

where d is the sample thickness. The reflection coefficient (r) is only slightly dependent on wavelength and was estimated therefore, from the measurements of the transmission coefficient at energies below the absorption edge. A computer programme was written to solve Equation 5.5 as a quadratic equation given the reflectivity r and the transmission coefficient T.

The measurements were made at room temperature and then repeated at 77K after filling the cold-finger with liquid nitrogen. The results were plotted as absorption coefficient versus photon energy, $h\nu$ where ν is the incident light frequency .

Fig. 5.12 Photograph showing the Zeiss Monochromator used for the optical absorption measurements.

CHAPTER VI : EXPERIMENTAL RESULTS AND DISCUSSION

6.1 D.C. CONDUCTIVITY

6.1.1 Introduction

The d.c. conductivity of the vanadium tellurite glass system was measured as a function of total vanadium content, vanadium valence ratio and temperature. Measurements were made on glasses prepared at increments of 10% over the glass-forming composition range from 10 mole % to 50 mole % V_2O_5. Glass melting was carried out in air at 900^{o}C and the vanadium valence ratio altered by the addition of elemental tellurium as described in the previous chapter. Figure 6.1 shows the region of glass formation in the form of a Gibbs triangle representing the ternary system V_2O_5 - V_2O_4 - TeO_2.

The conductivity increased with increasing vanadium content and rose to a broad maximum as the reduced vanadium content of the glass increased. It is interesting to note that the vanadium tellurite glasses have conductivites that are several orders of magnitude greater than vanadium phosphate glasses with the same molar vanadium content. Reasons for this are discussed later.

The tellurite glasses show a conductivity temperature dependence which can be discribed by the expression:

$$\sigma = \sigma_o \, \mathrm{Exp} \left(\frac{-W}{kT} \right) \qquad \ldots (6.1)$$

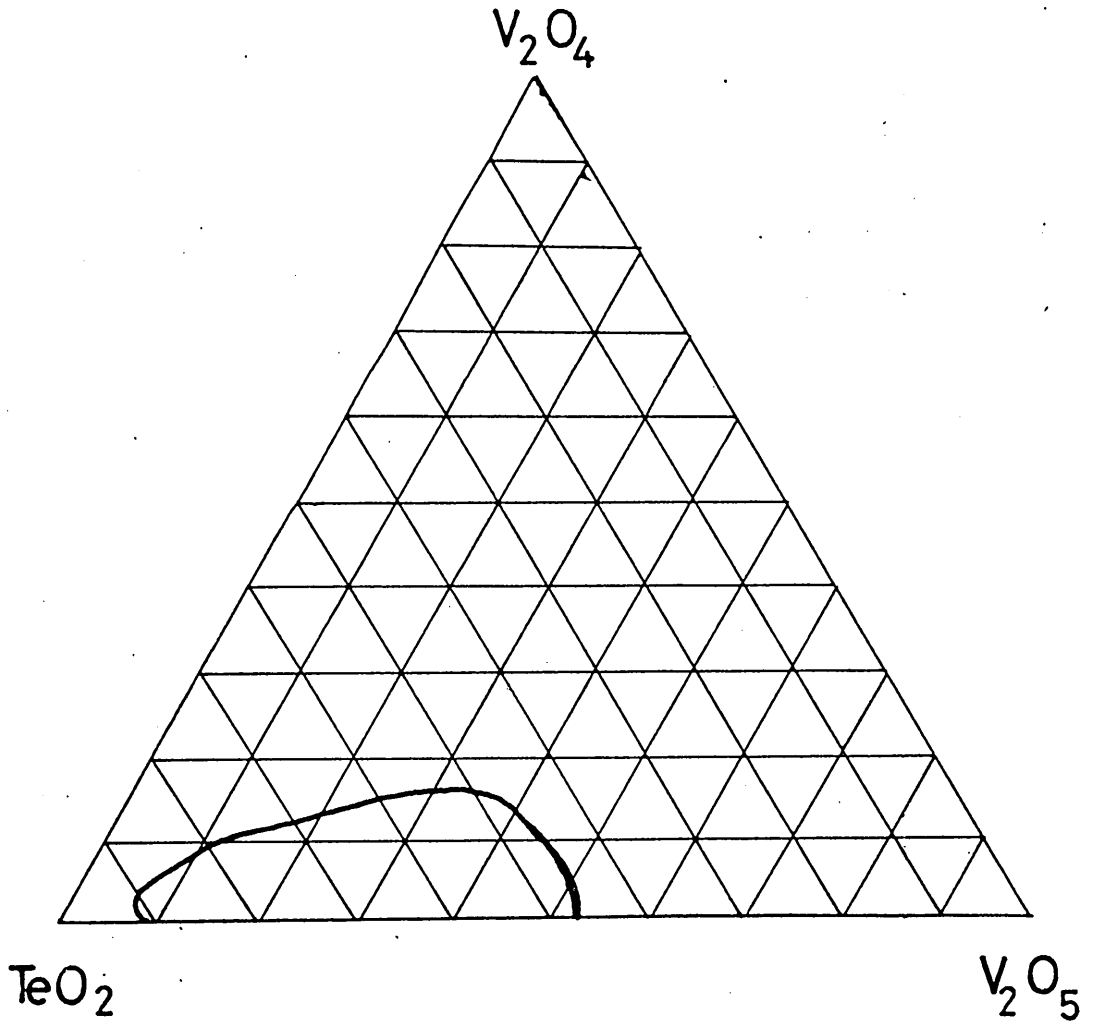

Fig. 6.1 Gibbs triangle showing glass-forming region in the V_2O_5 - V_2O_4 - TeO_2 system.

where σ_o is a pre-exponential constant, W is an activation energy for conduction and k is Boltzmanns constant. At temperatures below 200K the thermal activation energy (W) decreases producing a reduction in slope of a conductivity versus inverse temperature plot.

The use of an expression of the form of equation 6.1 to describe conduction in vanadate glasses where transport is thought to occur by means of hopping, is only valid in the special circumstance of a non degenerate semiconductor with a bandwidth > kT in which scattering by acoustic phonons predominates. Under these conditions

$$\mu \propto T^{-3/2}$$

and

$$n \propto T^{3/2}$$

therefore $\sigma = ne\mu = \sigma_o \exp\left(\frac{-W}{kT}\right)$.

In all other cases σ_o is expected to be temperature-dependent. The materials used in this work have bandwidths < kT, hence the pre-exponential term is temperature-dependent. Mott[56] uses the expression,

$$\sigma = \nu\frac{Ne^2a^2}{kT} \cdot c(1 - c) \cdot \exp(-2a\alpha) \cdot \exp\left(\frac{-W}{kT}\right) \quad \ldots (6.2)$$

thus $$\sigma \propto \frac{1}{T} \exp\left(\frac{-W}{kT}\right)$$

and strictly, log (σT) should be plotted as a function of inverse temperature. In practice, however, this does not significantly alter the curvature, or the slope of the plots from the values found by plotting log (σ) versus temperature. In the present work log (σ) has been plotted, unless otherwise indicated, because the bulk of the data in the literature is presented in this way and to do otherwise would make comparison difficult.

6.1.2 Temperature Dependence of Conductivity

Figure 6.2 shows the conductivity of different glasses of composition 50 mole % V_2O_5-50 mole % TeO_2 as a function of temperature. Data on glasses with different V^{4+}:V_{Tot} ratios are plotted as log conductivity versus $\frac{1}{T}$ in the temperature range 77 to 300 K. All compositions show a marked deviation from linearity below 200 K. The slope of the graph is constant above 200 K and below this temperature there is a continuous decrease in slope and hence activation energy. Figure 6.3 shows a plot of conduction activation energy, at temperatures greater than 200 K, as a function of total vanadium content for glasses whose V^{4+} : V_{Tot} ratio is around 0.1.

If the usual expression for the conductivity of transition-metal oxide glasses is used

$$\sigma = \sigma_o \exp \frac{-(W_H + \frac{1}{2}W_D)}{kT} \qquad \ldots (6.3)$$

two straight line portions on a log σ versus $\frac{10^3}{T}$ plot would be expected with a transition from the higher hopping activation energy (W_H) to half the disorder energy (W_D) in the range $\frac{1}{2}\theta_D > T > \frac{1}{4}\theta_D$ as the temperature decreases, (θ_D- Debye temperature). Experimentally this is not observed, as can be seen in Figure 6.2. Below 200 K the

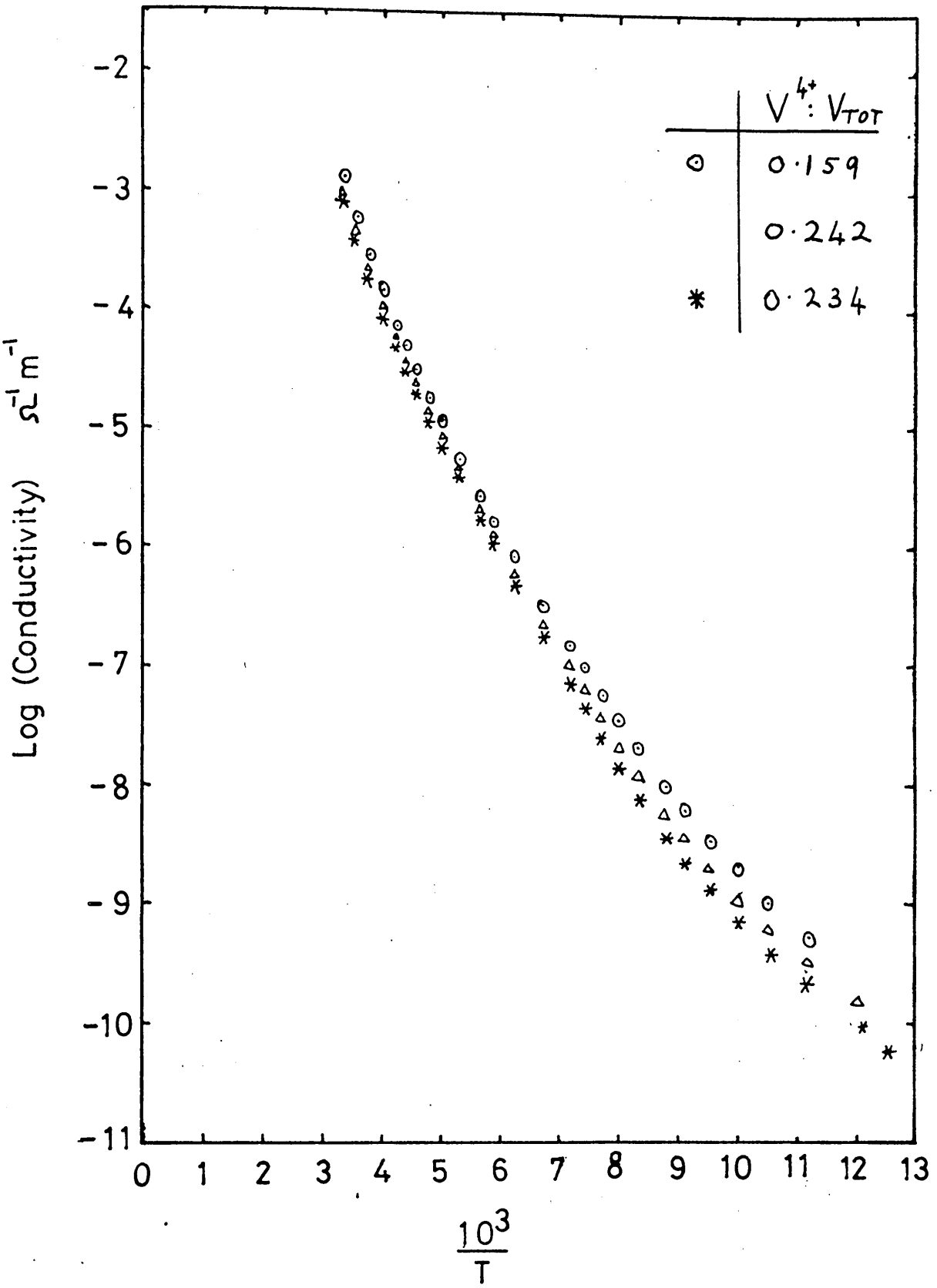

Fig. 6.2 Conductivity as a function of inverse temperature for some 50 V_2O_5 - 50 TeO_2 glasses compositions.

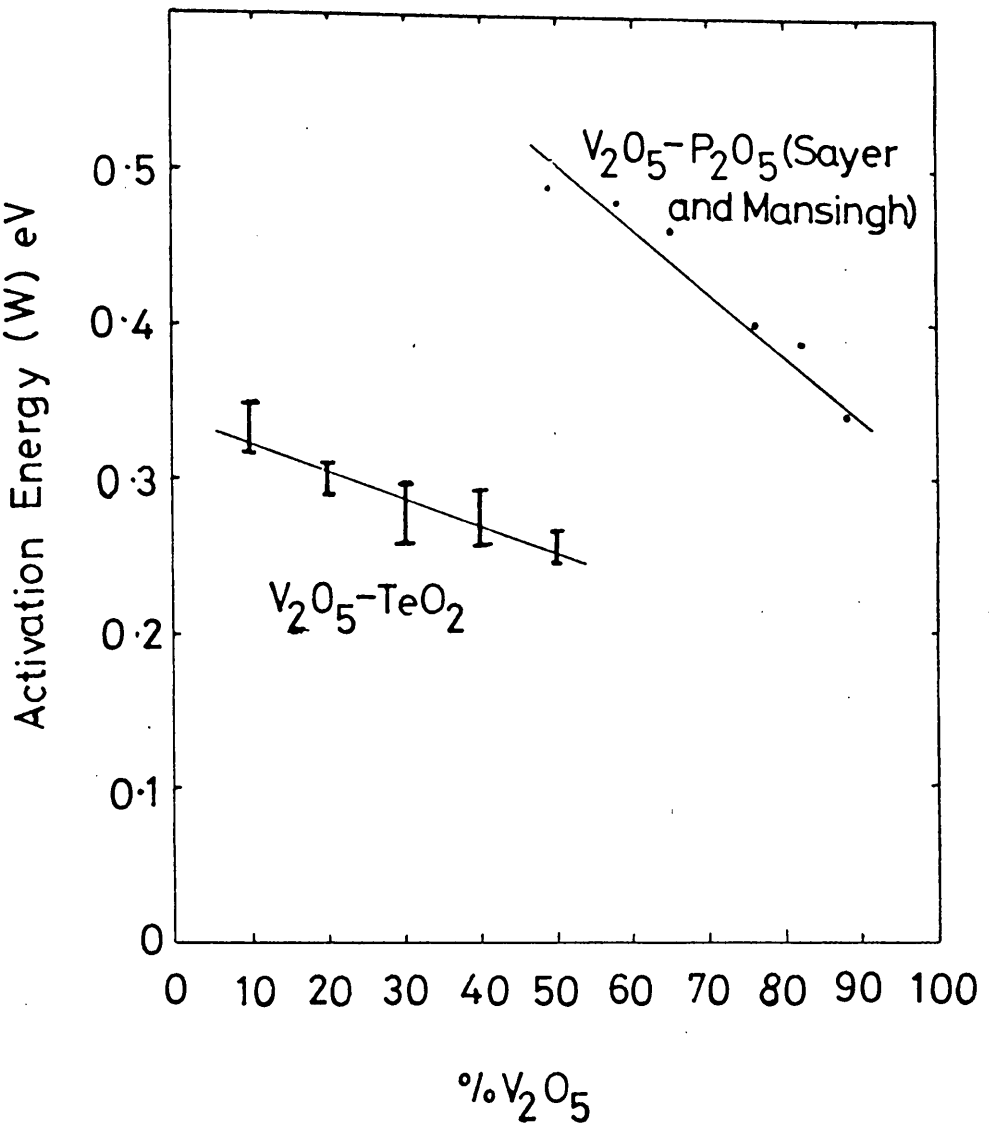

6.3 Conduction activation energy as a function of composition in V_2O_5 - TeO_2 and V_2O_5 - P_2O_5 glasses.

activation energy decreases continuously, but does not attain a constant value as the temperature approaches 77 K. This limit was imposed by the use of liquid nitrogen as the refrigerant and by the difficulty of measuring the sample conductance at these low temperatures.

This behaviour can be explained in general terms by the thermally activated hopping of small polarons in a disordered structure. In the high temperature regime ($T \geqslant 200$ K) the activation energy is constant and probably arises from the hopping of carriers plus a contribution ($\frac{1}{2} W_D$) from the structural disorder energy. At temperatures below 200 K there is a progressive reduction in the activation energy as expected from the continuous reduction in available phonon energy. Austin and Mott[22] suggest that as the temperature falls from $\frac{1}{2}\theta_D$ to $\frac{1}{4}\theta_D$ the hopping energy term W_H should fall to zero and W become equal to W_D. Emin[60] has proposed a theory for polaron conduction in non-crystalline materials which may overcome this difficulty. The jump rate (R) is determined as a function of temperature by a perturbation approach to the two-site jump rate. The jump rate (R) is related to the conductivity (σ)

$$\sigma = \frac{nc\ e^2a^2}{kT} \cdot R \qquad \ldots (6.4)$$

where nc is the carrier concentration and a the site separation. By comparison with the usual expression for conductivity in these materials.

$$\sigma = \nu \frac{nc\ e^2a^2}{kT} \exp(-2\alpha a) \exp\left(\frac{-W}{kT}\right) \qquad \ldots (6.5)$$

it can be seen that the temperature dependence of the conductivity will

be determined by that of the jump rate. The graphical solution for jump rate as a function of temperature in units of the Debye temperature is given by Emin and reproduced in Figure 6.4. This shows a high temperature region of constant activation energy down to a temperature around $\theta_D/2$ and a gradual fall off in activation energy corresponding to phonon freeze-out continuing down to temperatures around $\theta_D/8$ This suggests that there is still an appreciable thermally activated hopping contribution to the conduction activation energy down to temperatures around 60 - 70 K. This is beyond the range in which the conductivity in the oxide glasses is readily measurable so that it is likely that the low-temperature activation energy region has not yet been observed as it will be masked by a thermally activated hopping contribution. Exact correlation of the experimental data with Emin's expression for the jump rate is difficult since it depends upon a knowledge of factors which are not readily determined experimentally. The model curves given by Emin should, however, be of the same shape as the experimental data assuming that the phonon frequency does not vary with temperature. It will be seen later in this section that this assumption is not unreasonable. In Figure 6.4 a curve of the conductivity data is included with Emins theoretical curve for comparison (Figure 4.3).

Other theories have been used to explain the low-temperature behaviour of conductivity in vanadate glasses Linsley used Killias theory which predicts the temperature dependence from the activation energy as

$$W \propto \left(1 - \frac{\theta_R}{T}\right) \qquad \ldots (4.3)$$

where θ_R is a constant. This expression can be fitted to the present

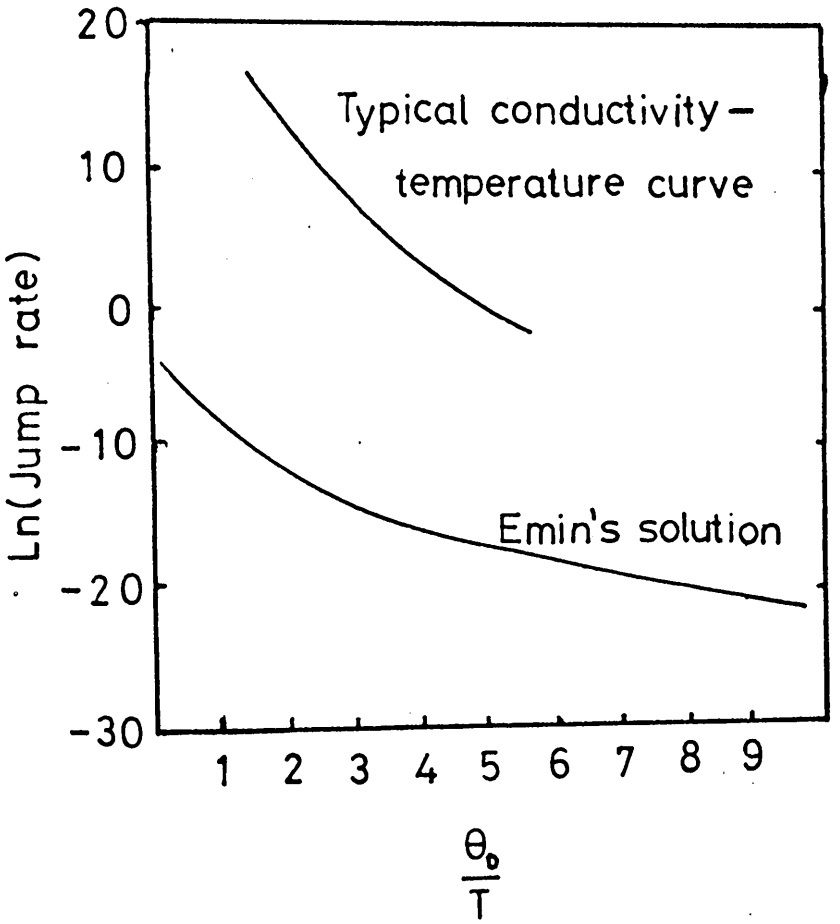

Fig. 6.4 Emins solution for the two-site jump-rate for carriers as a function of temperature (Figure 4.3) along with a curve showing the shape of a typical conductivity temperature plot for a V_2O_5 - TeO_2 glass.

data over limited ranges of temperature depending upon the values of θ_R chosen. A farther objection to this model is that it predicts a negative activation energy when $T > \theta_R$, consequently attempts to fit the data to this theory were discontinued.

Good fits of the data can be made to a $T^{-\frac{1}{4}}$ law (See section 1.7), however, the values of disorder energy (W_D) deduced from the slope of $\log \sigma$ - $T^{-\frac{1}{4}}$ plots are unrealistically high ($\simeq$ 0.8 eV). It is unlikely, therefore that a $T^{-\frac{1}{4}}$ analysis is valid in this case.

6.1.3 Dependence Upon Vanadium Valence Ratio

The dependence of the conductivity on the valence ratio (V^{4+}: V_{Tot}) was studied by preparing a series of glasses in which a proportion of the vanadium was reduced by adding elemental tellurium to the melt, as described in the previous chapter. It is convenient to consider the reduced glasses as belonging to the three component system V_2O_5 - V_2O_4 - TeO_2 in which the percentage of V_2O_4 represents the percentage of reduced vanadium oxide in the glass and the glass-forming region can be presented in the form of a Gibbs triangle (as in Figure 6.1). There is a well defined region of glass-formation onto which constant conductivity contours (at fixed temperature) can be drawn. Figure 6.5 shows a detail of the TeO_2 apex of the Gibbs triangle with conductivity contours in one-decade steps. In Figure 6.6 the conductivity (at 300 K) is plotted as a function of V^{4+}: V_{Tot} for different total vanadium concentrations. The conductivity increases with increasing V^{4+} content until V^{4+}: V_{Tot} = C$\simeq$ 0.2 after which the curves level out and show signs of a gradual decrease at higher V^{4+} concentrations. Theories of hopping

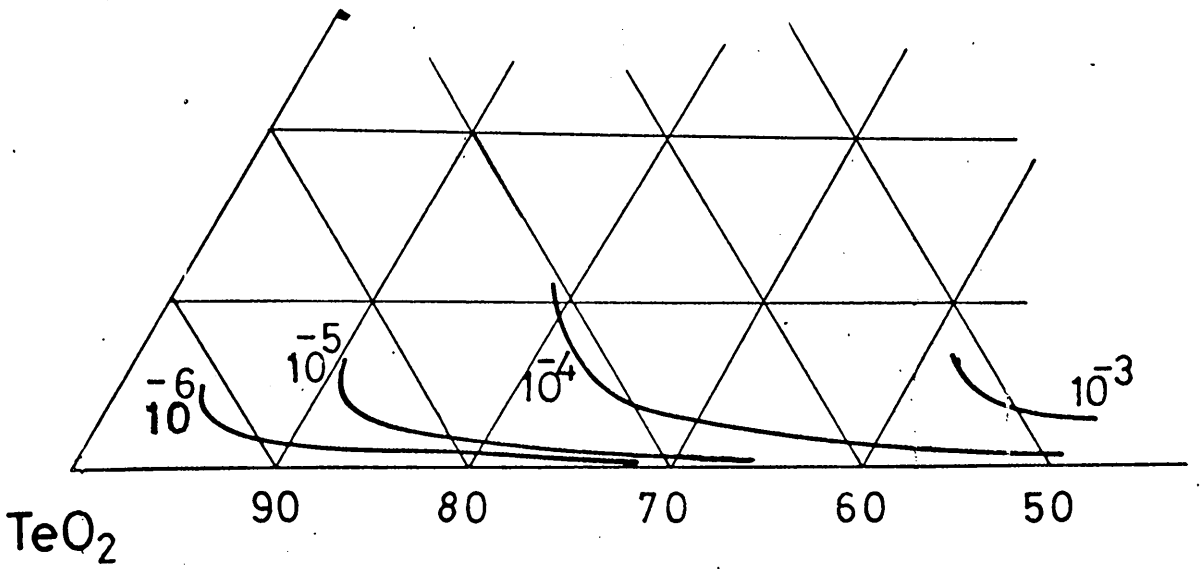

Fig. 6.5 Detail of a Gibbs triangle showing constant conductivity contours in the V_2O_5 - TeO_2 system.

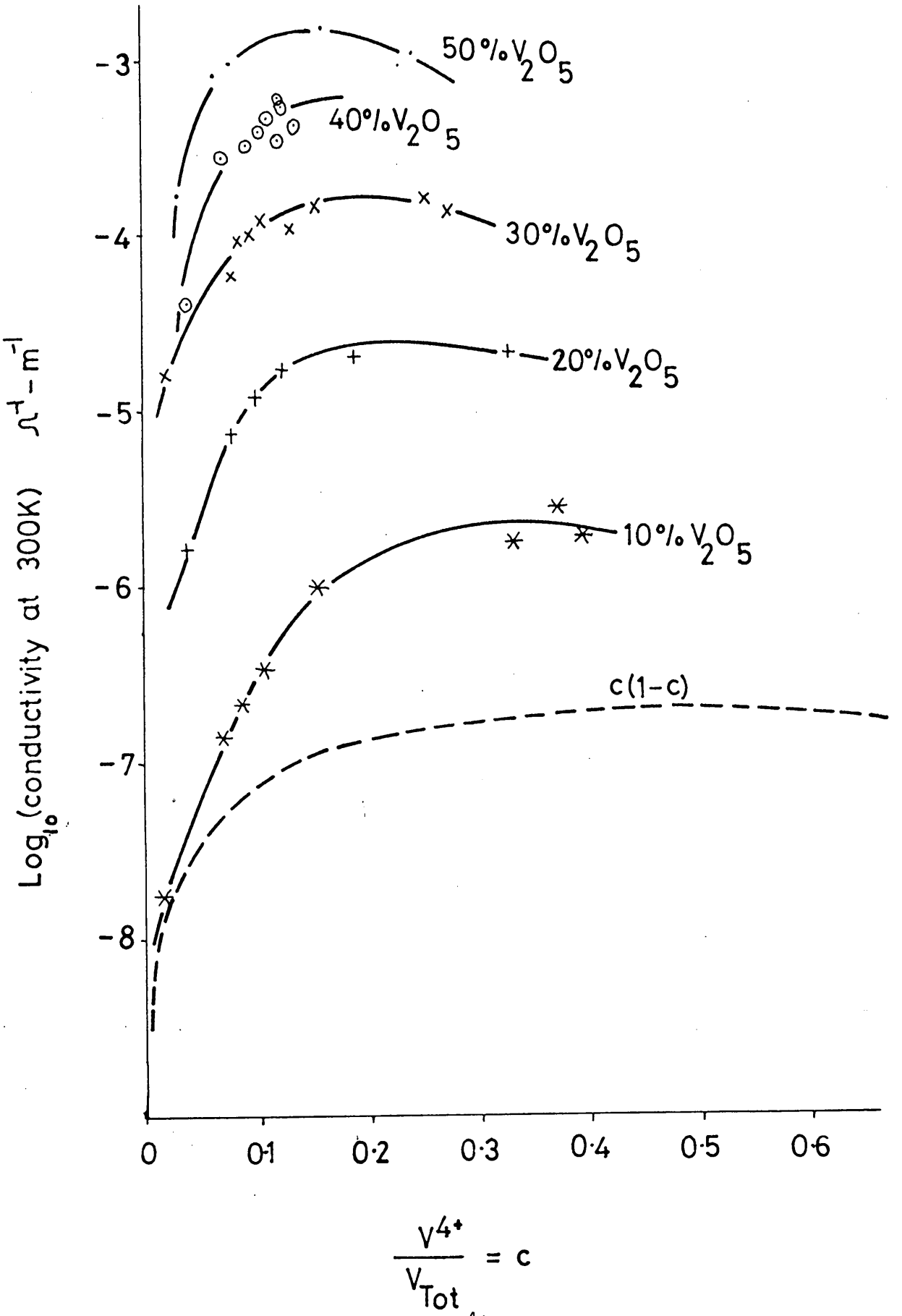

Fig. 6.6 Conductivity versus V^{4+}: V_{Tot} for different compositions of V_2O_5 - TeO_2 glass.

conduction in mixed valence semiconductors predict a conductivity maximum when there are equal numbers of occupied and unoccupied sites i.e. when C = 0.5. In the vanadium phosphate glass system Linsley[40] found a well defined maximum in conductivity at C ≃ 0.2 and this discrepancy between theory and experiment has also been observed by other workers[61],[54],[55]. Three explanations have been advanced:

1. That a portion of the V^{5+} ions are bound in structural complexes and are unable to participate in the conduction process. Linsley et al [61] have pointed that the vanadates and vanadophosphate salts are known[53] to form large polymeric molecules.

2. Kinser and Wilson[54] have suggested that the conductivity maximum at C ≃ 0.2 is caused by the formation of a homogeneous glass structure around this value. Evidence was also produced which suggested that in the phsophate system there may be a second maximum at around C ≃ 0.5.

3. Bogomolova et al[55] have suggested on the basis of E.S.R. and electron microscopy data, that a glass - glass phase separation occurs with one phase containing all of the V^{4+} ions while the other phase has only V^{5+} ions. Conduction can only occur in the phase containing both V^{4+} and V^{5+} ions thus the conductivity maximum will be displaced if the V^{4+}: V_{Tot} ratio is determined for the whole of the glass.

Information on the structural properties of V_2O_5 - TeO_2 glasses is scanty, making it difficult to theorise on reasons for the displacement of the conductivity maximum. The formation of large vanado-

tellurite complexes seems less likely than the formation of vanadophosphate complexes in V_2O_5 - P_2O_5 glasses, because of the structural dissimilarity of TeO_2 and P_2O_5. Less of the V^{5+} would be expected to be complexed into the interior of large molecules and hence on this basis a smaller shift in the conductivity maximum would be expected.

In general the tellurite glasses seem to show the same valence ratio dependence of conductivity as the vanadium phosphates, with the exception that the peak in conductivity is broader and flatter. Reasons for this are not immediately apparent but it is likely that there is greater structural homogeneity in the centre of the glass-forming region, which could broaden the maximum if the centres of the glass-forming region and the conductivity maximum do not coincide. The fact that the conductivity-valence ratio curve increases rapidly towards the centre of the glass-forming region lends support to this idea.

6.1.4 Conductivity Dependence on Total Vanadium Content

Figure 6.7 shows the relation found between conductivity and total vanadium content with bars indicating the spread caused by different V^{4+} : V_{Tot} ratios. Also plotted in this figure are data from Linsley[40] on the V_2O_5 - P_2O_5 system. The most striking result is that the conductivities of the V_2O_5 - TeO_2 glasses are 2½ to 3 orders of magnitude greater than those of V_2O_5 - P_2O_5 glasses with the same total vanadium content. This suggests that the glass-forming oxide is not simply a non-interacting solvent in the conduction process as suggested by Ioffe et al[82] for the V_2O_5 - P_2O_5 system.

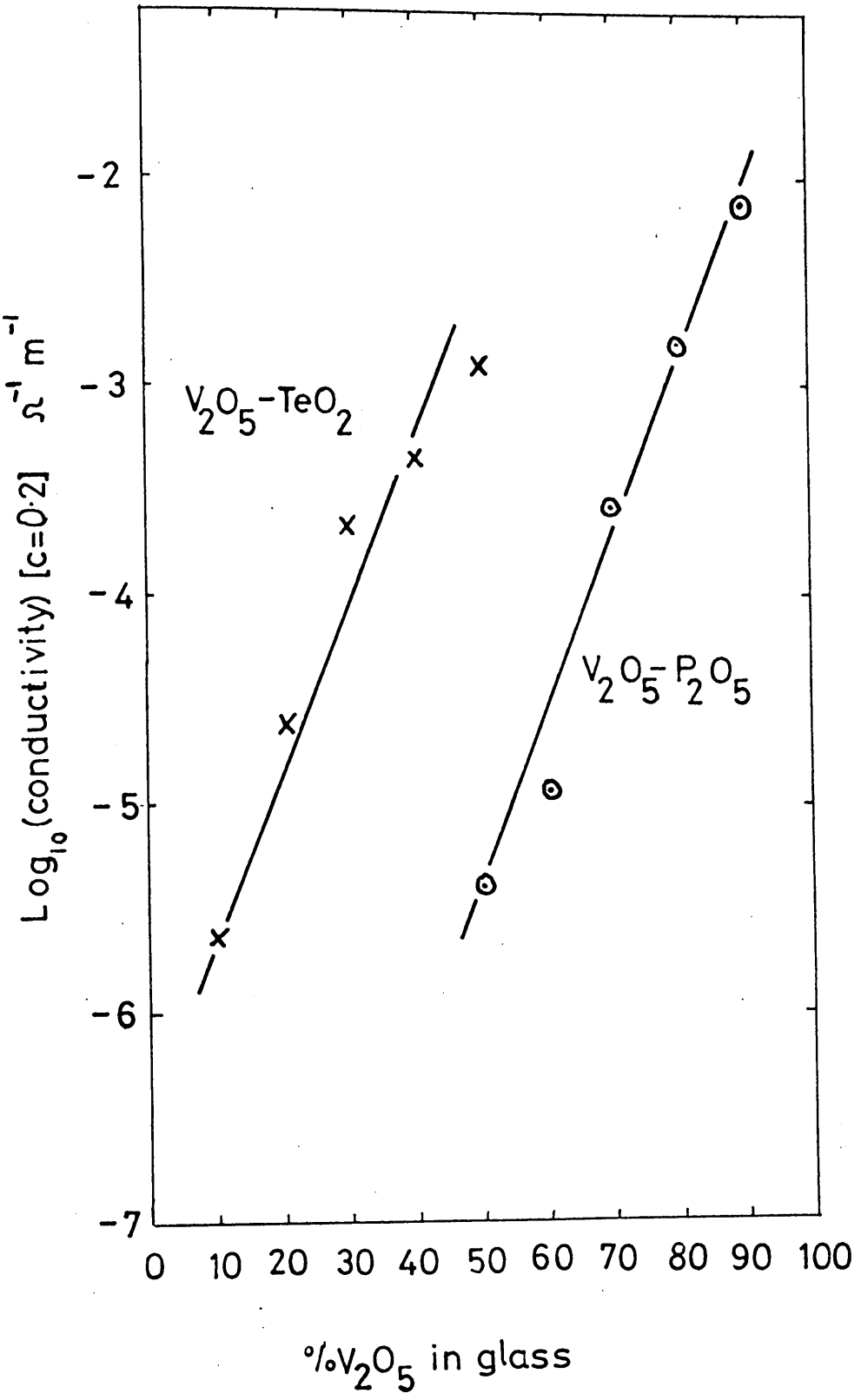

Fig. 6.7 Room temperature conductivity versus total vanadium content.

Sayer and Mansingh[39] noted that, at a fixed temperature, a plot of log (conductivity) versus activation energy (W) gives a common straight line of slope - (1/kT) for a wide variety of transition-metal phosphate glasses. This implies that the pre-exponential term (σ_0) in the Arrhennius-type expression for conductivity (Equation 6.1) is constant, thus

$$\log \sigma = \log \sigma_0 - \frac{W}{kT} \qquad \ldots (6.6)$$

and that the compositional variation is due almost entirely to variations in W. Whether this is true for other transition-metal oxide glass systems is difficult to determine since few have been studied in the same detail as the phosphates. A similar plot of log (conductivity at 300 K) and activation energy for the V_2O_5 - TeO_2 glasses used in the present work is shown in Figure 6.8 and by contrast to the phospates the slope is not -1/kT, indicating that σ_o varies markedly in the tellurite glasses. The variation of conductivity with composition, in the tellurites is caused by a variation in *both* the pre-exponential and the activation energy.

Figure 6.3 plots activation energy as a function of total vanadium content for both tellurite and phosphate glasses showing the lower activation energies of the tellurites, which along with the higher pre-exponentials accounts for their higher room temperature conductivity.

Conduction in transition-metal oxides can be described by the expression proposed by Mott[56] for conduction by hopping between

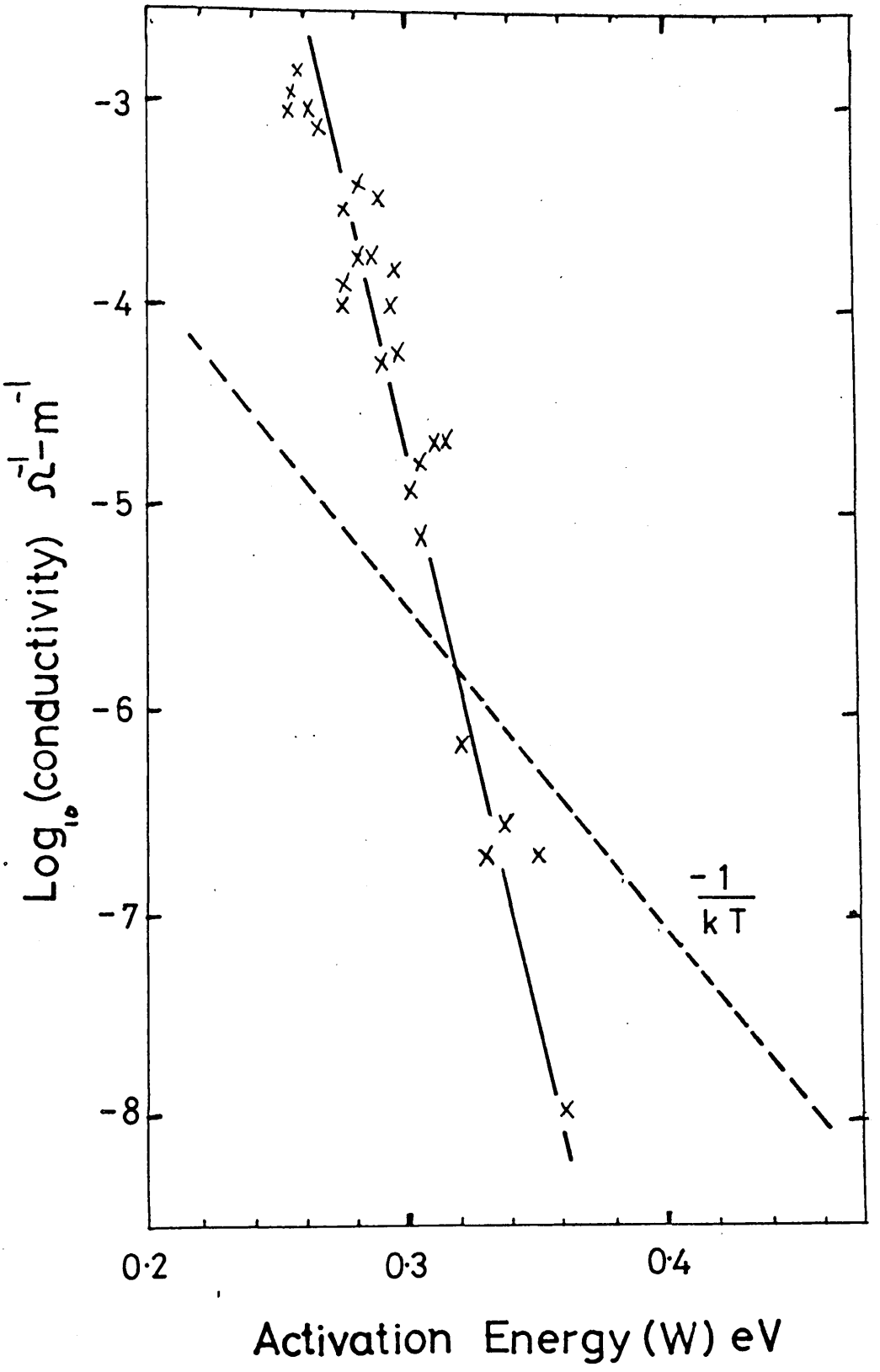

Fig. 6.8 Conductivity at 300 K versus activation energy.

localised states, namely (see Equation 4.6).

$$\sigma = \nu \frac{n e^2 a^2}{kT} \cdot c(1 - c) \exp(-2\alpha a) \exp\left(\frac{-W}{kT}\right) \quad \ldots (6.2)$$

where ν is a phonon frequency, N is the number of transition metal ion sites, a is site separation and α is a tunneling factor. The product $\nu e^{-2\alpha a}$ can be calculated from the experimental data by plotting log σT versus $\frac{I}{T}$ and extrapolating from 300 K to infinite temperature to obtain the pre-exponential term in Equation 6.5, i.e:

$$A = \nu \frac{n e^2 a^2}{kT} \cdot c(1 - c) \exp(-2a\alpha) \quad \ldots (6.7)$$

From density* and composition data on the glasses it was possible to obtain numerical values for the factors in Equation 6.7 and hence determine values of $\nu_e^{-2\alpha a}$, as tabulated in table 1 and the appendix:

Composition	Melt No.	$A(\Omega^{-1}m^{-1})$	$N(m^{-3})$	a(m)	c	νe^{-2a}
50% V_2O_5	45	1.6×10^{4}	1.12×10^{28}	4.2×10^{-10}	0.188	2.9×10^{10}
40% V_2O_5	40	1.0×10^{4}	9.0×10^{27}	4.4×10^{-10}	0.140	2.4×10^{10}
30% V_2O_5	34	3.0×10^{4}	8.5×10^{27}	4.7×10^{-10}	0.177	1.0×10^{10}
20% V_2O_5	28	1.0×10^{3}	5.5×10^{27}	5.4×10^{-10}	0.141	2.9×10^{9}
10% V_2O_5	51	1.8×10^{2}	3.3×10^{27}	6.3×10^{-10}	0.184	5.1×10^{8}

* The density data were determined for samples of bulk glass by weighing and measuring the volume of water displaced when the sample was placed in a calibrated vessel of water. The density of the glass, along with different crystal forms of V_2O_5 and TeO_2 is plotted as a function of composition in Fig 6.9.

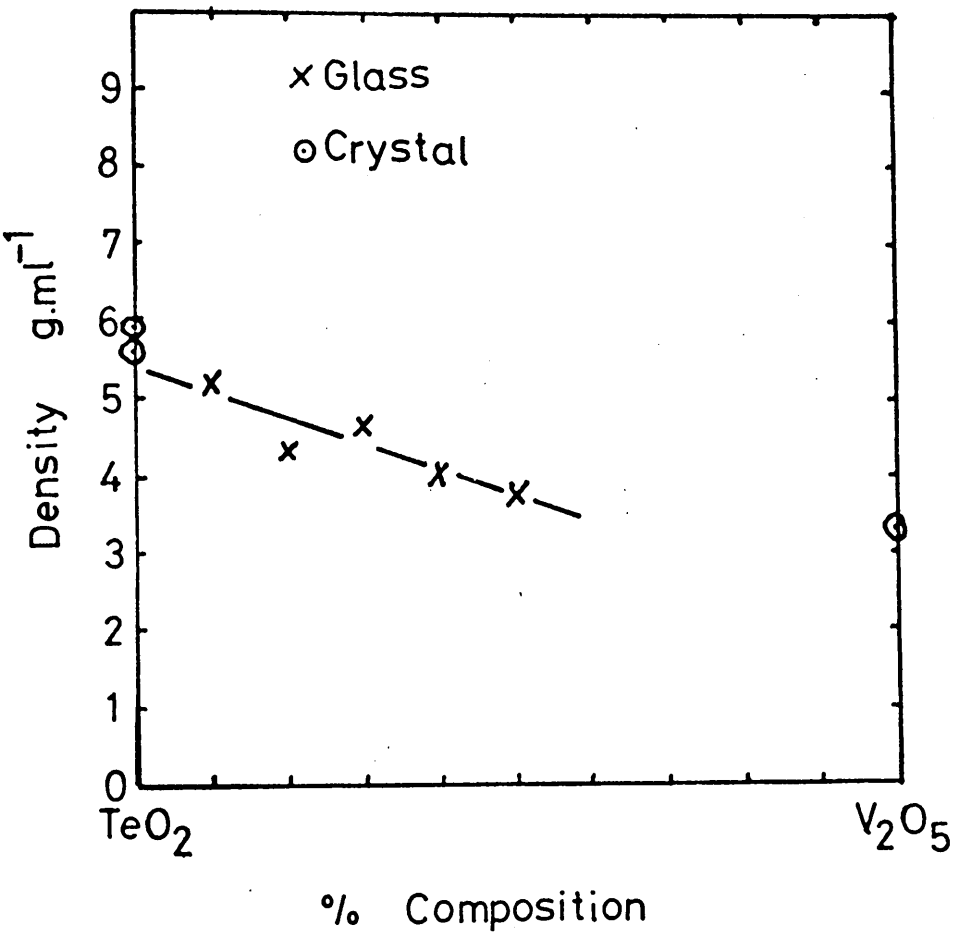

Fig. 6.9 Density versus composition for V_2O_5 - TeO_2 glass including points showing density of V_2O_5 and TeO_2.

The value of $\nu_{oe}^{-2\alpha a}$ is the number of site transitions a carrier makes per second. An estimate of α and ν can be made from Figure 6.11 in which log (νe^{-2a}) is plotted versus a, the site spacing. From the slope of this graph $\alpha \simeq 0.97$ Å^{-1}, in good agreement with data given by Austin and Garbett[75], and ν $6 \times 10^{13} S^{-1}$. The bars in Figure 6.10 indicate the spread caused by the different valence ratios of the different glasses. One feature worthy of note is that the tunneling factor can account for the exponential dependence of the pre-exponential on site spacing. This is in marked contrast to the phosphate glasses where no dependence of conductivity on site spacing is observed[39].

This analysis assumes that the phonon frequency is independent of site spacing but Sayer and Mansingh[39] found that it decreases as the site spacing is reduced. If this is also the case for V_2O_5 - TeO_2 glasses the estimate of the phonon frequency would be lowered from the rather high value of $6 \times 10^{13} S^{-1}$.

The reasons why V_2O_5 - TeO_2 glasses should be deifferent from V_2O_5 - P_2O_5 glasses in this respect are not obvious. One possibility is that Te sites can participate in the conduction process to a limited extent. Tellurium is known to exist in the valence states Te^{2-} and Te^{6+} as well as Te^{4+}. In the process of melting the glass it is likely that a small proportion of the TeO_2 is oxidised either by reaction with atmospheric oxygen above melt or by reaction with V_2O_5 thus:

$$TeO_2 + V_2O_5 \rightleftharpoons TeO_3 + V_2O_4$$

Under these conditions charge transfer could occur between Te ions

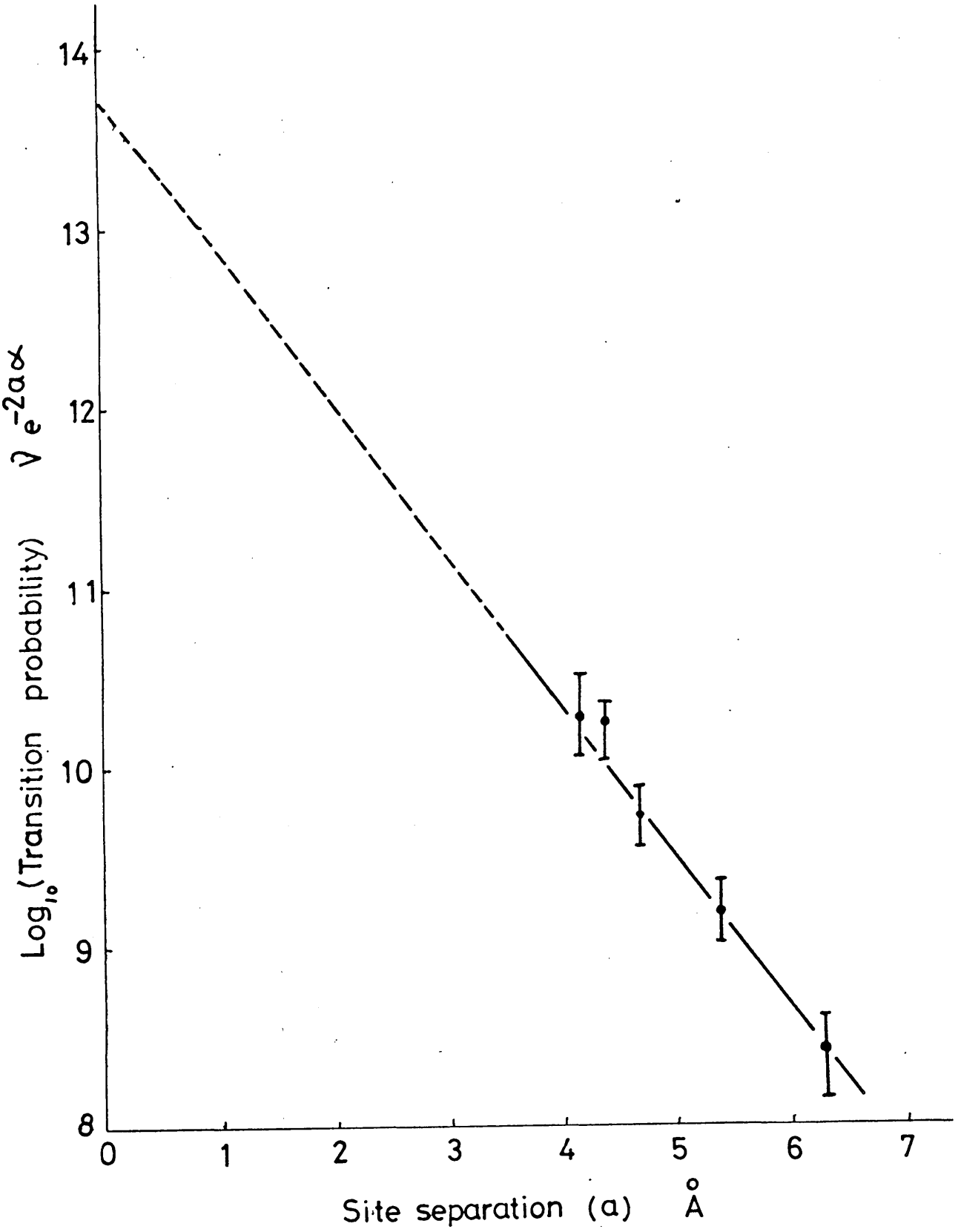

Fig. 6.10 Carrier transition probability versus site spacing.

or between Te and V ions enabling an additional range of possible charge transfer processes to occur.

6.2.1 Composition Dependence of Thermo-electric Power Above Room Temperature

The thermopower (or Seebeck coefficient α) of all specimens was measured in the range 290 K to 400 K and data for some typical compositions are shown in Figure 6.11 demonstrating that α is virtually independent of temperature in this region and influenced mainly by composition. Generally the thermopower becomes smaller on reducing the V_2O_5 content of the glass, probably in part because the V^{4+}: V_{Tot} ratio increases as the vanadium content of the glass decreases.

The results of the room temperature measurements of thermopower for glasses of different compositions are plotted in Figure 6.12 as a function of V^{4+}: V_{Tot} ratio. Also shown in this graph is a dotted line corresponding to Heikes and Ure's[21] expression for the thermopower in narrow-band semiconductors, assuming that the entropy term $\Delta S_R/k$ is negligibly small

$$\alpha = \frac{k}{e}\left\{\frac{\Delta S_R}{k} + \ln\left(\frac{c}{1-c}\right)\right\} \qquad \ldots (6.8)$$

where α = thermopower

c = fraction of sites occupied by an electron

Heikes and Ure[21] do not define the term $\Delta S_R/k$ but Austin and Mott[22] suggest that it has a value between 0.1 and 0.2 and consequently can be neglected.

The experimental results (Figure 6.12) do not agree well with

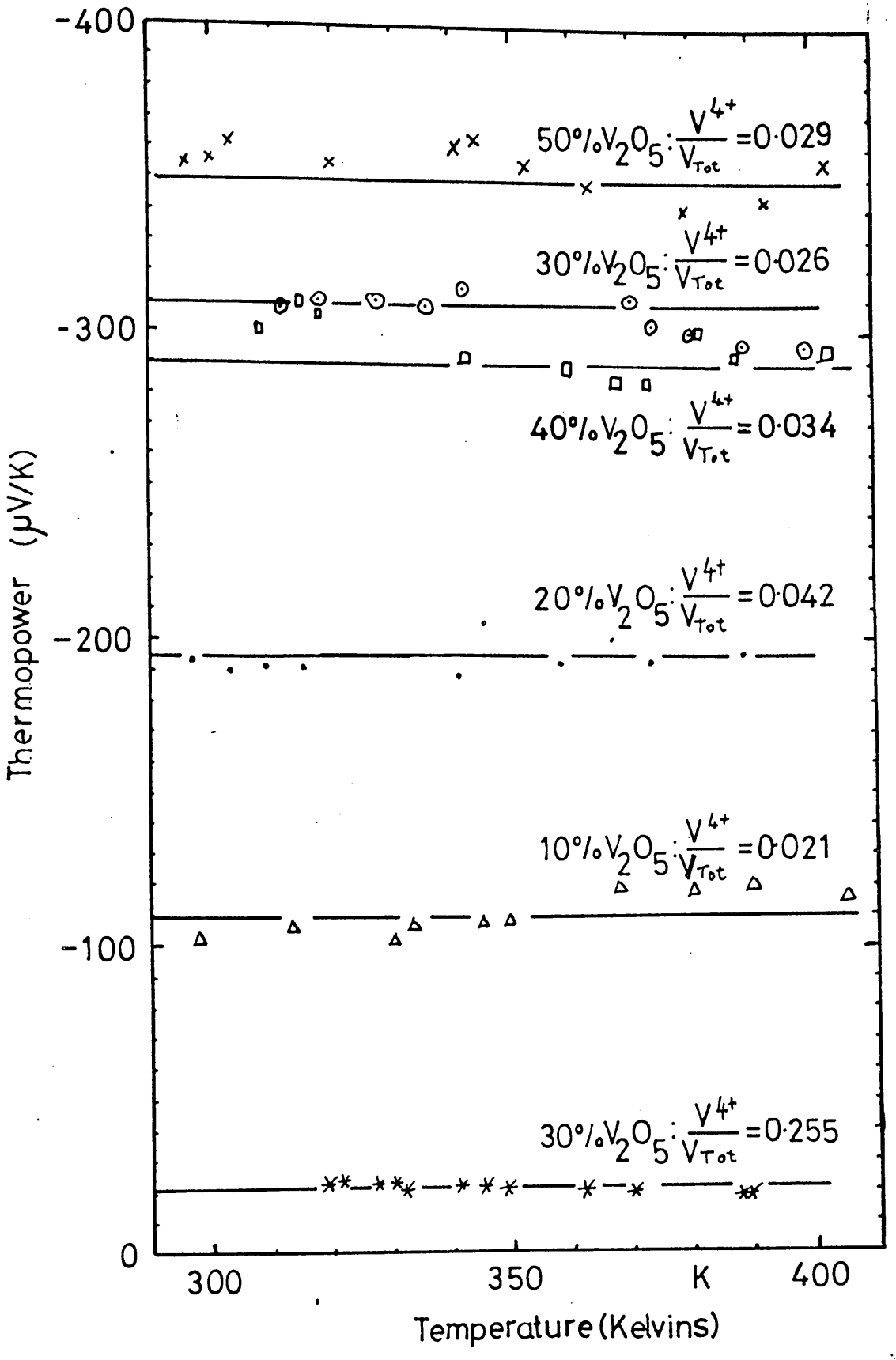

Fig. 6.11 Thermopower of some typical V_2O_5 - TeO_2 glasses as a function of temperature above room temperature.

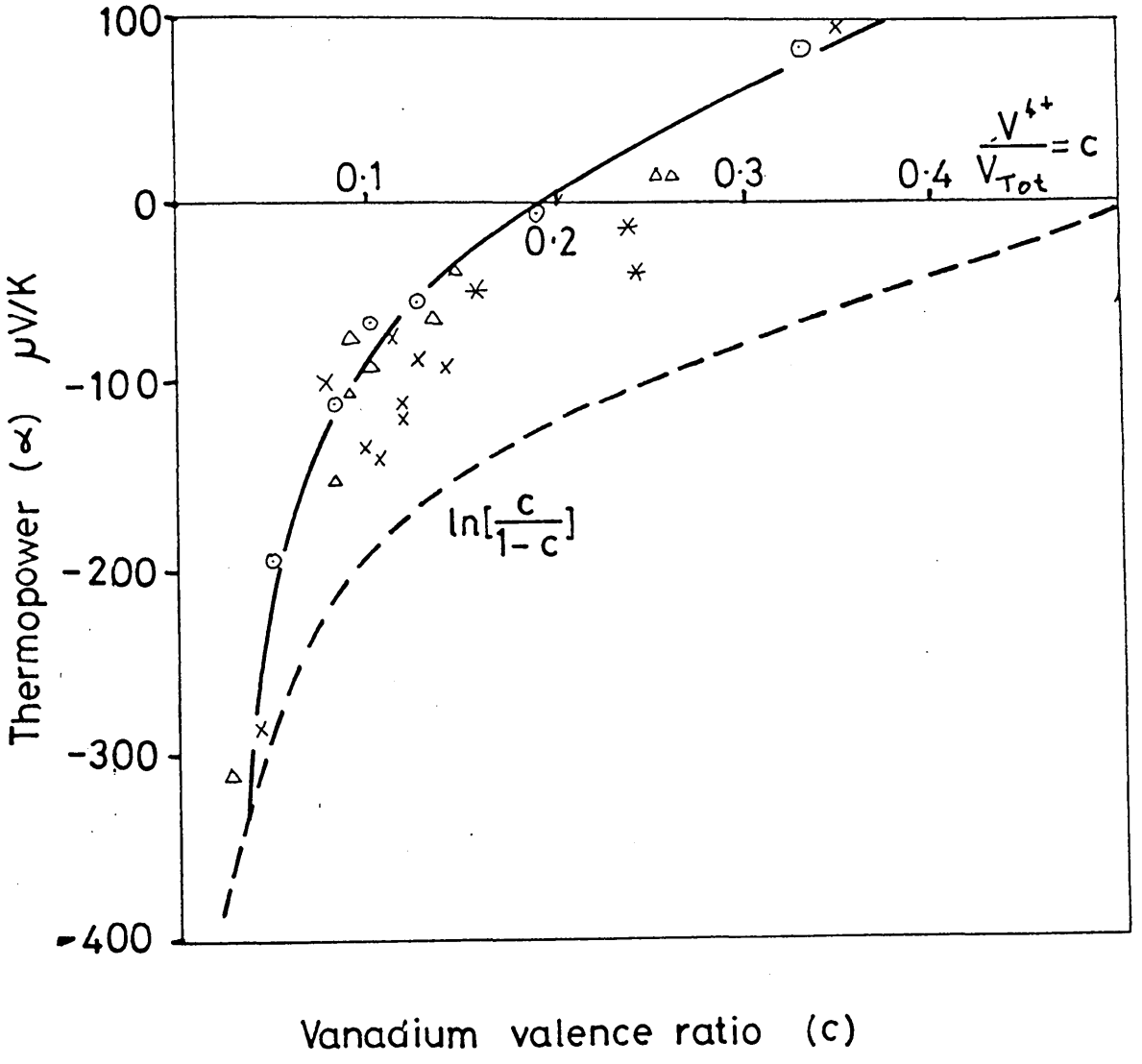

Fig. 6.12 Valence ratio dependence of thermopower.

values of α calculated from equation 6.8 using the (V^{4+}: V_{Tot}) ratios obtained from the chemical analyses (see Section 5.4), although the experimental and calculated curves do have the same shape. Note, however, that $\alpha = 0$ at (V^{4+}: V_{Tot}) $\simeq$ 0.2 which is the same ratio at which the conductivity goes through a maximum. Nester and Kingery[23] obtained surprisingly good agreement between the measured and calculated values, while Linsley[40] found that there is a considerable discrepancy.

Similar arguements are applicable to the variation of the thermopower with valence ratio, as were applied to the conductivity. Again it appears that not all of the five-valent vanadium is able to participate in the conduction process, suggesting that the structural complexing of vanadium ions into macromolecules within the glass where it is isolated from the conduction process. Another possibility is that glass-glass phase separation occurs, isolating a proportion of the V^{5+} ions in one phase. The remainder is left with a higher V^{4+}: V_{Tot} ratio than the glass as a whole causing a shift in the point at which the thermopower changes sign. Such glass-glass phase separation has been observed by Bogomolova et al in vanadium phosphate glasses, by means of electron microscopy,and used by them to explain the shift in the conductivity maximum.

6.2.2 Temperature Dependence of Thermopower at Low Temperatures

The thermopower in several V_2O_5 - TeO_2 glasses of different composition was measured as a function of temperature from 400 K to 120 K. As mentioned in the previous section α is virtually temperature-independent down to about 200 K but thereafter it decreases with temperature.

There is some confusion in the literature about the low-temperature variation of α in V_2O_5 - P_2O_5 glasses. Brown[63] reported a very rapid *increase* with decreasing temperature, while according to Nester and Kingery[23] α *decreases*, apparently linearly with temperature. In figure 6.13 the thermopower of various V_2O_5 - TeO_2 glasses is plotted as a function of temperature over the range 400 - 120 K. For each composition the thermopower is constant at temperatures above about 200 K, but below this temperature it decreases to a point where measurement was limited by the resistance of the sample. Measurements were made down to 120 K on the more conducting samples while on the more resistive compositions it was not possible to extend the measurements as far.

From this data it is possible to estimate the disorder energy (W_D) in two ways. Mott[56] argues that for conduction in a material having an impurity bandwidth (W_D in this case) greater than kT, whether transport is by hopping or not, the "metallic" type formula for thermopower applies, i.e:

$$\alpha = \frac{\pi^2}{3} \cdot \frac{k^2 T}{e} \frac{d(\ln \sigma)}{dE} \quad \text{when } W_D > kT \qquad \ldots (6.9)$$

Substituting the Arrhennius-type of temperature dependence for conductivity the thermopower becomes

$$\alpha = \frac{\pi^2 k}{3e} \left\{ \frac{d(\ln \sigma)}{dE} - \frac{dW_D}{dE} \right\} \quad \text{when } W_D > kT \qquad \ldots (6.10)$$

ie, α is temperature-dependent when $W_D > kT$

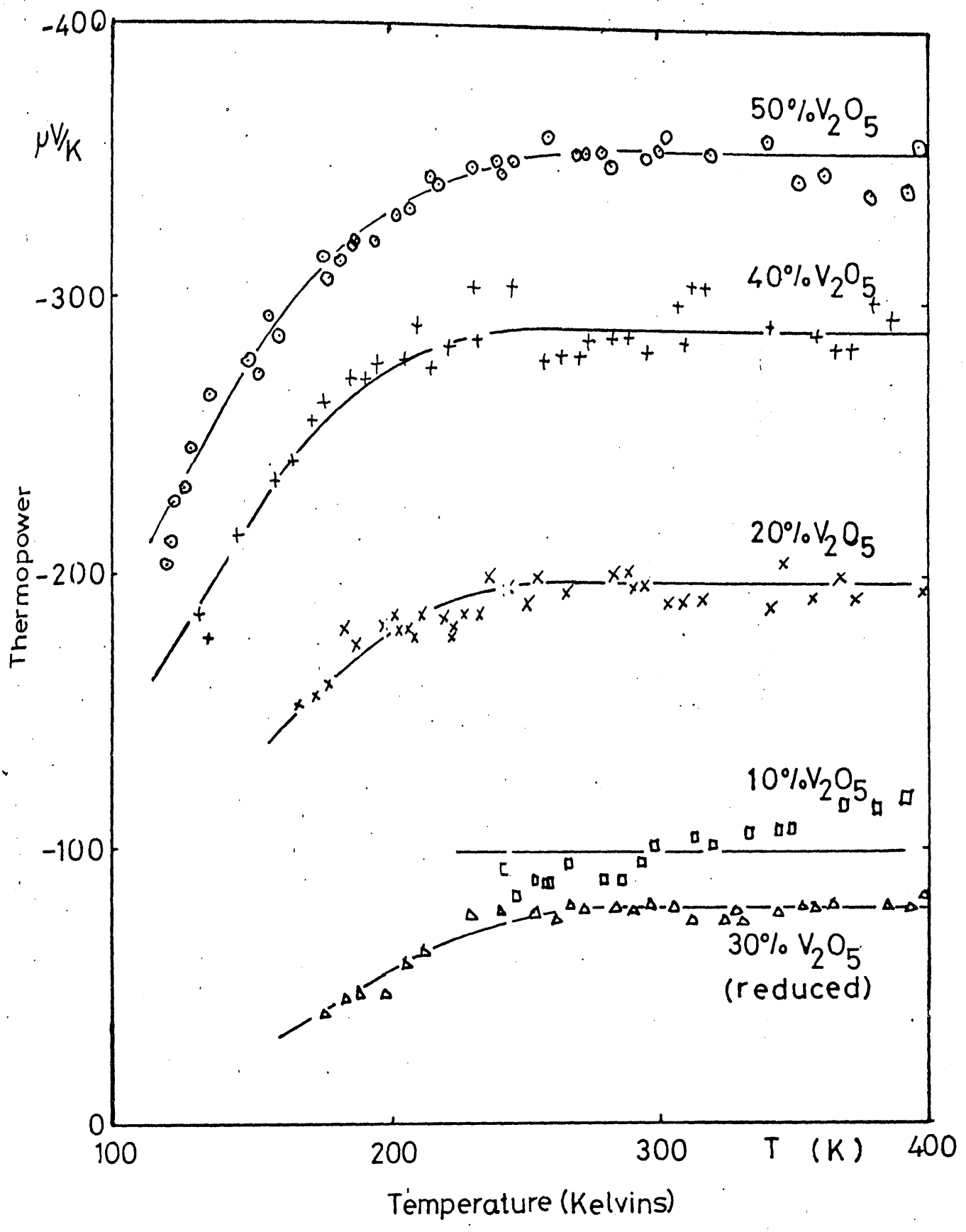

Fig. 6.13 Thermopower as a function of temperature below room temperature.

When $kT > W_D$, however, the thermopower is known to obey the Heikes[21] relationship (Equation 6.8) and be temperature-independent. This implies that the thermopower changes from being temperature-independent to temperature-dependent when $kT \approx W_D$. Experimentally this is found to occur at about 200 K, (Figure 6.13) giving a value W_D a value of $\simeq$ 0.0 2 eV. This is rather lower than some other published data. Other authors have estimated W_D in yet different ways. Sayer and Mansingh[39], for example, equated W_D with the activation energy for conduction at the lowest temperatures of measurement ($\tilde{\sim}$ 80 K) and they estimate $W_D \sim$ 0.1 eV. Even at 80 K, however, their results for log σ versus (1/T) are still exhibiting a decreasing slope which suggests that 0.1 eV can only be an upper limit for W_D. Greaves[88] obtains a very high value of 0.4 eV on the assumption of variable range hopping occuring at low temperatures[56]. This procedure is probably not valid for the vanadate glasses in view of the unacceptably high disorder energy obtained.

Alternatively one can regard the disorder energy W_D as the energy required to produce an equilibrium number of carriers at low temperatures and according to Emin[60] the themopower associated with a charge e moving in a molecular crystal lattice is then given by (using Emins notation)

$$\alpha = \frac{-k}{e} \left(\frac{Eo}{kT}\right) = \frac{Eo}{eT} \qquad 6.11$$

where Eo is the energy for the thermal generation of carriers, and corresponds to W_D in the present context.

In Figures 6.14 α is plotted versus (I/T) and the activation energy for the thermopower (i.e. W_D) at low temperature is approximately

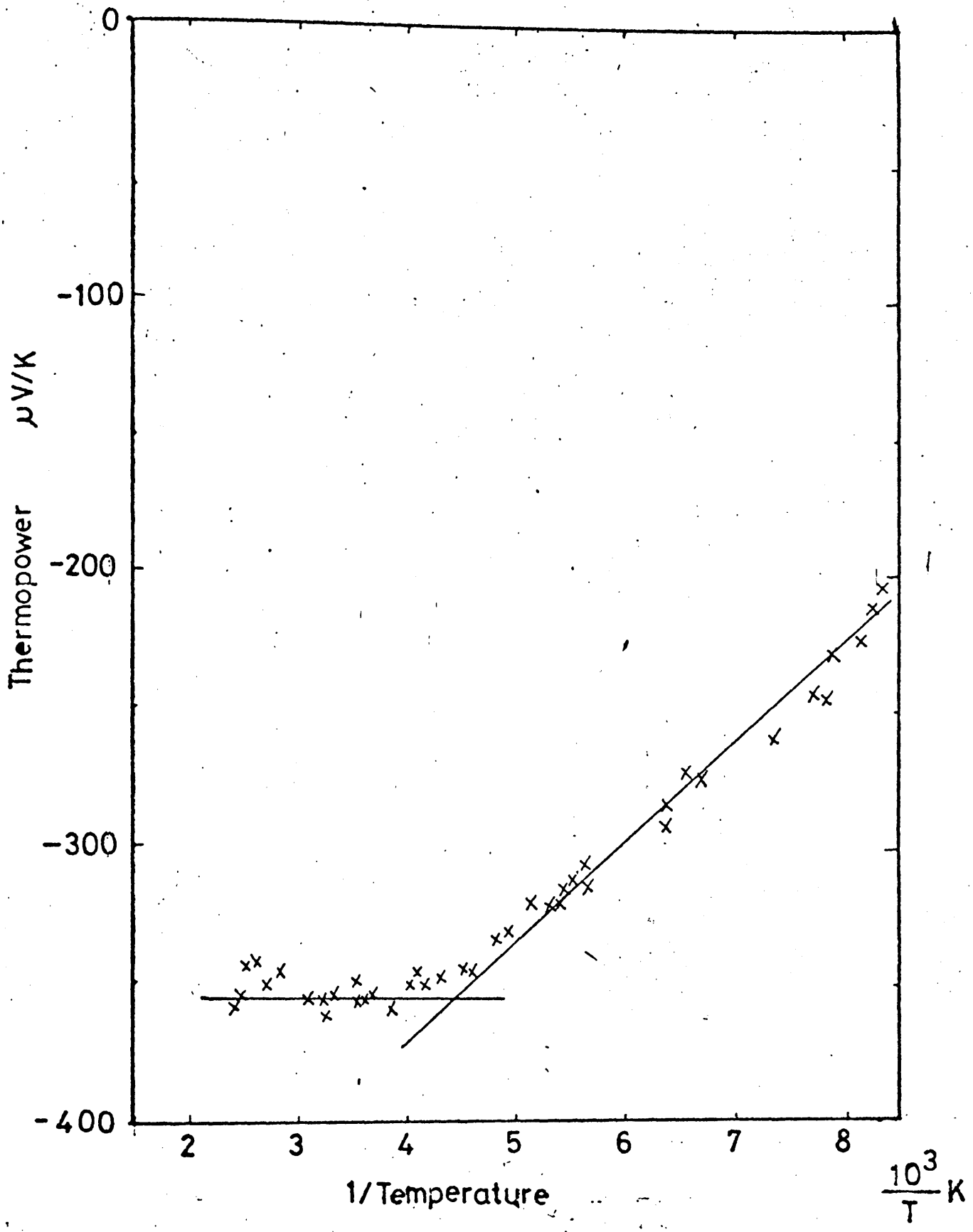

Fig. 6.14a Thermopower versus inverse temperature in a 50% V_2O_5 - 50% TeO_2 glass.

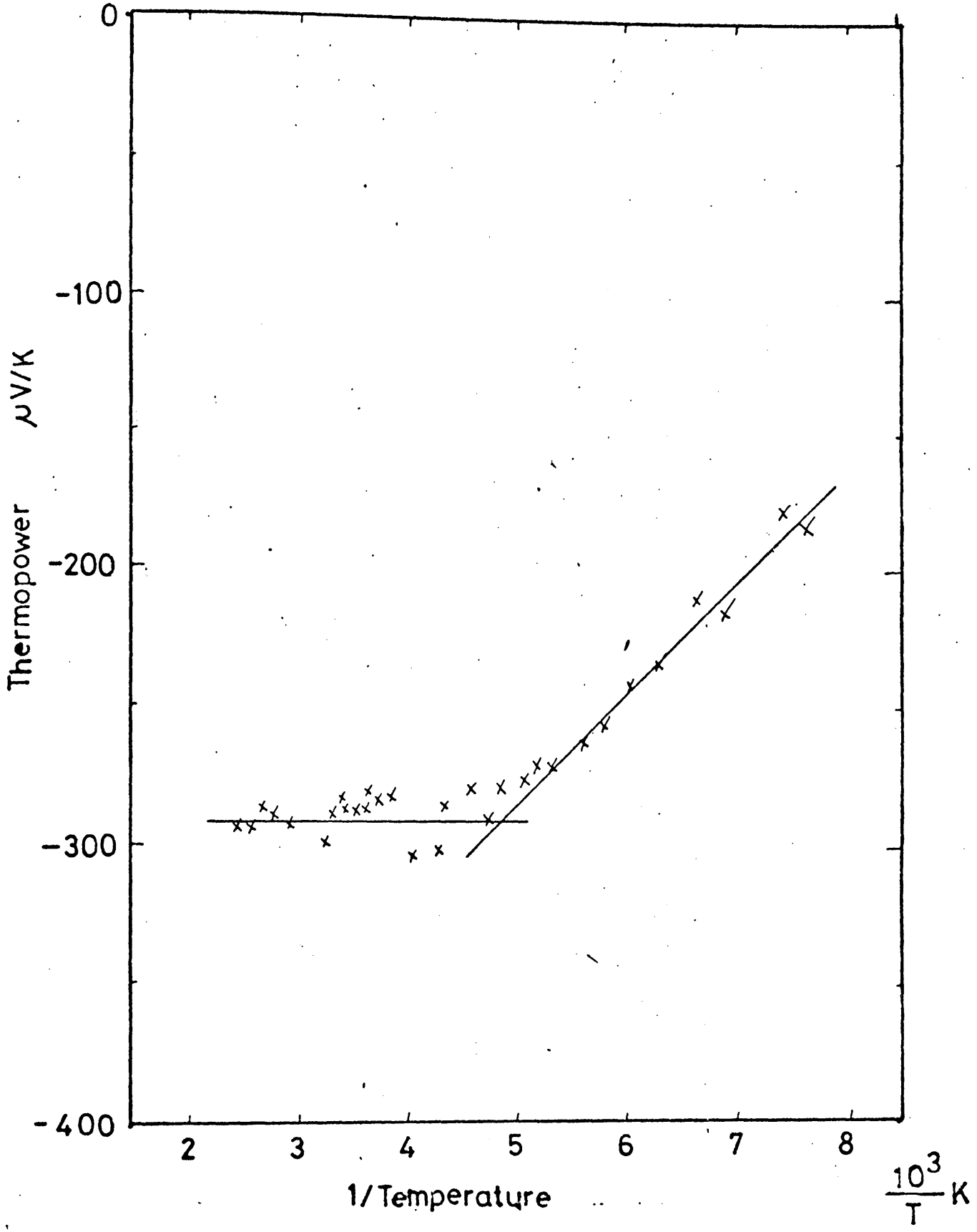

Fig. 6.14b Thermopower versus inverse temperature in a 40% V_2O_5 - 60% TeO_2 glass.

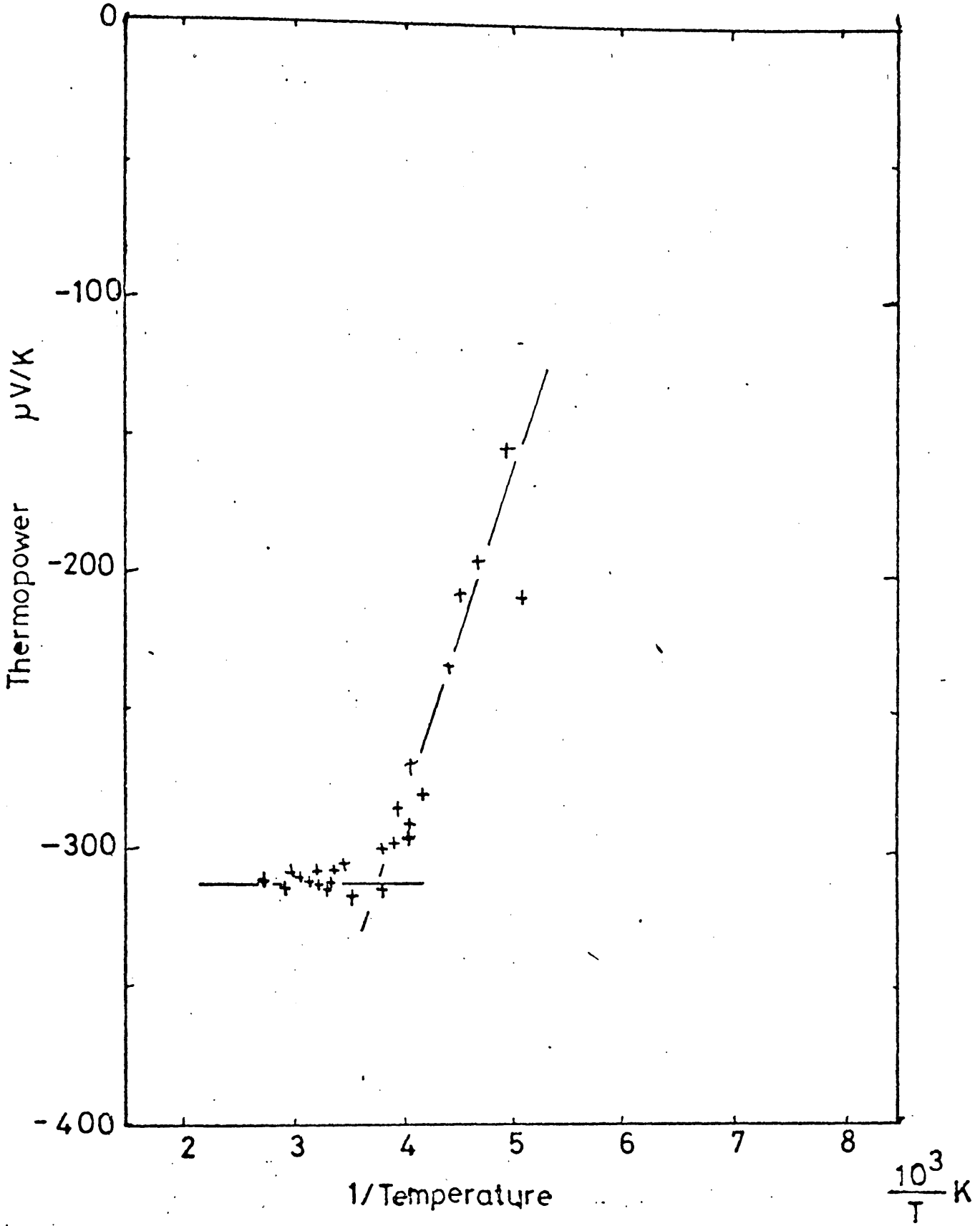

Fig. 6.14c Thermopower versus inverse temperature in a 30% V_2O_5 - 70% TeO_2 glass.

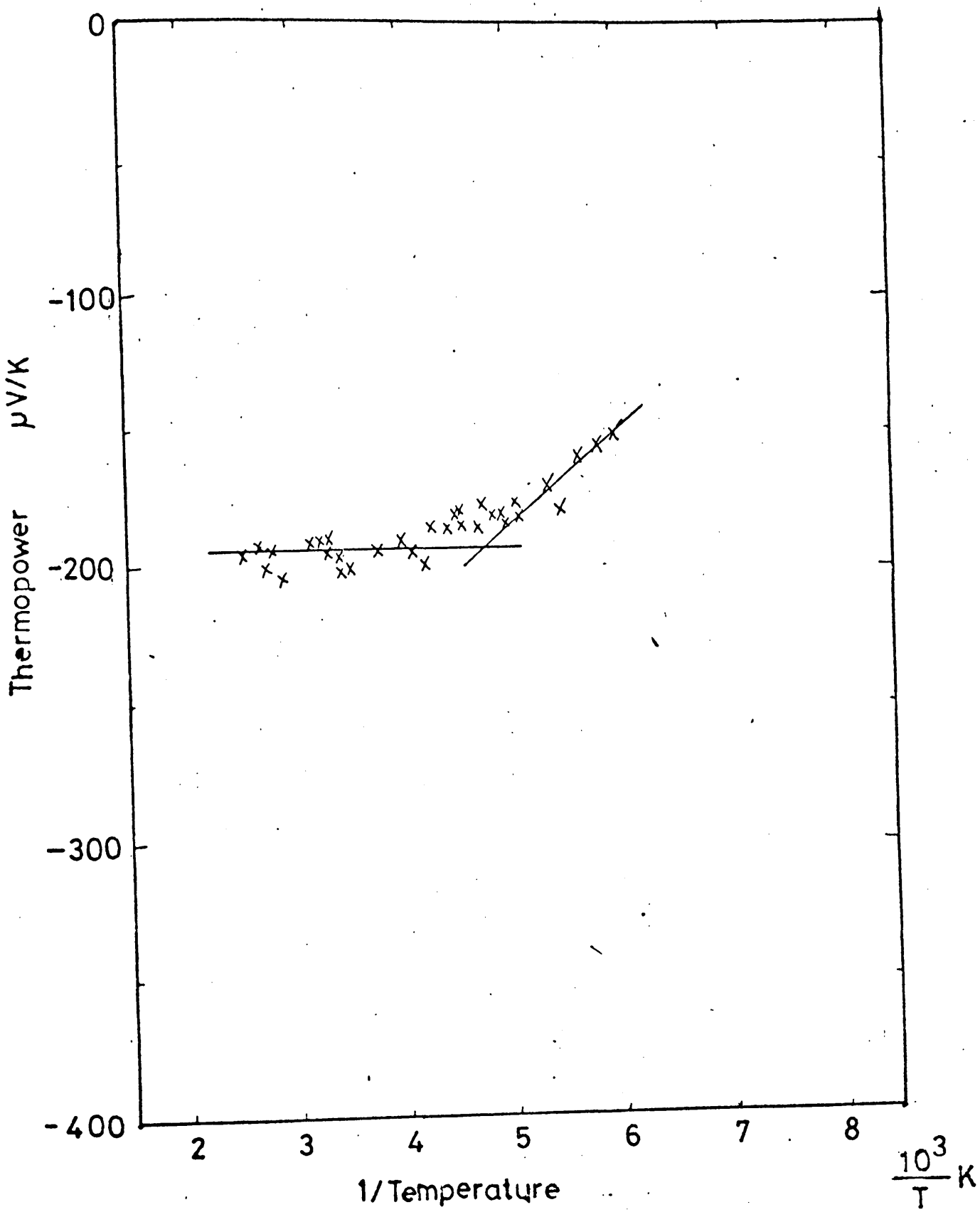

Fig. 6.14d Thermopower versus inverse temperature in a 20% V_2O_5 - 80% TeO_2 glass.

0.02 eV for each of the glasses studied. This is in good agreement with the value obtained from the temperature at which the transition occurs between temperature-dependent and temperature-independent behaviour, but both methods give smaller results than previously suggested measurements of conductivity activation energy at low temperatures. This supports Emin's theory of conduction by phonon assisted jumping of carriers, according to which thermally activated hopping of carriers can occur at much lower temperatures than predicted by Snakenberg[57]. Because the phonon freeze-out is much slower it is reasonable to expect that a small disorder energy would be masked by the contribution to the conductivity activation energy from the residual hopping energy. Only at temperatures below $T \simeq \frac{\theta_D}{8}$ where the activation energy is solely due to disorder should conductivity plot as a straight line with a slope corresponding to the disorder energy W_D. It is likely that such temperatures are never reached in the present measurements since an estimate of the Debye temperature based on the first break in the conductivity-temperature curve indicates that θ_D is around 400 K. The present measurements were limited, by the use of liquid nitrogen as the refrigerent to temperatures > 77 K, so W_D will be smaller than the activation energy observed at this temperature. This estimate of θ_D is close to others appearing in the literature for other vanadate glass systems. Farley and Saunders[87] estimate it to be about 400 K from studies of the elastic properties of vanadium phosphate glasses.

An intuitive estimate of the upper limit for the size of W_D can be made from the transition temperature of the glass. This is the temperature at which the disorder is "frozen" into the glass, thus it is

reasonable to expect that

$$W_D \simeq kTg \qquad \ldots (6.12)$$

where Tg is the glass transformation temperature in Kelvins. This gives an estimate of 0.06 eV for most vanadate which is reduced slightly by annealing.

6.3 OPTICAL PROPERTIES OF THE V_2O_5 - TeO_2 GLASS SYSTEM

6.3.1 Introduction

All of the glasses in the composition range 10 - 50 mole % V_2O_5 were opaque to the eye in all but very thin (< 5 μm) sections. In sections 2 μm or less they appear reddish-brown in transmission when only slightly reduced. When heavily reduced (V^{4+}: $V_{Tot} \simeq 0.25$) they have a marked greenish tinge in transmission. The bulk glass appears black in reflection.

The optical absorption ($\propto$ opt) was measured as a function of incident photon energy E = hν over the composition range 10 - 50 mole % V_2O_5, both at 77 K and room temperature. The effects of varying the (V^{4+}: V_{Tot}) ratio on a glass with 40 mole % V_2O_5 were observed at low $\propto$.

6.3.2 Optical Absorption Variation With Vanadium Concentration and Temperature

The results of the optical absorption measurements as a function of photon energy at room temperature (∿ 300 K) and 77 K are shown in Figures 6.15. A steep absorption edge is observed for each glass at

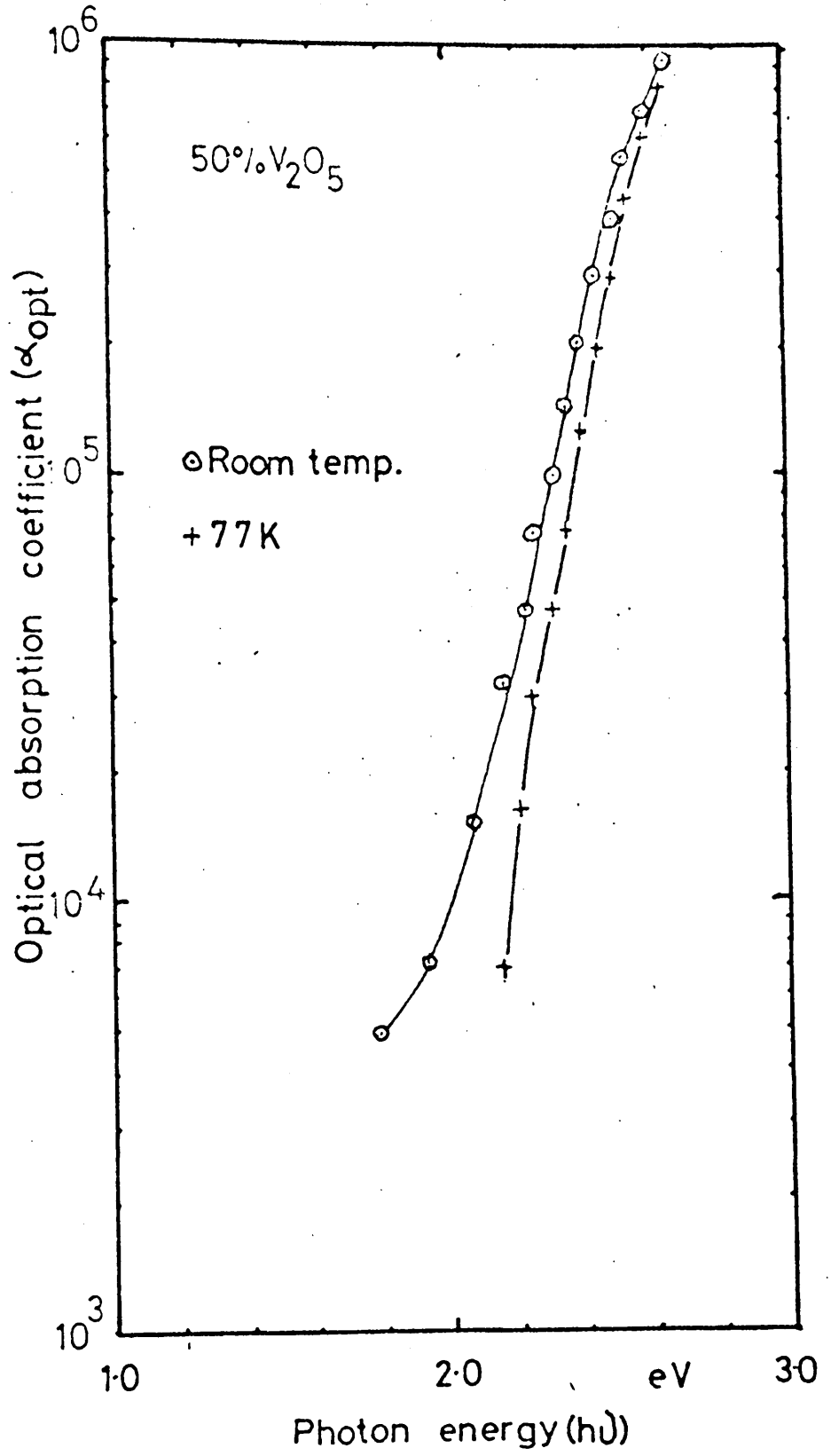

Fig. 6.15a Optical absorption coefficient versus photon energy in a 50% V_2O_5 - 50% TeO_2 glass.

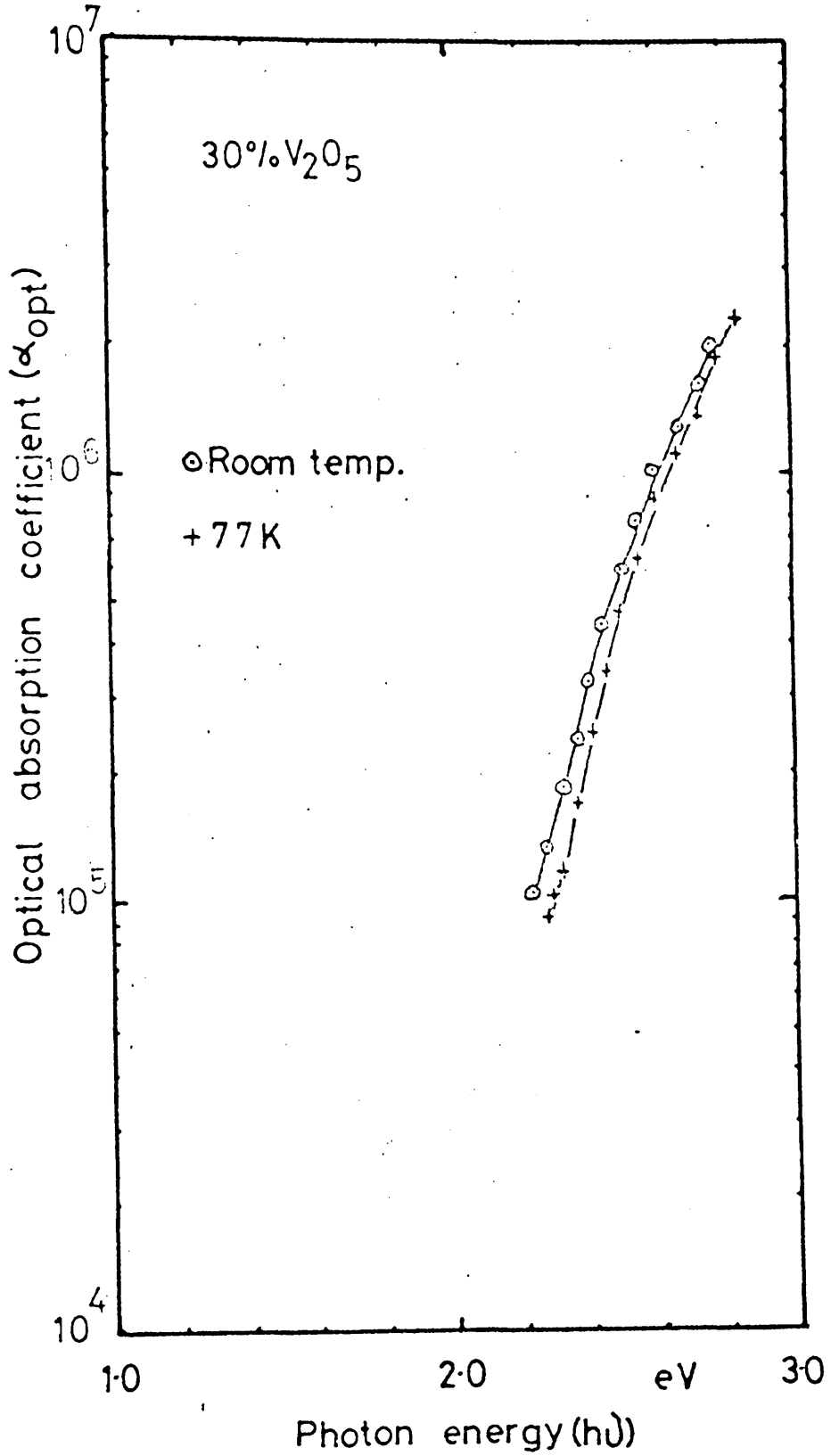

Fig. 6.15b Optical absorption coefficient versus photon energy in a 30% V_2O_5 - 70% TeO_2 glass.

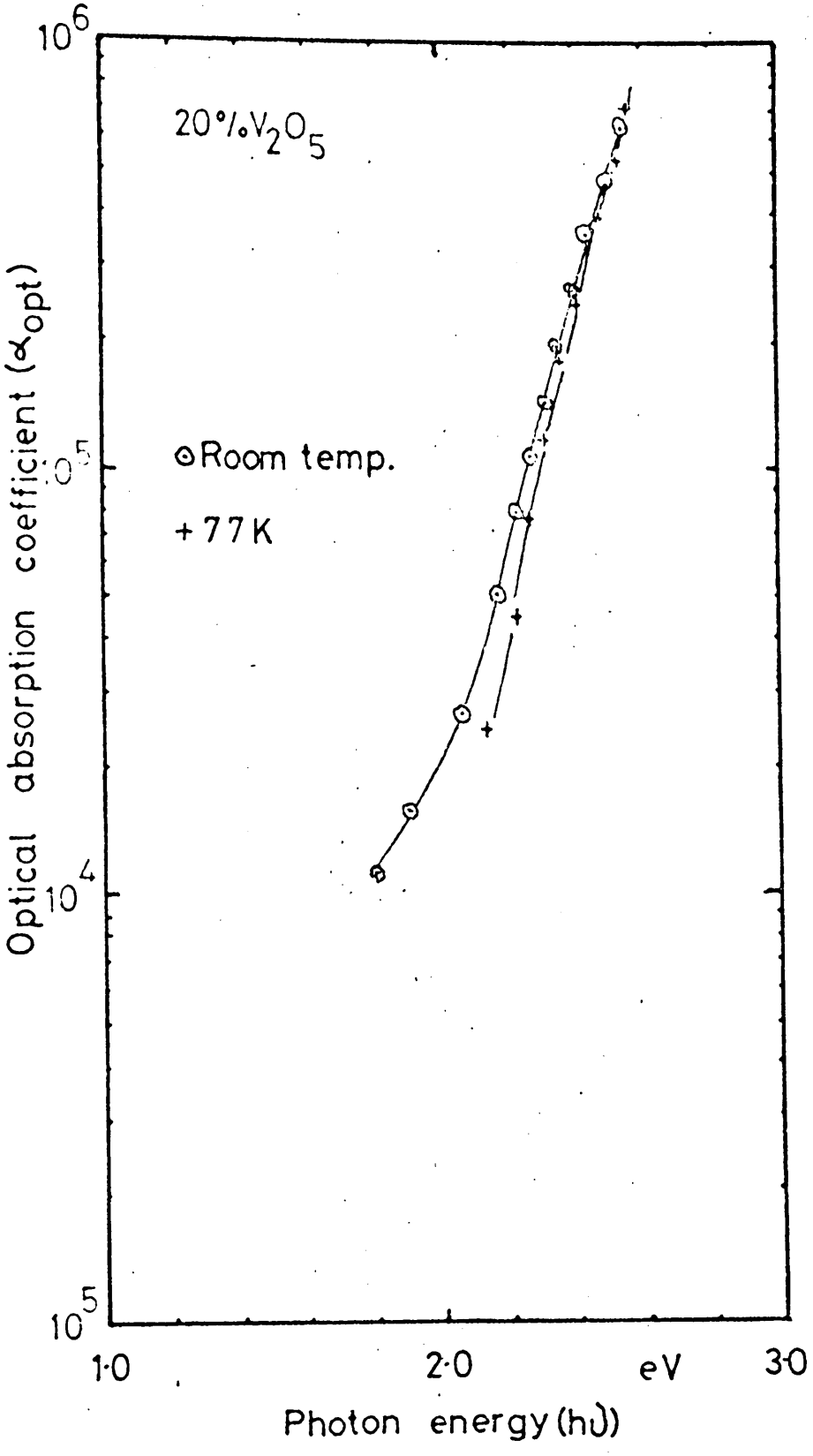

Fig. 6.15c Optical absorption coefficient versus photon energy in a 20% V_2O_5 - 80% TeO_2 glass.

about 2.2 to 2.4 eV, at room temperature, with a small shift of about 0.05 eV to higher energies on lowering the temperature to 77 K. In the vanadium phosphate glasses the fundamental edge is thought[52] to arise from direct forbidden transitions between the oxygen 2p bands and the vanadium 3d bands of the V_2O_5 in the glass. The fundamental absorption edge in the V_2O_5 - TeO_2 glasses probably arises from the same mechanism. The position of the edge at 2.2 eV was found to be independent of total vanadium content and the percentage of reduced vanadium, supporting the conclusion that the fundamental edge is the result of direct forbidden transitions between the oxygen 2p bands and the vanadium 3d band of the V_2O_5. Farther support for this view is supplied by the optical absorption behaviour of crystalline V_2O_5. Kenny et al[89] measured the absorption coefficient in V_2O_5, along the different crystal axes, and found, for each, a fundamental absorption edge increasing from 2.2 eV, which they attribute to direct forbidden transitions.

6.3.3 Variation of Optical Absorption with $(V^{4+}:V_{Tot})$ Ratio

The absorption of glasses of the composition $(V_2O_5)_{40}(TeO_2)_{60}$ was studied at low values of α_{opt} in the region of the absorption tail in order to observe the effects of varying the $(V^{4+}:V_{Tot})$ ratio. It was necessary to use samples 10 to 50 m thick to produce a measureable amount of absorption and they were produced by blowing bubbles from different melts having known $(V^{4+}:V_{Tot})$ ratios. Typical results are shown in Figure 6.16 for two samples of 40 mole % V_2O_5 glass with different $(V^{4+}:V_{Tot})$ ratios. At the lower end of the absorption curve a shoulder appears which increases in intensity as the vanadium in the glass is progressively reduced. This shoulder is interpreted as being the combination of a broad absorption band and the tail

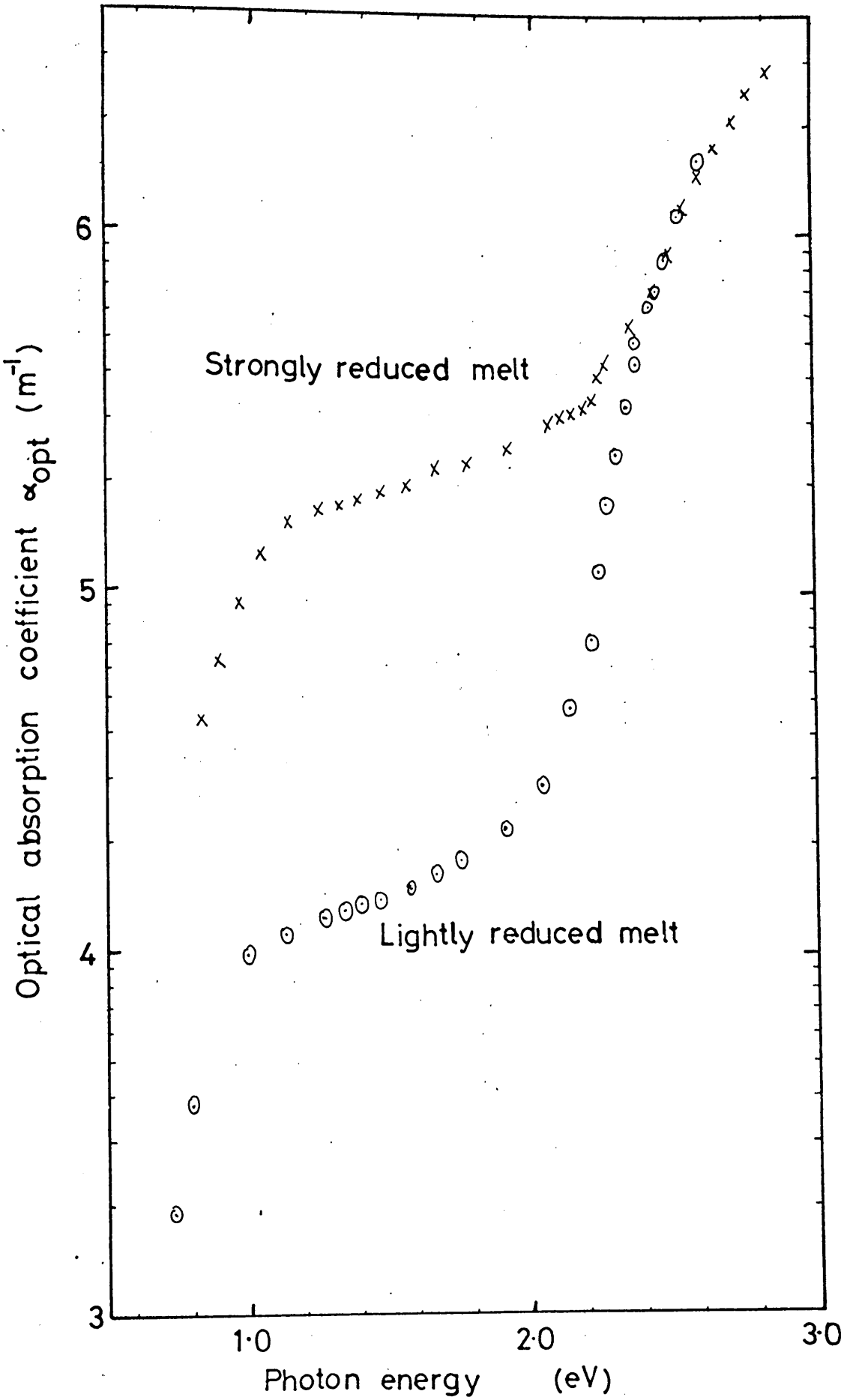

Fig. 6.16 Optical absorption versus photon energy for different V^{4+}: V_{Tot} ratios in a 40% V_2O_5 - 60% V_2O_5 glass.

of the absorption edge.

Small polaron theory predicts[22] a series of absorption lines at multiples of twice the polaron binding energy (W_p), which are broadened by thermal motion of the lattice, resulting in a series of Gaussian absorption peaks. This absorption arises from the optical excitation of a carrier from its polarisation well and subsequent transfer to another lattice site, corresponding, in a vanadate glass, to the transfer of an electron from a V^{4+} site to a V^{5+} site. In the vanadate glasses it is only possible, in practice, to observe the first absorption peak since the fundamental absorption edge arising from the 2p and 3d direct forbidden transitions of the V_2O_5 masks the higher order peaks.

The position of the polaron absorption peak can be related to the d.c. conductivity and the thermopower data through

$$h\nu = E_{opt} = 2 W_p \qquad \ldots (6.13)$$

where E_{opt} is the incident photon energy and Wp is the polaron binding energy. The polaron binding energy is related to the hopping energy W_H[22] by

$$W_H = \tfrac{1}{2} W_p \qquad \ldots (6.14)$$

Therefore, $$h\nu = E_{opt} = 4 W_H \qquad \ldots (6.15)$$

But $$W_H = W - \tfrac{1}{2} W_D \qquad \ldots (6.16)$$

where W is the conduction activation energy and W_D is the disorder energy.

Typically for a 40 mole % V_2O_5 glass W is 0.28 eV and the thermopower data gives a value of 0.02 eV for W_D.

$$\text{Therefore,} \qquad E_{opt} \simeq 1.1 \text{ eV}$$

This agrees well with the position of the shoulder in the absorption edge (1.1 - 1.3 eV), shown in Figure 6.16, indicating a polaron binding energy of 0.6 eV.

It is reasonable, therefore, to interpret the shoulder in terms of polaron hopping but the present evidence is not sufficient to discount the possibility of it arising from an internal d-d excitation of electrons in the vanadium atoms. To make this distinction unequivicically it would be necessary to measure the electro-modulation spectra and observe whether or not the position of the peak was shifted by the application of an electric field.

6.4 HIGH ELECTRIC FIELD BEHAVIOUR OF d.c. CONDUCTIVITY IN V_2O_5 - TeO_2 GLASSES

The d.c. conductivity was measured as a function of electric field in the composition range 20 - 50 mole % V_2O_5 using voltage pulses of 10 μ S duration. Figures 6.17 shows the data from these measurements plotted as the conductivity enhancement factor, i.e. the ratio of high to low field conductivity ($\frac{\sigma(E)}{\sigma(0)}$), versus the product of applied electric field and inverse temperature.

The data can be fitted to a curve of the form

$$Y = \frac{\text{Sinh } (mx)}{mx} \qquad \ldots (6.17)$$

A field dependence of this form is typical for a simple field assisted hopping process where all of the carriers are localised. Figure 6.18 is a simple model of a typical high field hopping process where all the carriers are localised in potential wells. The jump of hopping distance is a_j and the applied electric field is E. The potential barrier in the direction of the field is lowered by

$$E \cdot a_j/2$$

while in the direction against the field it is raised by the same amount, thus, neglecting the effects of structural disorder, the jump rates for hopping up and down the field are :

$$\text{Jump rate up field} = \nu \exp\left(\frac{-W}{kT} - \frac{eaE}{2kT}\right) \qquad \ldots(6.18)$$

$$\text{Jump rate down field} = \nu \exp\left(\frac{-W}{kT} + \frac{eaE}{2kT}\right) \qquad \ldots(6.19)$$

$$\therefore \mu = \frac{\nu a}{E}\left\{\exp\left(\frac{-W}{kT} + \frac{eaE}{2kT}\right) - \exp\left(\frac{-W}{kT} - \frac{eaE}{2kT}\right)\right\} \qquad \ldots(6.20)$$

$$\mu = 2\frac{\nu a}{E} \cdot \exp\left(\frac{-W}{kT}\right) \cdot \sinh\left(\frac{eaE}{2kT}\right) \qquad \ldots(6.21)$$

where ν is a phonon frequency

a is the jump distance

W is the activation energy for conduction

but $\sigma = ne\mu$ when n is the carrier concentration.

$$\therefore \sigma(E) = 2\frac{nea}{E}\nu \cdot \exp\left(\frac{-W}{kT}\right) \cdot \sinh\left(\frac{eaE}{2kT}\right)$$

$$= \frac{ne^2a^2}{kT}\nu \exp\left(\frac{-W}{kT}\right) \cdot \frac{2kT}{eaE} \sinh\left(\frac{eaE}{2kT}\right)$$

$$= \sigma(0) \cdot \sinh\left(\frac{eaE}{2kT}\right) \cdot \frac{2kT}{eaE} \qquad \ldots(6.22)$$

where $\sigma(0) = \frac{ne^2a^2}{kT}\nu \exp\left(\frac{-W}{kT}\right)$, ie, the low field conductivity.

By fitting a $(\frac{\sinh mx}{x})$ -curve to the experimental data values of the jump distance a can be estimated. Figure 6.17 includes such curves (shown dotted). The values of the site spacing, calculated from the composition and the jump distance are given in Table 6.2.

Table 6.2

Composition	Site spacing(a) from chemical data	Jump distance (a_j) (m)	$\frac{a_j}{a}$
50% V_2O_5	4.2×10^{-10} m	18.7×10^{-10} m	4.45
40% V_2O_5	4.4×10^{-10} m	18.6×10^{-10} m	4.22
30% V_2O_5	4.7×10^{-10} m	21.4×10^{-10} m	4.55
20% V_2O_5	5.4×10^{10} m	17.4×10^{-10} m	3.22

There is only approximate agreement between experiment and the theoretical curve, with the experimental data generally having a more gradual transition to field-dependence. The introduction of a cosh nx factor into the theoretical expression would improve the agreement but this would imply that free carriers were generated by the field and that the carrier concentration was thermally activated[(90)], in contradiction to E.S.R. and thermopower data which indicate a temperature-independent carrier concentration.

From Table 6.2 it can be seen that the jump distance calculated from the high field data is considerably greater than the site spacing calculated from the carrier concentration obtained from chemical

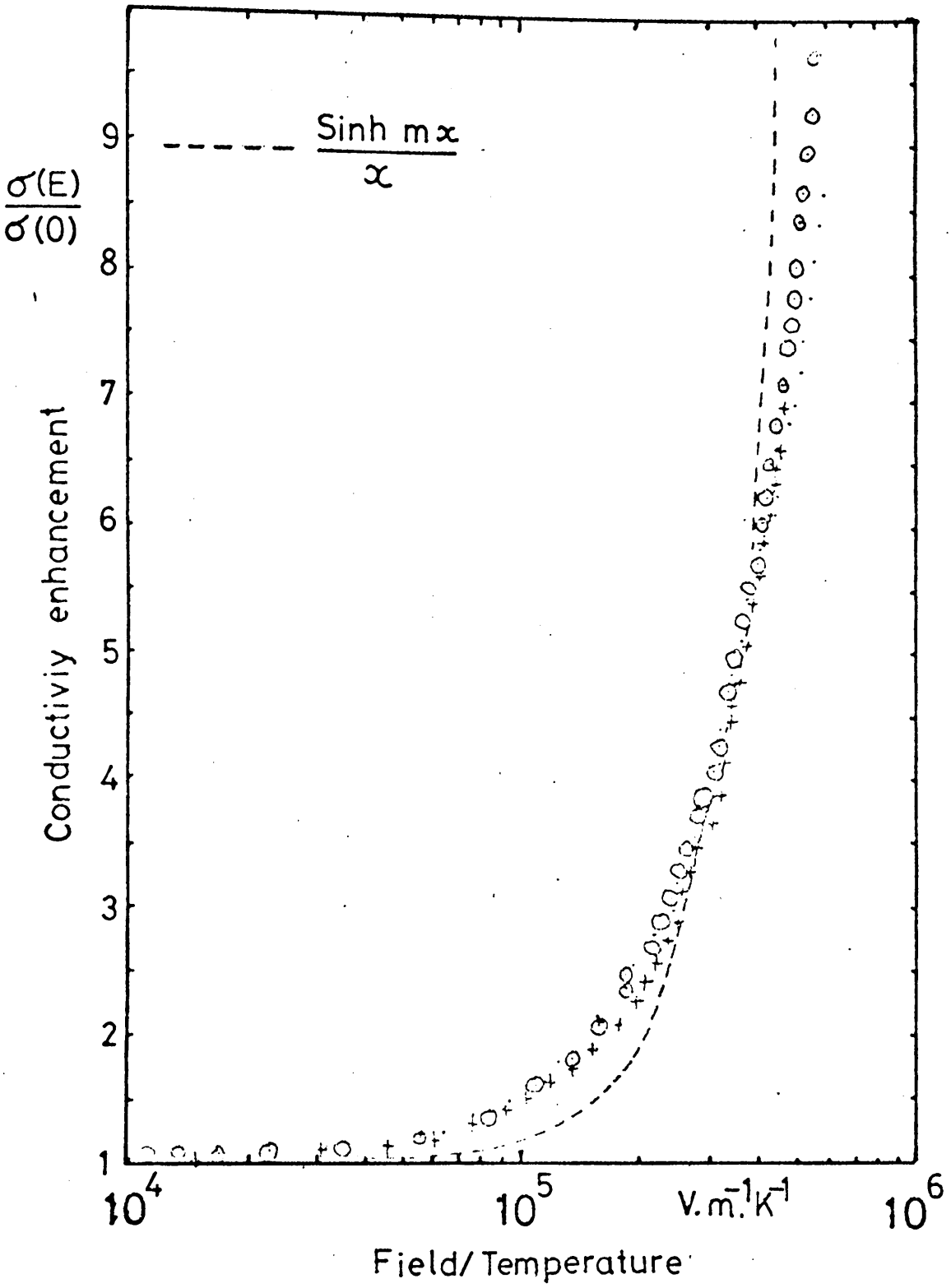

Fig. 6.17a High field conductivity enhancement factor versus field X recipricol temperature for a 50 V_2O_5 - 50 TeO_2 glass.

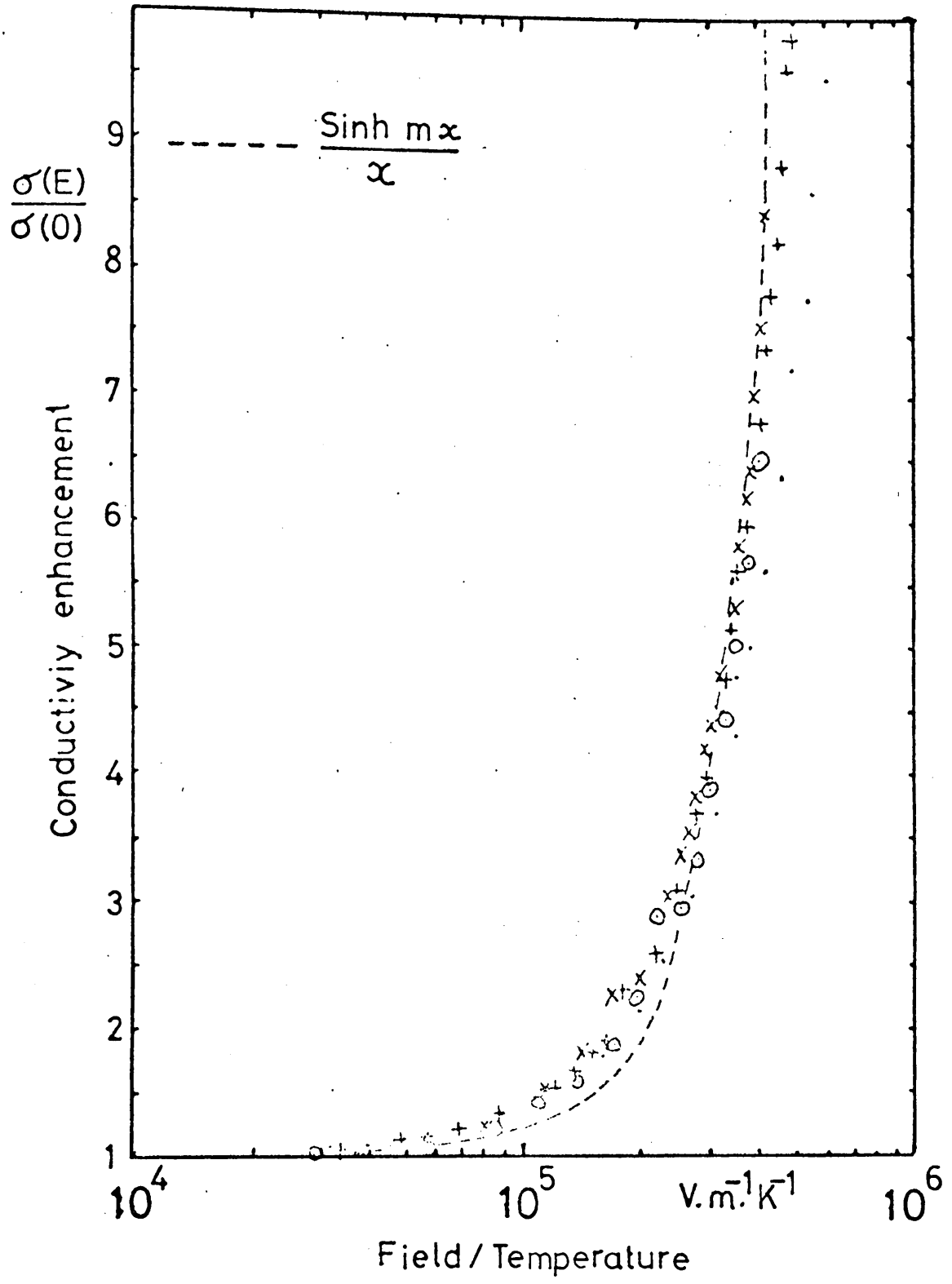

Fig. 6.17b High field conductivity enhancement factor versus field X recipricol temperature for a 40 V_2O_5 - 60 TeO_2 glass.

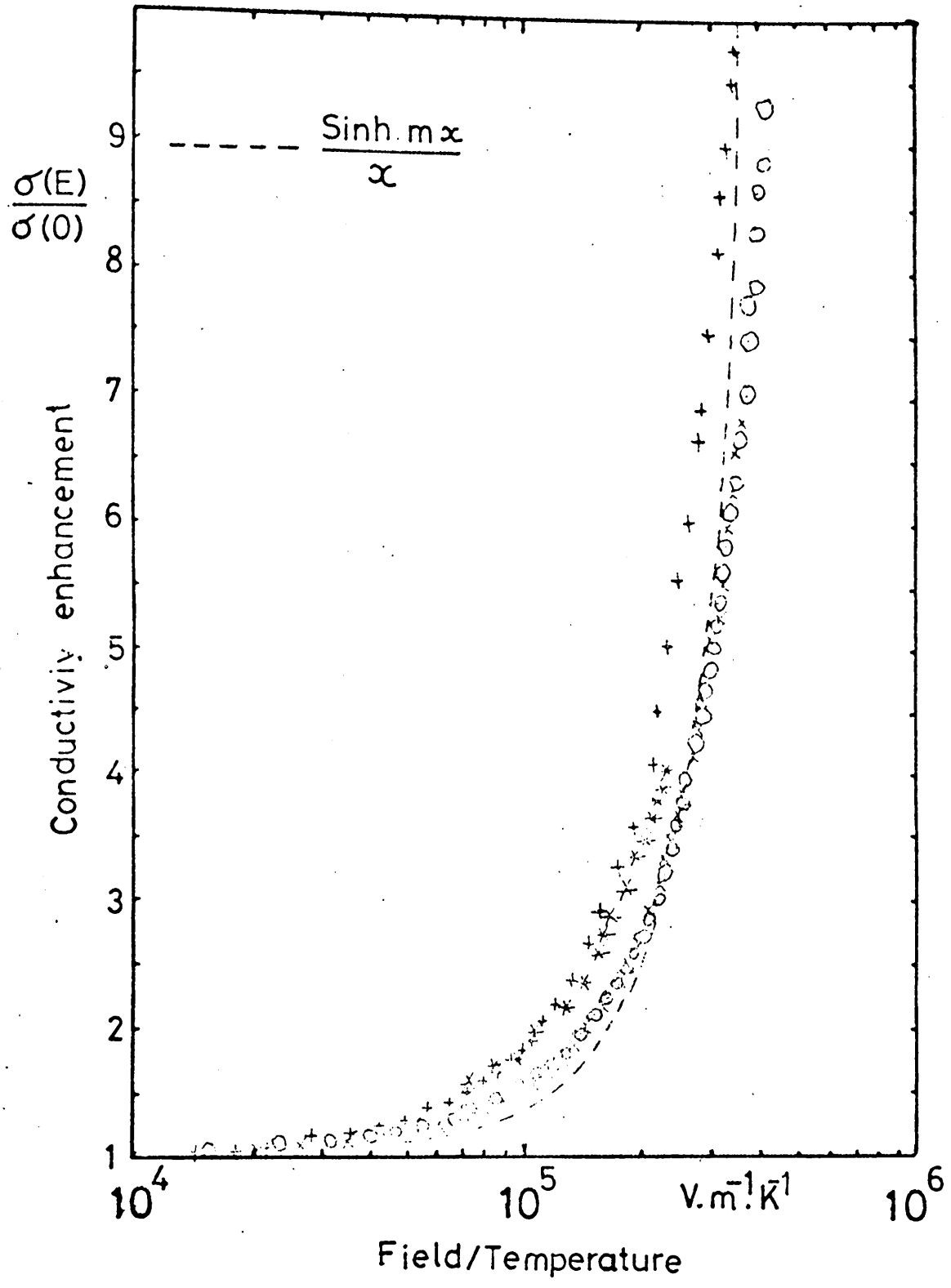

Fig. 6.17c High field conductivity enhancement factor versus field X recipricol temperature for a 30 V_2O_5 - 70 TeO_2 glass.

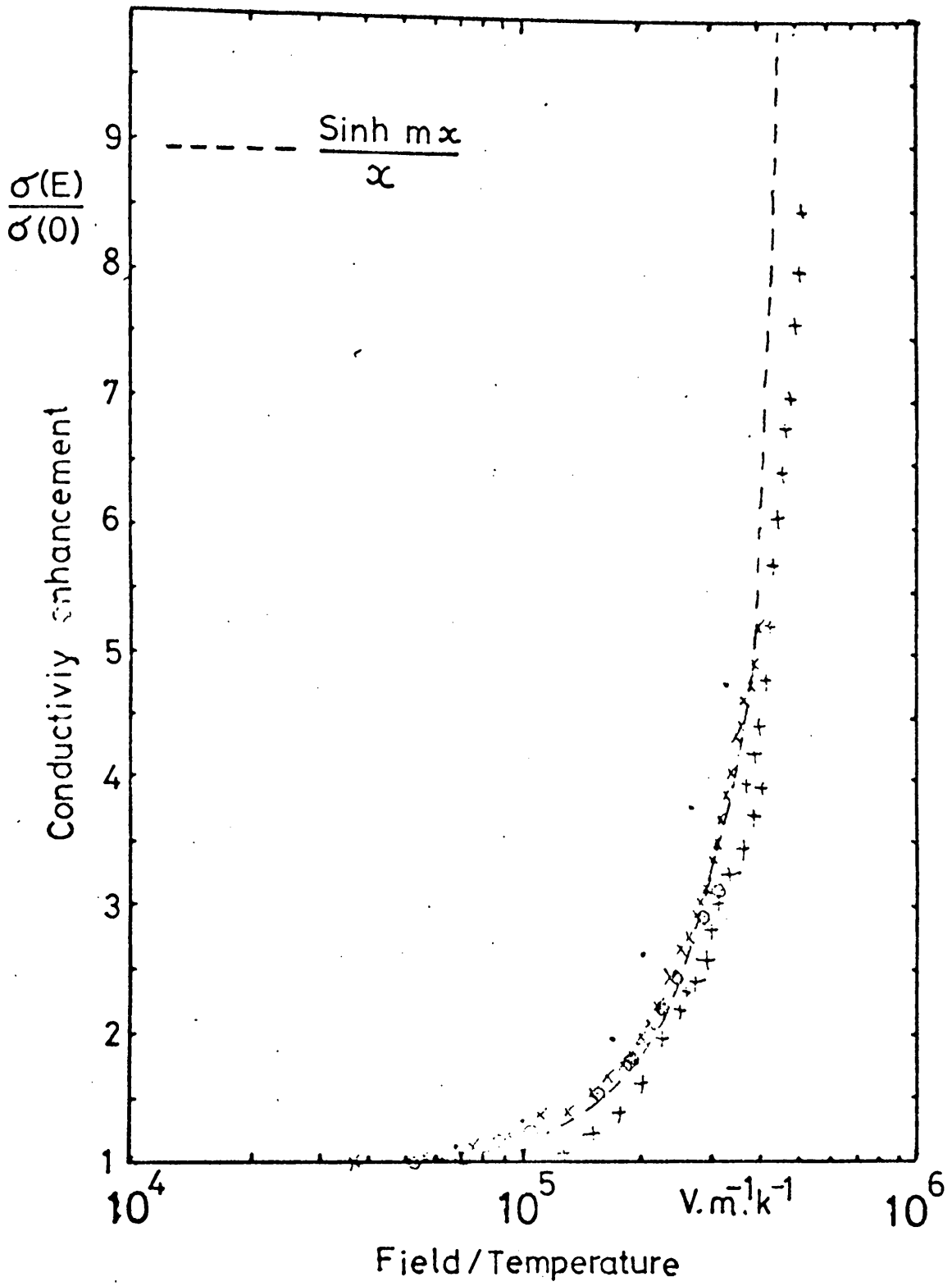

Fig. 6.17d High field conductivity enhancement factor versus field X recipricol temperature for a 20 V_2O_5 - 80 TeO_2 glass.

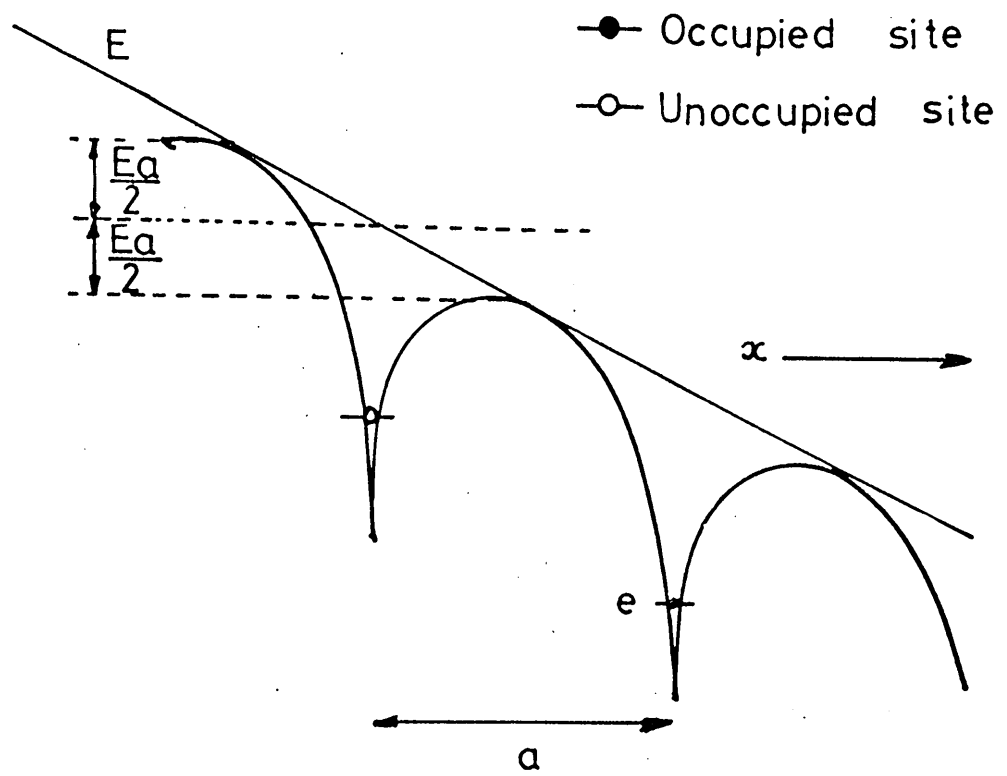

Fig. 6.18 High field hopping model for localised carriers.

analysis. Austin and Sayer[73] show that, depending on the value of the disorder energy, W_D, the effect of structural disorder is to increase the jump distance by around 20% in a typical vanadate glass. This increase is not large enough to account for the difference between the site separation and the jump distance calculated from the high-field data. To explain this anomoly Austin and Sayer[73] propose a model in which certain of the hops require a greater energy than the rest. There is, therefore, an *apparent* enhancement in the jump distance whereas it is, in fact, the local field at the sites of the hard hops which is enhanced over the applied field. The hard hops present high impedence links in a chain of lower impedences and an applied field will fall mainly across them, while the field at the other links in the chains is reduced from the average value. Consequently it is the field dependent conductivity of the hard hops with an enhanced local field which determines that of the bulk.

The origin of the hard hops is not obvious. One possibility is suggested by the observation of a maximum in d.c. conductivity at V^{4+}: V_{Tot} ratios which are much lower than the theoretically predicted value of 0.5 (See Section 6.1.3). It was suggested that this arose because a fraction of the V^{5+} sites were bound-up in structural complexes and unable to take part in the conduction process. These complexes would present areas which carriers could only cross with difficulty, i.e. would act as 'hard hops'. Recently Bogomolova **et al**[55] have presented evidence based on E.S.R. spectra and electron microscopy of V_2O_5 - P_2O_5 - CaO glass showing that phase separation occurs into two distinct phases, one of which is rich in V^{4+} and would dominate the low-field conduction process. At high fields these regions would

present 'easy hops' while in the regions deficient in V^{4+} the carriers would have to hop greater distances, thus presenting the 'hard hops'. This situation would apply if phase separation is on a fine or a gross scale.

6.5 A.C. CONDUCTIVITY IN V_2O_5 - TeO_2 GLASSES

The frequency dependence of conductivity of several V_2O_5 - TeO_2 glasses from 10 to 50 mole % V_2O_5 is shown in Figure 6.19 over the frequency range 100 Hz to 10 MHz. In the low frequency region ($f < 10$ kHz) the conductivity is independent of frequency and approximately equal to the d.c. conductivity. The a.c. conductivity data ($\sigma_{a.c.}$) is obtained from the frequency dependent conductivity $\sigma(\omega)$:

$$\sigma_{a.c.} = \sigma(\omega) - \sigma_{d.c.} \qquad \ldots (6.23)$$

In Figure 6.20 the a.c. conductivity is plotted as a function of frequency demonstrating the usual frequency dependence of the form :

$$\sigma_{a.c.} \propto \omega^n \quad \text{where } n \simeq 0.85 \qquad \ldots (6.24)$$

This behaviour is typical of hopping conduction but, as pointed out by Jonscher[91], cannot in itself be taken as sufficient evidence of such.

Figure 6.20 includes a scale showing the range of the d.c. conductivities of the glasses used for the a.c. conduction measurements and it is clear that the latter is much less dependent on composition. This observation will be discussed in terms of "Maxwell-Wagner" polarisation.

The inhomogeneous glass can be modelled as a dielectric separated

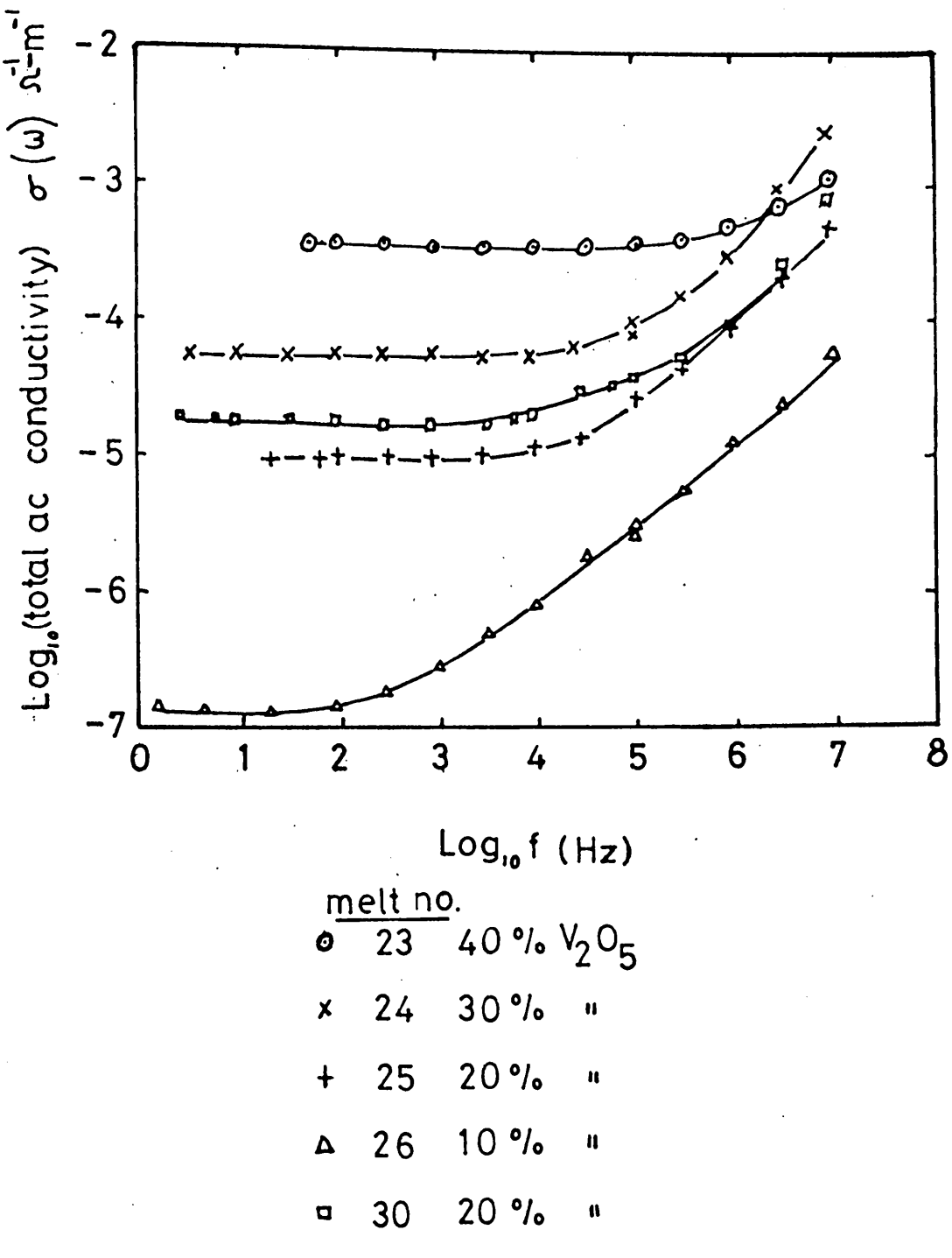

Fig. 6.19 Frequency dependence of conductivity for some V_2O_5 - TeO_2 glasses.

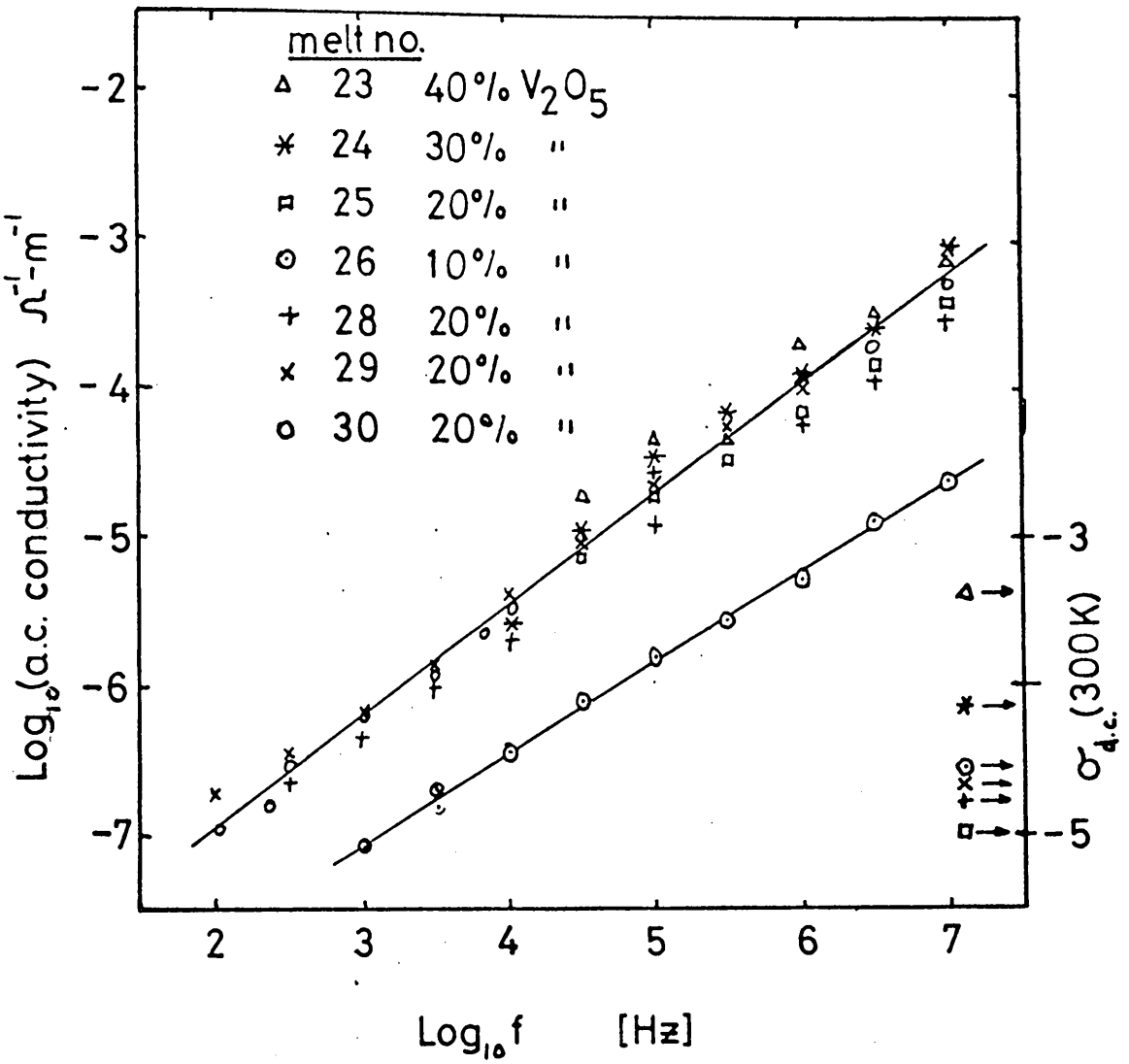

Fig. 6.20 Frequency dependence of the a.c. conductivity of some V_2O_5- TeO_2 glasses.

into regions of high and low conductivity. The exact nature of these regions is not known but they could arise from the formation of long-chain polymeric ions or macro-molecules as described in Section 6.13 on the d.c. conductivity. Another possibility is phase separation, within the glass, either of glassy regions with differing conductivities or the formation of micro-crystalline regions. A.C. losses due to "Maxwell-Wagner" or interfacial polarisation would then occur through the accumulations of charge at the boundaries between the different regions.

The heterogeneous glass can be considered represented in a highly simplified form as the two-layer structure of Figure 6.21. The resistors R_1 and R_2 represent the resistances of the two different regions, while C_1 and C_2 represent the capacitances. Analysis of this model leads to the result[92]

$$\frac{1}{R} = \frac{1}{R_1 + R_2} + \frac{(C_s - C_\infty)\omega^2\tau}{1 + \omega^2 \tau^2} \qquad \ldots (6.25)$$

and

$$C = C_\infty + \frac{C_s - C_\infty}{1 + \omega^2 \tau^2} \qquad \ldots (6.26)$$

where R and C are the components in the equivalent circuit shown in Figure 6.21 and

$$C_s = \frac{C_1 R_1^2 + C_R R_2^2}{(R_1 + R_2)^2} \qquad \ldots (6.27)$$

$$C_\alpha = \frac{1}{C_1^{-1} + C_2^{-1}} \qquad \ldots (6.28)$$

$$\tau = \frac{C_1 + C_2}{R_1^{-1} + R_2^{-1}} \qquad \ldots (6.29)$$

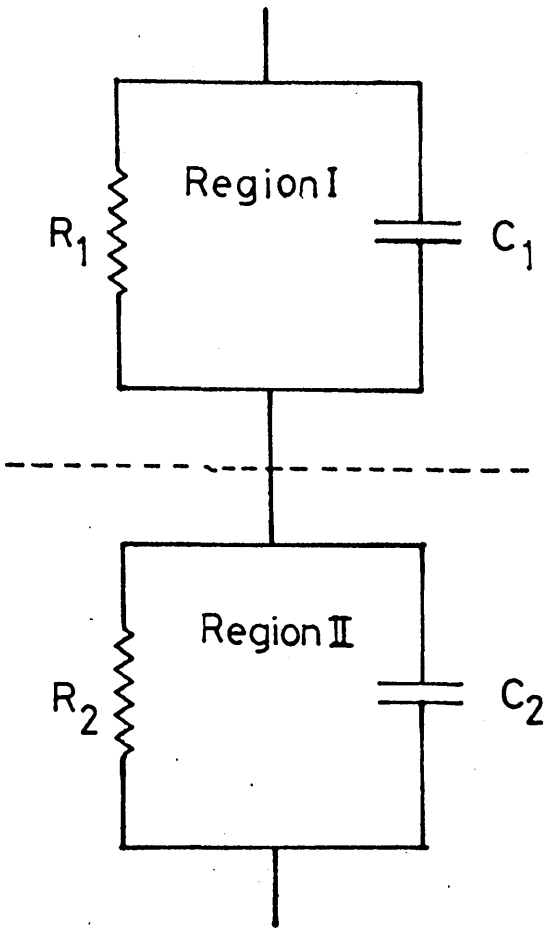

Fig. 6.21 "Two-layer" model of phase separated glass.

At low frequencies the term $(R_1 + R_2)^{-1}$ in equation 6.25 will dominate and the conductivity will approach the d.c. value of equation 6.2 . At high frequencies the term

$$\frac{(C_s - C_\infty)^2}{1 + \omega^2\tau^2}$$

will dominate and give a frequency dependent conductivity.

This simple model, based on the assumption that a single relaxation time (τ) occurs within the glass, does not give a $\sigma \propto \omega^{\sim 1}$ dependence. It is likely, however, that a distribution of relaxation times exists in a disordered material such as a glass resulting in a modified frequency dependence of $\sigma_{a.c.}$ from that predicted by equation 6.25. One source of this distribution of relaxation times is the variation in barrier heights between localised states due to disorder.

If one phase dominates conduction, ie, $R_1 << R_2$, then the composition dependence of R_2 will determine that of the glass as a whole. The wide range of composition dependence observed at low frequencies ($f < 10$ kHz) implies that R_2 varies widely with composition. The weak dependence of τ on composition, indicated by the small composition variation in conductivity in the high frequency ($f > 100$ kHz) region, implies that R_1 should have a weaker composition dependence than R_2. This result is in agreement with the conclusion reached by Bogomolova et al[55], as a result of E.S.R. and scanning electron microscopy, that V_2O_5 - P_2O_5 glasses are separated into two phases, one of which controls the conduction.

Figure 6.22 shows the dielectric constant (E) of some V_2O_5 - TeO_2 glasses containing 80 mole % V_2O_5. It increases with decreasing frequency to unusually high values (e.g. approaching 150) at frequencies below 100 Hz. In the high frequency region ($f > 10^6$ Hz) it is virtually independent of frequency and has a value of about 20. This low frequency behaviour could be accounted for either by electrode polarisation or by polarisation of the interfacial regions between separate phases within the glass. If the former were the case, non-ohmic contact effects would be expected in the low-field d.c. behaviour. No such effects were observed suggesting that the exceptionally high ε_r values are a property of the bulk glass.

A possible explanation is the occurence of "hyperelectronic polarisation" in the glass. This mechanism was postulated by Pohl and Rosen[93],[94] to explain the extremely large (50 - 300,000) dielectric constants observed in certain conducting organic polymers. The long-chain molecules occurring in these materials are suggested to act as macrodipoles, on the basis that electrons are known to be delocalised within such molecules. The resulting polarisability of these molecules, each hundreds, or even thousands, of Angstroms long would be large. This mechanism should be applicable to the present glasses if the long-chain vanado-tellurite complexes discussed in section 6.1.3 are formed. These macro-molecules could act as highly polarisable dipoles, which, because of their large size would have long relaxation times giving rise to the high dielectric constants at low frequencies.

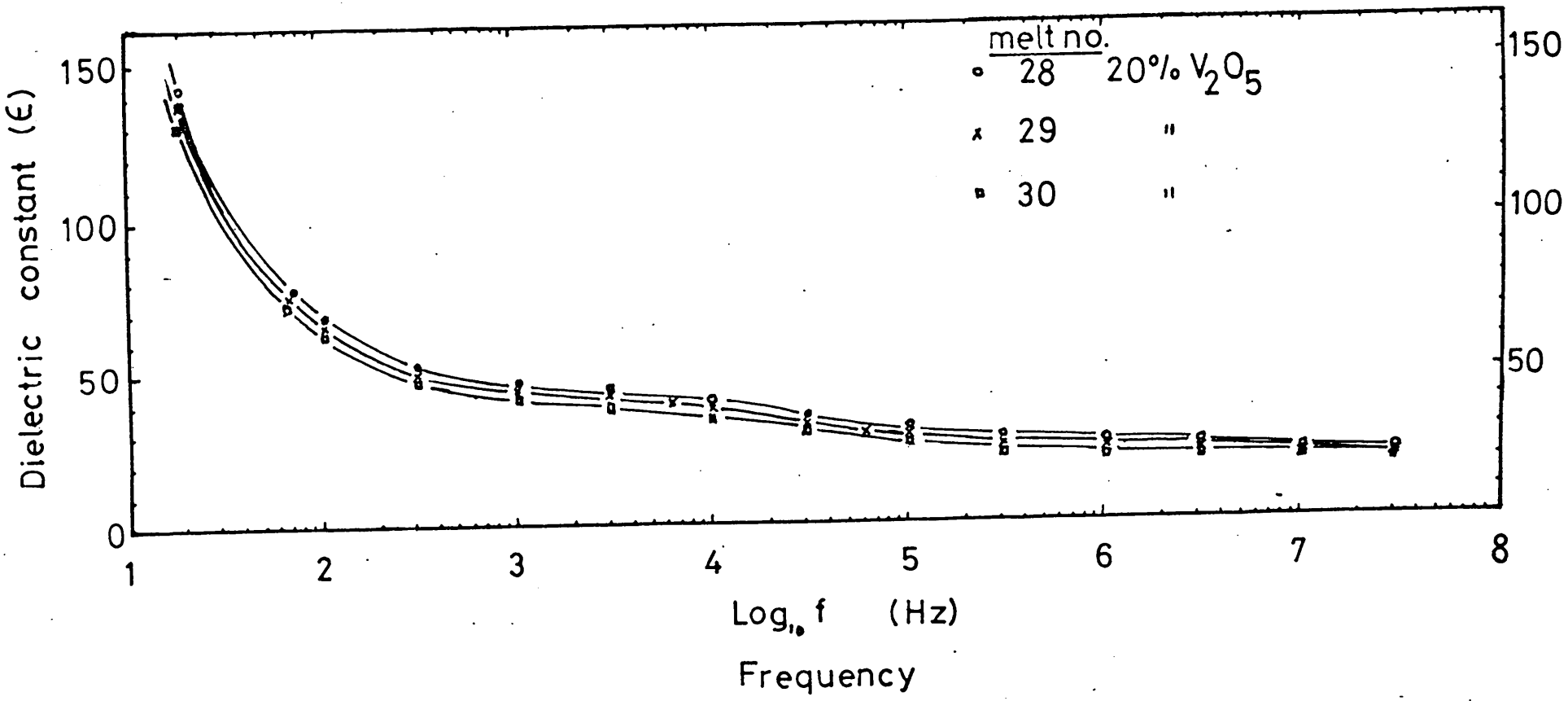

Fig. 6.22 Frequency dependence of ε for some 20 V_2O_5-80 TeO_2 glasses.

CHAPTER 7 : CONCLUSIONS AND SUGGESTIONS FOR FURTHER WORK

7.1 CONCLUSIONS

The object of this work was to investigate the conduction process in V_2O_5-TeO_2 glasses. Earlier studies of the system have been limited in scope and concerned primarily with the temperature dependent conductivity and electrical switching behaviour. In the present work, however, detailed studies were made of conductivity, thermopower, optical absorption, a.c. conductivity and high field d.c. conductivity as functions of temperature, composition and vanadium valence ratio. Similar studies have previously been carried out on V_2O_5-P_2O_5 glasses and, where appropriate comparisons were made and contrasts drawn between the two systems.

The most striking difference between the two systems is that the conductivity of V_2O_5-TeO_2 glasses is $2\frac{1}{2}$ to 3 orders of magnitude higher than V_2O_5-P_2O_5 glasses with similar vanadium contents. Furthermore, the pre-exponential term in the Arrhenius-type expression for conductivity is dependent on composition and valence ratio, while in the phosphate glasses it is independent of composition. The constancy of σ_o in the phosphate glasses implies that the variation in conductivity is due entirely to compositional dependence of the activation energy W. In contrast, σ_o for the V_2O_5-TeO_2 glasses varies with composition and valence ratio and σ varies

exponentially with site spacing, suggesting non-adiabatic hopping and α(the parameter characterising the rate of decay of the localised wave function) is estimated to be 0.97 $A^{o\ -1}$.

The conduction activation energy (W) was found constant above 250 K, but below this temperature the slope of log σ versus (1/T) decreased continuously, down to the lowest temperature at which measurements were made (77 K), implying that there is still an appreciable hopping contribution, and that the disorder energy is probably lower than previous estimates made by equating W_D to the "activation energy" at low temperatures. This is consistent with values of around 0.02 eV obtained from the behaviour of the thermopower at low temperatures.

The higher conductivity of the tellurites, by comparison to the phosphates has allowed measurements of thermopower to be made at low temperatures (>100 K). Previous attempts to make such measurements on the vanadium phosphates have lead to some confusion in the literature. Brown[63] reported an increasing negative thermopower at low temperatures, while Nester and Kingery[23] observed an apparently linear decrease with temperature below about 250 K. The present work on the V_2O_5-TeO_2 glasses establishes that the thermopower decreases in an activated manner, at temperatures below about 250 K, with an activation energy of approximately 0.02 eV. This is interpreted as being the disorder energy W_D.

The results of the a.c. conductivity and high-field data are consistent with hopping conduction. The a.c. behaviour appears to be the result of Maxwell-Wagner polarisation with a distribution of relaxation times, while the high-field conduction is consistent with the Austin-Sayer[73] "hard-hop" model.

Throughout the experimental data there are indirect indications that the glass is not completely homogeneous. The shift in the position of the maximum in d.c. conductivity from the theoretical $V^{4+}:V_{tot}$ ratio of 0.5 , the a.c. conductivity, the increase in dielectric constant to very high values at low frequencies and the high field conduction properties, could all be interpreted in terms of inhomogeneity in the composition and structure on a macroscopic scale. Scanning electron micrographs, with a resolution of 500 Å, were made on freshly fractured glass surfaces. These did not reveal any inhomogeneity, but it is likely that it occurs on a smaller scale.

7.2 SUGGESTIONS FOR FURTHER WORK

A more detailed knowledge of the structure of V_2O_5-TeO_2 glasses is necessary if a more complete description of the conduction process is to be made. This is especially true as regards the macro-structure. Techniques such as the paper chromatography experiments used by Ohashi on the V_2O_5-P_2O_5 glasses would be useful in revealing the existence of chain

molecules and large vanado-tellurite complexes. A more detailed knowledge of the local environments of the V^{4+} and V^{5+} ions is also desirable in determining the microstructure. To this end E.S.R. and N.M.R. studies would be helpful.

The optical absorption spectra revealed an absorption band apparently due to charge transfer between V^{4+} and V^{5+} ions, although this could also be interpreted as an interval d-d excitation of the vanadium 3d electrons. Electro-modulation of the absorption spectrum could establish the source of this band, a shift in position indicating a charge transfer band.

APPENDIX

CONDUCTIVITY AND THERMOPOWER DATA ON GLASS MELTS

50/50 mole per cent V_2O_5/TeO_2 Glasses

Melt Number	$V^{4+}:V_{Tot}$	σ(300 K) ($\Omega^{-1}.m^{-1}$)	σ_o ($\Omega^{-1}.m^{-1}$)	W (eV)	$\nu\, e^{-2a\alpha}$ (s^{-1})	α ($\mu V/K$)
9	0.03	1.7×10^{-4}	3.3×10^{-1}	0.270	-	-335
15	0.62	7.9×10^{-4}	2.0×10^{-1}	0.266	-	-220
44	0.077	9.7×10^{-4}	1.0×10^{-1}	0.250	3.4×10^{10}	-200
45	0.159	1.59×10^{-3}	2.0×10^{-1}	0.255	2.3×10^{10}	- 55
46	0.242	1.17×10^{-3}	1.0×10^{-1}	0.250	1.0×10^{10}	- 48
47	0.234	9.7×10^{-4}	1.5×10^{-1}	0.260	1.2×10^{10}	- 15

40/60 mole per cent V_2O_5/TeO_2 Glasses

Melt Number	$V^{4+}:V_{Tot}$	σ(300 K) ($\Omega^{-1}.m^{-1}$)	σ_o ($\Omega^{-1}.m^{-1}$)	W (eV)	$\nu\, e^{-2a\alpha}$ (s^{-1})	α ($\mu V/K$)
10	0.033	2.5×10^{-5}	1.0×10^{1}	0.320	-	-290
16	0.071	3.05×10^{-4}	1.1×10^{1}	0.278	-	-120
23	0.108	4.0×10^{-4}	1.4×10^{1}	0.280	1.8×10^{10}	- 85
37	0.092	3.1×10^{-4}	1.2×10^{1}	0.273	2.1×10^{10}	- 88
38	0.102	4.1×10^{-4}	1.4×10^{1}	0.267	2.4×10^{10}	-136
39	0.120	3.9×10^{-4}	1.3×10^{1}	0.274	1.7×10^{10}	-110
40	0.123	6.1×10^{-4}	1.6×10^{1}	0.260	1.9×10^{10}	- 90
41	0.134	4.4×10^{-4}	9.0×10^{0}	0.259	1.6×10^{10}	- 95
42	0.107	2.95×10^{-4}	5.0×10^{0}	0.290	1.2×10^{10}	-140
43	0.121	4.2×10^{-5}	1.8×10^{1}	0.268	2.2×10^{10}	-116

30/70 mole per cent V_2O_5/TeO_2 Glasses

Melt Number	$V^{4+}:V_{Tot}$	σ(300 K) ($\Omega^{-1}.m^{-1}$)	σ_o ($\Omega^{-1}.m^{-1}$)	W (ev)	$\nu\, e^{-2a\alpha}$ (s^{-1})	α ($\mu V/K$)
11	0.025	1.7×10^{-5}	2.5×10^{-2}	0.355	-	-310
17	0.077	5.5×10^{-5}	3.0×10^{0}	0.290	-	-155
20	0.134	1.23×10^{-4}	6.0×10^{0}	0.275	-	- 75
24	0.096	3.9×10^{-4}	5.0×10^{0}	0.287	3.8×10^{9}	- 90
32	0.082	1.3×10^{-4}	2.0×10^{0}	0.254	6.1×10^{9}	-130
33	0.103	1.3×10^{-4}	2.5×10^{0}	0.266	7.7×10^{9}	-105
34	0.151	1.83×10^{-4}	6.0×10^{0}	0.285	5.1×10^{9}	- 48
35	0.256	1.75×10^{-4}	8.0×10^{0}	0.280	6.6×10^{9}	+ 22
36	0.273	1.69×10^{-4}	1.5×10^{1}	0.295	4.2×10^{9}	+ 13

20/80 mole per cent V_2O_5/TeO_2 Glasses

Melt Number	$V^{4+}:V_{Tot}$	σ(300 K) $(\Omega^{-1}.m^{-1})$	σ_o $(\Omega^{-1}.m^{-1})$	W (ev)	$\nu\, e^{-2a\alpha}$ (s^{-1})	α $(\mu V/K)$
12	0.042	1.7×10^{-6}	2.5×10^{1}	0.370	-	-195
18	0.077	6.2×10^{-6}	3.0×10^{0}	0.302	-	-125
25	0.100	1.28×10^{-5}	2.0×10^{0}	0.300	1.5×10^{9}	- 75
28	0.124	1.8×10^{-5}	3.0×10^{0}	0.290	2.4×10^{9}	- 65
29	0.188	2.3×10^{-5}	2.5×10^{0}	0.310	1.5×10^{9}	- 5
30	0.333	2.4×10^{-5}	2.0×10^{0}	0.305	1.06×10^{9}	+ 70

10/90 mole per cent V_2O_5/TeO_2 Glasses

Melt Number	$V^{4+}:V_{Tot}$	σ(300 K) $(\Omega^{-1}.m^{-1})$	σ_o $(\Omega^{-1}.m^{-1})$	W (ev)	$\nu\, e^{-2a\alpha}$ (s^{-1})	α $(\mu V/K)$
13	0.020	1.7×10^{-8}	-	0.410	-	-100
19	0.071	2.0×10^{-7}	-	0.350	-	- 85
26	0.086	2.4×10^{-7}	5.0×10^{-1}	0.330	-	- 60
50	0.105	3.6×10^{-7}	6.0×10^{-1}	0.337	2.2×10^{8}	-120
51	0.156	1.05×10^{-6}	8.0×10^{-1}	0.320	4.1×10^{8}	- 38
52	0.375	3.0×10^{-6}	1.0×10^{0}	0.340	1.4×10^{8}	- 60
53	0.400	2.1×10^{-6}	1.3×10^{0}	0.338	-	+100
54	0.335	1.88×10^{-6}	1.1×10^{0}	0.340	-	+140

REFERENCES

1. Zachariasen, W H, J Amer Chem Soc, 54, pp 3841-3853, 1932.
2. Jones, G O, "Glass", Methuen's Monographs, 1956.
3. Van Wazer , J R, J Amer Ceram Soc, 72, p 639, 1950.
4. Stevels, J M, J Soc Glass Tech, 35, p 284, 1951.
5. Mott, N F and Twose, W D, Adv in Phys, 10, p 107, 1961.
6. Anderson, P W, Phys Rev, 109, p 1492, 1958.
7. Davis, E A and Mott, N F, Phil Mag, 22, p 903, 1970.
8. Mott, N F, Phil Mag, 19, p 835, 1969.
9. Mott, N F and Davis, E A, "Electronic Processes in Non-Crystalline Materials", Clarendon Press, Oxford, 1971.
10. Morin, F J, Bell Sys Tech J, 37, p 1047, 1958.
11. Slater, J C, "Handbuch der Physik", 19, J Springer, Berlin, 1956.
12. de Boer, J H and Verwey, E J W, Proc Phys Soc, (London), 49, p 66, 1937.
13. Mott, N F, Proc Phys Soc (London), 62A, p 416, 1949.
14. Van Houten, S, J Phys Chem Solids, 23, p 1045, 1962.
15. "Atomic Energy Levels", NBS Circular, 467, Vols 1949 and 1952.
16. Mott, N F and Littleton, M J, Trans Faraday Soc, 34, p 485, 1938.
17. Tanabe, Y and Sugano, S, J Phys Soc Japan, 9, p 753, 1954.
18. Verleur, H W, Barker, A S and Berglund, C N, Phys Rev, 172, p 788, 1968.
19. Kahn, A H and Leyendecker, A J, Phys Rev, 135, p A1321, 1964.
20. Goodenough, J B, Proc 2nd Int Conf on Conduction in Low-Mobility Materials, Taylor and Francis, London, p 87, 1971.
21. Heikes, R R in Chapter 4 of "Thermoelectricity : Science and Engineering", Interscience, NY - London, 1961.

22. Austin, I G and Mott, N F, Adv in Phys, 18, 71, p 41, 1969.

23. Nester, N H and Kingery, W D, Proc 7th Int Cong on Glass, Brussels, p 106, 1965.

24. Holstein, T, Ann Phys, NY, 8, p 343, 1959.

25. Mott, N F and Gurney, R W, "Electronic Processes in Ionic Crystals", Oxford, London, 1950.

26. Gibbons, D J and Spear, W E, J Phys Chem Solids, 27, p 1917, 1966.

27. Street, G B and Gill, W D, Phys Stat Sol, 18, p 601, 1966.

28. Loveland, R J, Le Comber, P G and Spear, W E, Phys Rev B, 6, p 3121, 1972.

29. Bosman, A J and van Daal, H J, Adv in Phys, 19, p 1, 1970.

30. Van Daal, H J, Proc 2nd Int Conf on Conduction in Low-Mobility Materials, Taylor and Francis, London, p 17, 1971.

31. Emin, D, Phys Rev Lett, 25, p 1751, 1970.

32. Kennedy, T N, Hakim, R and Mackenzie, J D, Mat Res Bull, 2, p 193, 1967.

33. Kennedy, T N and Mackenzie, J D, J Non-Cryst Sols, 1, p 326, 1969.

34. Denton, E P, Rawson, H and Stanworth, J E, Nature, 173, p 1030, 1954.

35. Roscoe, H E, Phil Trans Roy Soc, 158, p 1, 1968.

36. Hansen, K W, J Electro-Chem Soc, 112, 10, p 994, 1965.

37. Hansen, K W and Splann, M T, ibid, 113, 9, p 895, 1966.

38. Kinser, D L, ibid, 117, 4, p 546, 1970.

39. Sayer, M and Mansingh, A, Phys Rev B, 6, 12, p 1629, 1972.

40. Linsley, G S, PhD Thesis, Univ of Sheffield, 1968.

41. Kennedy, T N and Mackenzie, J D, Phys Chem Glasses, 8, p 169, 1967.

42. Dimitriev, Y, Marinov, M, Ivanova, Y and Popov, M, C R l'Acad Bulg Sci, 23, 5, p 507, 1970.

43. Dimitriev, Y, Marinova, M and Ivanova, Y, ibid, 24, 3, p 319, 1971.

44. Drake, C F, Scanlan, I F and Engel, A, Phys Stat Sol, 32, p 193, 1969.

45. Munakata, M, Sol State Electronics, 1, p 159, 1960.

46. Lynch, G F, Sayer, M, Segel, S L and Rosenblatt, G, J App Phys, 42, 7, p 2587, 1971.

47. Kitiagorodskii, I I, Frolov, V K and Kuo-Cheng, Steklo i Keramika, 17, 5, 1960.

48. Landsberger, F R and Bray, P J, J Chem Phys, 53, 7, p 2757, 1970.

49. Mackenzie, J D, "Semiconducting Glasses", Tech Report 5, Contract Nonr-591 (21).

50. Harper, H and McMillan, P W, Phys Chem Glasses, 15, p 148, 1974.

51. Sayer, M, Mansingh, A, Reyes, J M and Lynch, G F, Proc 2nd Int Conf on Conduction in Low-Mobility Materials, Taylor and Francis, London, p 115, 1971.

52. Anderson, G W and Compton, W D, J Chem Phys, 52, 12, p 6166, 1970.

53. Ohashi, S, "Topics in Phosphorous Chemistry", 1, p 217, Interscience, 1964.

54. Kinser, D L and Wilson, L K, Proc 2nd Cairo Sol State Conf, Cairo, 1973.

55. Bogomalova, L D, Dolgolenko, T F, Lazukin, V N and Filatova, I V, Sov Phys Sol State, 16, p 5, 1974.

56. Mott, N F, J Non-Cryst Sol, 1, p 1, 1968.

57. Schnakenberg, J, Phys Stat Sol, 28, p 623, 1968.

58. Schmid, A P, J App Phys, 39, 7, p 3140, 1968.

59. Killias, H R, Phys Letts, 20, 1, p 5, 1966.

60. Emin, D, Proc 13th Session of Scottish Univ Summer School in Physics, Academic Press, London and NY, 1973.

61. Linsley, G S, Owen, A E and Hayatee, F M, J Non-Cryst Sols, 4, p 208, 1970.

62. Sayer, M, Private communication.

63. Brown, R M, PhD Thesis, University of Illinois, 1966.

64. Sayer, M, Mansingh, A, Reyes, J M and Rosenblatt, G, J App Phys, 42, 7, p 2857, 1971.

65. Heikes, R R, Maradudin, A A and Miller, R C, Ann Phys, 8, p 733, 1963.

66. Chaudhari, P K and Li, S S, Phys Stat Sol (a), 24, p 231, 1974.

67. Kennedy, T N and Mackenzie, J D, Phys and Chem of Glasses, 8, p 169, 1967.

68. Pollak, M, Phys Rev, 133, p A564, 1964.

69. Pollak, M, Phys Rev, 138, p A1822, 1965.

70. Hayatee, F M, PhD Thesis, Univ of Edinburgh, 1971.

71. Kinser, D L, Clark, A E and Hench, L L, Bull Am Ceram Soc, p 398, 1969.

72. Mansingh, A, Vaid, J K and Tandon, R P, J Phys C, 8, p 1023, 1975.

73. Austin, I G and Sayer, M, J Phys C, 7, p 905, 1974.

74. Anderson, G W, J App Phys, 44, 1, p 406, 1973.

75. Austin, I G and Garbett, E S, Proc 13th Session of Scottish Univ Summer School in Physics, Academic Press, London, and NY, 1973.

76. Reik, H G, Sol State Comms, 8, p 1737, 1970.

77. Austin, I G, Sayer, M and Sussman, R S, "Amorphous and Liquid Semiconductors", Ed J Stuke and W Brenig (Taylor and Francis, London), Proc 5th Int Conf on Amorphous and Liquid Semiconductors, Garmisch, Partenkirchen, Sept 1973, 2, p 1343, 1974.

78. Gaman, V I, Beznikov, U A, Fedyaninova, N I and Kusnetsov, V D, Izv.Vuz.Fiz. 2, p 57, 1972.

79. Kalygina, V M and Gaman, V I, Izv. Viz. Fiz., 3, p 45, 1972.

80. Kalygina, V M and Gaman, V I, ibid, 8, p 31, 1972.

81. Rhee, C, Yoon, S W and Lim, H J, Proc Xth Int Cong on Glass, Kyoto, p 7, 1974.

82. Ioffe, V A, Patrina, J B and Poberovshaya, I S, Sov Phys Sol State, 2, p 609, 1960.

83. Mackenzie, J D, "Modern Aspects of the Vitreous State", 3, p 126, Butterworths, London, 1965.

84. Baynton, P L, Rawson, H and Stanworth, J E, J Electrochem Soc, 104, p 237, 1957.

85. Hamblen, D P, Weidel, R A and Blair, G E, J Amer Ceram Soc, 46, p 499, 1963.

86. Lynch, A C, Proc IEE, 104B, p 363, 1957.

87. Farley, J M and Saunders, G A, Phys Stat Sol (a), 28, p 199, 1975.

88. Greaves, G N, J Non-Cryst Sol, 11, p 429, 1972.

89. Kenny, N, Kannewurf, C R and Whitmore, D H, J Phys Chem Solids, 27, p 1237, 1966.

90. Adamec, V and Calderwood, J H, J of Phys, 8, p 551, 1975.

91. Jonscher, A K, Proc 13th Session of Scottish Univ Summer School in Physics, Academic Press, London and NY, p 329, 1973.

92. Koops, C G, Phys Rev, 83, 121, 1951.

93. Rosen, R and Pohl, H A, J Polymer Sci, C17, p 13, 1967.

94. Pohl, H A and Wyhof, J R, J Non-Cryst Sol, 11, p 137, 1972.